

THERMOPHYSICAL PROPERTIES OF METHANOL BASED
NANOFLUIDS

MOHD. MOSTAFIZUR RAHMAN

DISSERTATION SUBMITTED IN FULFILMENT OF THE
REQUIREMENT FOR THE DEGREE OF MASTER OF
ENGINEERING SCIENCE

FACULTY OF ENGINEERING
UNIVERSITY OF MALAYA
KUALA LUMPUR

2015

UNIVERSITI MALAYA

ORIGINAL LITERARY WORK DECLARATION

Name of Candidate: **Mohd. Mostafizur Rahman** (I.C/Passport No:

Registration/Matric No: **KGA120095**

Name of Degree: **Master of Engineering Science**

Title of Project Paper/Research Report/Dissertation/Thesis (“this Work”):
Thermophysical Properties of Methanol Based Nanofluids

Field of Study: **Energy**

I do solemnly and sincerely declare that:

- (1) I am the sole author/writer of this Work;
- (2) This Work is original;
- (3) Any use of any work in which copyright exists was done by way of fair dealing and for permitted purposes and any excerpt or extract from, or reference to or reproduction of any copyright work has been disclosed expressly and sufficiently and the title of the Work and its authorship have been acknowledged in this Work;
- (4) I do not have any actual knowledge nor do I ought reasonably to know that the making of this work constitutes an infringement of any copyright work;
- (5) I hereby assign all and every rights in the copyright to this Work to the University of Malaya (“UM”), who henceforth shall be owner of the copyright in this Work and that any reproduction or use in any form or by any means whatsoever is prohibited without the written consent of UM having been first had and obtained;
- (6) I am fully aware that if in the course of making this Work I have infringed any copyright whether intentionally or otherwise, I may be subject to legal action or any other action as may be determined by UM.

Candidate’s Signature

Date

Subscribed and solemnly declared before,

Witness’s Signature

Date

Name:

Designation:

ABSTRACT

Nanofluids are defined as colloidal suspension of solid particles with the size smaller than 100 nanometer. In this study, Al_2O_3 , SiO_2 and TiO_2 nanoparticles were suspended into methanol without any surfactant to investigate their characteristics, stability and thermophysical properties. Nanoparticles size, shape, elemental proportion and suspension uniformity were characterized. The stability of methanol based nanofluids was analyzed using Uv-Vis spectrometer and zeta potential. Thermophysical properties of nanofluids, namely thermal conductivity, viscosity and density of nanofluids were measured by KD_2 pro analyzer, LVDV III ultra-programmable rheometer and KEM-DA 130N density meter, respectively. All experiments were conducted at five different volume concentrations (0.005, 0.01, 0.05, 0.10 and 0.15 vol%) and five different temperatures (1, 5, 10, 15 and 20 °C). In this study, Al_2O_3 -methanol nanofluid appeared to be more stable compared to SiO_2 -methanol and TiO_2 -methanol nanofluids. It was found that thermal conductivity increased with the increase of volume concentration of nanoparticles for all types of nanoparticles. Thermal conductivity enhancements is shown between 1–8% for every 0.05 vol% increase with Al_2O_3 having the highest enhancement increase in nanoparticle volume concentration. Thermal conductivity also increased between 0.5–3.9% for every 5 °C increment in temperature with SiO_2 showing the least change. The shear stress and viscosity increased with volume concentration but decreased with increase in temperature and shear rate. The results showed that the fluids appeared as a non-Newtonian fluid with a shear thickening or dilatant behavior. The increment was higher in TiO_2 -methanol nanofluids compared to the other two with the highest increment of 17.8%. Besides, density of the methanol based nanofluids increased with volume concentrations. However, density decreased accordingly with increased temperature. This study demonstrates that thermal conductivity, viscosity and density of methanol based nanofluids depend on the volume concentration and temperature.

ABSTRAK

Nanofluids ditakrifkan sebagai penyuraian koloid zarah pepejal dengan saiz yang lebih kecil daripada 100 nanometer. Dalam kajian ini, Al_2O_3 , SiO_2 dan TiO_2 nanopartikel diurai dalam metanol tanpa surfaktan untuk menyiasat ciri-cirinya, kestabilan dan sifat termofizikal. Nanopartikel saiz, bentuk, bahagian unsur dan keseragaman penyuraian telah dikaji. Kestabilan nanofluids berasaskan metanol dianalisis menggunakan Uv-Vis spektrometer dan potensi zeta. Sifat termofizikal dnanofluids, iaitu, kekonduksian terma kelikatan dan ketumpatan nanofluids diukur masing-masing dengan KD_2 pro analyzer, reometer boleh-program-ultra LVDV III dan meter ketumpatan KEM-DA 130N. Semua ujikaji telah dijalankan di lima kepekatan yang berbeza isipadu (0.005, 0.01, 0.05, 0.10 dan 0.15 vol%) dan lima suhu yang berbeza (1, 5, 10, 15 dan 20 °C). Dalam kajian ini, nanofluid Al_2O_3 -metanol didapati lebih stabil berbanding dengan nanofluid SiO_2 -metanol dan TiO_2 -metanol. Ia telah mendapati bahawa kekonduksian haba meningkat dengan peningkatan kepekatan jumlah nanopartikel untuk semua jenis partikel nano. Kekonduksian terma meningkat sebanyak 1-8% untuk peningkatan setiap 0.05 vol% dan Al_2O_3 mempunyai peningkatan yang tertinggi dalam kepekatan jumlah nanopartikel. Kekonduksian haba juga meningkat antara 0.5-3.9% untuk setiap kenaikan suhu 5 °C dengan SiO_2 menunjukkan perubahan yang paling kurang. Keicihan dan kelikatan meningkat dengan kepekatan jumlah tetapi menurun dengan peningkatan suhu dan kadar ricih. Hasil kajian menunjukkan bahawa cecair muncul sebagai cecair bukan Newtonian dengan penebalan ricih atau tingkah laku Perisai Cecair. Peningkatan ini lebih tinggi dalam nanofluids TiO_2 -metanol berbanding yang lain dengan kenaikan tertinggi sebanyak 17.8%. Selain itu, ketumpatan nanofluid berdasarkan metanol meningkat dengan kepekatan jumlah. Walau bagaimanapun, ketumpatan menurun pada kadar yang sama dengan suhu meningkat. Kajian ini menunjukkan bahawa kekonduksian haba, kelikatan dan ketumpatan nanofluids berasaskan metanol bergantung kepada kepekatan isipadu dan suhu nanofluids.

ACKNOWLEDGEMENTS

In the Name of Allah, The Beneficent, The Merciful, I would like to express my utmost gratitude and thanks to the almighty Allah (s.w.t) for the help and guidance that He has given me through all these years. My deepest appreciation is to my family for their blessings and supports.

I would like to express my gratitude and profound respect to my supervisors, Professor Dr. Saidur Rahman and Professor Ir. Dr. Abdul Aziz Bin Abdul Raman for their brilliant guidance, supports and encouragement to carry out this research work. I am deeply indebted to them.

Finally, thanks to University of Malaya for financial support, privileges, and opportunities to conduct this study. This project was carried out under the Ministry of Higher Education of Malaysia and the University of Malaya, Kuala Lumpur, Malaysia for the financial support under the project UM.C/HIR/MOHE/ENG/40. I gratefully acknowledge to the members of Energy Laboratory in helping me and for suggestion, ideas, discussions, and advices in completing this research work.

TABLE OF CONTENTS

ORIGINAL LITERARY WORK DECLARATION	ii
ABSTRACT	iii
ABSTRAK	iv
ACKNOWLEDGEMENTS	v
TABLE OF CONTENTS	vi
LIST OF FIGURE	x
LIST OF TABLE	xv
LIST OF SYMBLES AND ABBREVIATIONS	xvi
LIST OF APPENDICES	xviii
CHAPTER 1 : INTRODUCTION	1
1.1 Background	1
1.2 Importance of this study	4
1.3 Problem statement	5
1.4 Objectives of this study	5
1.5 Outline of the thesis.....	6
CHAPTER 2 : LITERATURE REVIEW	7
2.1 Introduction	7
2.2 Nanofluids	7
2.2.1 Preparation of nanofluids.....	8
2.2.1.1 One step method.....	8

2.2.1.2 Two-step method.....	9
2.3 Characterization of nanoparticles and nanofluids	11
2.3.1 XRD, SEM and TEM.....	11
2.4 Stability of nanofluids	13
2.4.1 Sediment photograph capturing	13
2.4.2 UV-Visible spectrophotometer	13
2.4.3 Zeta potential and Zetasizer	14
2.5 Thermophysical properties of nanofluids.....	16
2.5.1 Thermal conductivity.....	16
2.5.1.1 Theoretical study on thermal conductivity.....	16
2.5.1.2 Experimental study on thermal conductivity	19
2.5.1.2.(a) Effect of volume fraction on thermal conductivity of nanofluids	22
2.5.1.2.(b) Influence of temperature on thermal conductivity of nanofluids	22
2.5.2 Viscosity of nanofluids	23
2.5.2.1 Theoretical study on viscosity.....	23
2.5.2.2 Experimental study on viscosity	26
2.5.2.2.(a) Viscosity of nanofluids as a function of volume fraction.....	27
2.5.2.2.(b) Effect of temperature on viscosity of nanofluids	28
2.5.3 Density of nanofluids.....	28
2.6 Summary of literature review	30
CHAPTER 3 : METHODOLOGY.....	32
3.1 Introduction	32

3.2 Experimental setup	32
3.2.1 Materials	32
3.2.2 List of equipment	34
3.3 Preparation of methanol based nanofluids	34
3.4 Characterization of nanoparticles and methanol based nanofluids	37
3.4.1 Determination of particle shape, size and suspension uniformly	38
3.5 Stability of methanol based nanofluids	38
3.5.1 Sediment photograph capturing	39
3.5.2 UV-Visible spectrophotometer	39
3.5.3 Zeta potential and zetasizer.....	39
3.6 Thermophysical properties of methanol based nanofluids.....	40
3.6.1 Thermal conductivity measurement.....	40
3.6.2 Viscosity measurement	42
3.6.3 Density measurement.....	44
CHAPTER 4 : RESULTS AND DISCUSSIONS	46
4.1 Introduction	46
4.2 Characterization of nanoparticles and methanol based nanofluids	46
4.2.1 X-ray Diffraction (XRD) image analysis.....	46
4.2.2 Scanning electron microscope (SEM) image Analysis.....	48
4.2.3 TEM image analysis	49
4.3 Stability of methanol based nanofluids	51
4.3.1 Sedimentation image analysis.....	51

4.3.2 Inspection stability by Uv-Visible spectrophotometer	52
4.3.3 Stability inspection by Zeta potential and Zetasizer test	54
4.4 Thermophysical properties of methanol based nanofluids.....	56
4.4.1 Thermal conductivity of methanol based nanofluids.....	56
4.4.2 Viscosity of methanol based nanofluids	63
4.4.3 Density of methanol based nanofluids.....	69
4.5 Implication of this study.....	72
CHAPTER 5 : CONCLUSIONS AND RECOMMENDATIONS.....	73
5.1 Introduction	73
5.2 Conclusions	73
5.3 Recommendations for future work.....	74
REFERENCES.....	76
LIST OF PUBLICATION AND PRESENTATION.....	86
APPENDIXES	87

LIST OF FIGURE

Figure 2.1: Common basefluids, nanoparticles, and surfactants for synthesizing nanofluid	10
Figure 2.2: XRD pattern of Ag nanoparticles (Philip & Shima, 2014).....	12
Figure 2.3: SEM (left) and TEM (right) image of Al ₂ O ₃ -water nanofluids (Shukla et al., 2005)	12
Figure 2.4: Zeta potential of methanol nanofluids as a function of nanoparticle volume fraction (Pang et al., 2012).....	14
Figure 2.5: Particle size of methanol based nanofluids as a function of nanoparticle volume fraction (Pang et al., 2012)	16
Figure 2.6: Thermal conductivity versus particle volume fraction	22
Figure 2.7: Thermal conductivity versus temperature	23
Figure 2.8: Viscosity increases with the increase of particle volume fraction	27
Figure 2.9: Viscosity increases with the increase of temperature.....	28
Figure 2.10: Density increases with the increase of particle volume fraction	29
Figure 2.11: Density increases with the increase of temperature.....	30
Figure 3.1: Flowchart of experimental analysis.....	32
Figure 3.2: Cluster size at different ultrasonication time (0.05vol% of Al ₂ O ₃ concentration).....	35
Figure 3.3: Effect of evaporation on ultrasonication duration of Al ₂ O ₃ -methanol (0.05 vol%) nanofluids (a) before ultrasonication (b) after 2h ultrasonication.....	37
Figure 3.4: Using thermal bath to control temperature during ultrasonication time to prepare nanofluids.....	37

Figure 3.5: Schematic diagram of KD ₂ pro thermal properties analyzer.....	41
Figure 3.6: Thermal conductivity comparison with measured and reference data	42
Figure 3.7: Schematic diagram of viscosity measurement.....	43
Figure 3.8: Viscosity comparison with measured and reference data.....	44
Figure 3.9: Density comparison with measured and reference data	45
Figure 4.1: XRD pattern of Al ₂ O ₃ nanoparticles	47
Figure 4.2: XRD pattern of SiO ₂ nanoparticles	47
Figure 4.3: XRD pattern of TiO ₂ nanoparticles	47
Figure 4.4: SEM image of Al ₂ O ₃ nanoparticles	48
Figure 4.5: SEM image of SiO ₂ nanoparticles	49
Figure 4.6: SEM image of TiO ₂ nanoparticles.....	49
Figure 4.7: TEM image of Al ₂ O ₃ -methanol nanofluid (0.05 vol%)	50
Figure 4.8: TEM image of SiO ₂ -methanol nanofluid (0.05 vol%)	50
Figure 4.9: TEM image of TiO ₂ -methanol nanofluid (0.05 vol%)	51
Figure 4.10: Photograph of methanol based nanofluids just after preparation and after 7 days preparation	52
Figure 4.11: UV–Vis spectrum of Al ₂ O ₃ –methanol nanofluids	53
Figure 4.12: UV–Vis spectrum of SiO ₂ –methanol nanofluids.	54
Figure 4.13: UV–Vis spectrum of TiO ₂ –methanol nanofluids	54
Figure 4.14: Zeta potential of methanol based nanofluids as a function of nanoparticle volume concentration	55
Figure 4.15: Particle size in methanol based nanofluids as a function of volume concentration	56
Figure 4.16: Thermal conductivity of Al ₂ O ₃ –methanol as a function of temperature and particle volume concentration.	57

Figure 4.17: Thermal conductivity of SiO ₂ –methanol as a function of temperature and particle volume concentration.	58
Figure 4.18: Thermal conductivity of TiO ₂ –methanol as a function of temperature and particle volume concentration.	58
Figure 4.19: Experimental values of thermal conductivity (Al ₂ O ₃ –methanol) compared with the values from existing correlation	59
Figure 4.20: Experimental values of thermal conductivity (SiO ₂ –methanol) compared with the values from existing correlation	60
Figure 4.21: Experimental values of thermal conductivity (TiO ₂ –methanol) compared with the data from existing correlation.....	60
Figure 4.22: Comparison of thermal conductivity enhancement with reference data.	61
Figure 4.23: Comparison of thermal conductivity ratio measured data with proposed correlation	63
Figure 4.24: Shear stress and viscosity of Al ₂ O ₃ –methanol nanofluids for 0.05 vol% as a function of shear rate and temperature.	64
Figure 4.25: Shear stress and viscosity of SiO ₂ –methanol nanofluids for 0.05 vol% as a function of shear rate and temperature.	65
Figure 4.26: Shear stress and viscosity of TiO ₂ –methanol nanofluids for 0.05 vol% as a function of shear rate and temperature.	65
Figure 4.27: Viscosity of Al ₂ O ₃ –methanol as a function of temperature and particle volume concentration.	66
Figure 4.28: Viscosity of SiO ₂ –methanol as a function of temperature and particle volume concentration.	67
Figure 4.29: Viscosity of TiO ₂ –methanol as a function of temperature and particle volume concentration.	67

Figure 4.30: Comparison of measured viscosity with the values from existing correlation	68
Figure 4.31: Comparison of viscosity ratio measured values with proposed correlation	69
Figure 4.32: Density of Al ₂ O ₃ -methanol as a function of temperature and particle volume concentration.	70
Figure 4.33: Density of SiO ₂ -methanol as a function of temperature and particle volume concentration.	71
Figure 4.34: Density of TiO ₂ -methanol as a function of temperature and particle volume concentration.	71
Figure 4.35: Comparison of density increment with the values from existing correlation.	72
Figure A.1: SEM image of Al ₂ O ₃ nanoparticles during EDS analysis with the marking of point 1	87
Figure A.2: EDS analysis of Al ₂ O ₃ nanoparticles at point 1.....	87
Figure A.3: SEM image of SiO ₂ nanoparticles during EDS analysis with the marking of point 2.	88
Figure A.4: EDS analysis of SiO ₂ nanoparticles at point 2.	89
Figure A.5: SEM image of TiO ₂ nanoparticles during EDS analysis with the marking of point 3.	89
Figure A.6: EDS analysis of TiO ₂ nanoparticles at point 3.	90
Figure B.1: TEM image of Al ₂ O ₃ -methanol nanofluids with the approximate measurement of some particle's diameter.	91
Figure B. 2: TEM image of SiO ₂ -methanol nanofluids with the approximate measurement of some particle's diameter.	92
Figure B.3: TEM image of TiO ₂ -methanol nanofluids with the approximate measurement of some particle's diameter.	92
Figure C.1: Volume distribution of nanoparticle size within the 0.10 vol% of Al ₂ O ₃ -methanol nanofluids	93

Figure C.2: Volume distribution of nanoparticle size within the 0.05 vol% of SiO ₂ -methanol nanofluids	93
Figure C.3: Volume distribution of nanoparticle size within the 0.01 vol% of TiO ₂ -methanol nanofluids.....	94

LIST OF TABLE

Table 2.1: Summary of methanol based nanofluids synthesis process that followed by the researchers.....	11
Table 2.2: Zeta potential absolute value and stability.....	15
Table 2.3: List of Classical models for nanofluid thermal conductivity.....	17
Table 2.4: List of nanofluid thermal conductivity models derived from Classical models.....	18
Table 2.5: List of experimental studies on nanofluid thermal conductivity	20
Table 2.6: List of Classical models for nanofluid viscosity.....	24
Table 2.7: List of nanofluid viscosity models derived from classical models	24
Table 2.8: List of experimental studies on nanofluid viscosity	26
Table 2.9: Summary of the available literature about methanol based nanofluids	30
Table 3.1: Properties of nanoparticles.....	33
Table 3.2: Properties of Methanol.....	33
Table 3.3: List of equipment used in experiment.....	34
Table 3.4: Experimental condition.....	36
Table A.1: Chemical Elemental composition of Al ₂ O ₃ nanoparticles by EDS analysis at point 1.....	88
Table A.2: Chemical Elemental composition of SiO ₂ nanoparticles by EDS analysis at point 2.....	89
Table A.3: Chemical Elemental composition of TiO ₂ nanoparticles by EDS analysis at point 3.....	90

LIST OF SYMBLES AND ABBREVIATIONS

Abbreviations

DW	Distilled Water
DIW	Deionized Water
EG	Ethylene Glycol
EDS	Energy dispersive spectrometry
HVAC	Heating, ventilation and air conditioning system
JCPDS	Joint Committee on Powder Diffraction Standards
KB	Boltzmann constant
M	Methanol
MBNF	Methanol based nanofluids
SEM	Scanning Electron Microscopy
TEM	Transmission Electron Microscopy
W	Water
XRD	X-Ray Diffraction

Nomenclature

C_p	Specific heat (J/g K)
d	Diameter of nanoparticles (nm)
h	Inter particle spacing
k	Thermal conductivity (W/m K)
m	Mass (kg)
n	Shape factor

r	Radius of particle (nm)
T	Temperature (K)
T_0	Initial temperate (K)
Vol.	Volume concentration of nanoparticles (%)

Greek Symbols

φ	Volume concentration (%)
ρ	Density (kg/m ³)
μ	Viscosity (mPas)
β	Ratio of nanolayer thickness (nm)
α	Empirical constants

Dimensionless numbers

Re	Reynolds number
Pr	Prandtl number

Subscripts

np	Nanoparticle
nf	Nanofluid
bf	Base fluid

LIST OF APPENDICES

APPENDIX A:	CHEMICAL ELEMENTS COMPOSITION OF NANOPARTICLES.....	87
APPENDIX B:	NANOPARTICLES SIZE MEASUREMENT.....	91
APPENDIX C:	VOLUME DISTRIBUTION WITHIN THE NANOFLUIDS	93

CHAPTER 1 : INTRODUCTION

1.1 Background

Heat transfer plays an important role in industrial process, where heat must be efficiently managed by adding, removing or moving into the system. Heat transfer fluids such as water, ethylene glycol (EG), pumping oil, etc., have reached their limits for cooling applications in the modern high performance devices due to their poor thermal performance. It has been proved that adding solid particles to these conventional fluids could enhance their thermal performance. However, the large size of particles in the scale of milli or even micro-sized particle (Philip & Shima, 2014) suspension showed insufficient enhancement for high-tech applications due to several technical problems (Krishnamurthy et al., 2006) like slugging, faster settling time, abrasion of the surface, erosion of the pipelines and increasing pressure drop. Therefore, researchers are looking for highly efficient heat transfer fluids to solve the drawbacks of traditional fluids in the cooling performance. However, from the last decade, Nanoscience and Nanotechnology have offered nanofluids (NFs), which showed advancements of its thermophysical properties as well as enhanced heat transfer performance of diverse field of modern high-tech applications.

Nanofluids are defined as a colloidal suspension of solid nanoparticles with the size of less than 100 nm dispersed in a conventional fluids and the solid particle concentration of lower than 5 vol%. For the first time, Choi and Eastman (1995) at Argonne National Laboratory in the USA coined the term nanofluids for fluids with suspended nanoparticles. Nanofluids apply in different areas such as biomedical applications, lubrication, surface coating, heat exchangers, automotive industry, power generation, solar industry and petroleum industry (Saidur et al., 2011). The importance of nano-sized particles and their benefits compared to micro particles has been investigated and it could be stated that nanoparticles possess (Das et al., 2003): (a) longer suspension time (more

stable), (b) much higher surface area, (c) larger surface area/volume ratio (1000 times larger), (d) higher thermal conductivity, (e) lower erosion and clogging, (f) lower demand for pumping power, (g) reduction in inventory of heat transfer fluid and (h) significant energy saving.

In order to evaluate the effectiveness of a nanofluid for heat transfer applications, it is necessary to identify the thermophysical properties such as thermal conductivity, viscosity, density, and specific heat of nanofluids. The thermophysical and transport properties of nanofluids are influenced by several factors, which affect the heat transfer coefficient as well as thermal performance of the system. The performance of nanofluids depends on base fluids, concentration of nanoparticles, temperature, particle size, stability of nanofluids, surfactants and pH of the base fluids (Beck et al., 2009; Duangthongsuk & Wongwises, 2009; Xia et al., 2014). In heat transfer, one of the most significant thermophysical properties of nanofluids, which is required to study in order to determine the capability of nanofluids for heat transfer applications. This property influences the Nusselt and Prandtl numbers, which are the most important parameters to know the heat transfer characteristics of a flowing fluid in a system (Aravind et al., 2011). The effectiveness of nanofluids depends on higher thermal conductivity for heat transfer applications.

However, only higher thermal conductivity is not sufficient for using nanofluids as a heat transfer fluid in the cooling applications. In order to choose the efficient nanofluids with optimal characteristics for cooling applications, it is also essential to know the viscosity of the nanofluids. Viscosity of nanofluids plays a critical role in all thermal applications due to the internal resistance of the fluid to flow. The viscosity of nanofluids is expected to be greater than their base fluids when nanoparticles are added. However, the enhancement of viscosity creates a negative effect on the pumping power and the heat transfer coefficient. For example, in the laminar flow regime, the pressure drop is directly

proportional to the viscosity (Herold & Rasooly, 2005). Further, Reynolds and Prandtl numbers are also affected by the viscosity of the fluids which affects the heat transfer coefficient (HTC). Thus, viscosity is as essential as thermal conductivity in all thermal systems.

The density of the nanofluids is directly proportional to the volume ratio of the nanoparticles in the base fluid. Moreover, the density of the nanoparticles is higher than that of the base fluids. Therefore, it is expected that the density of nanofluids increases with the dispersion of nanoparticles to the base fluid. Further, an extensive property named the specific heat of the nanofluid is considered in the calculation of heat transfer performance of a device. Generally, the solid nanoparticles have lower specific heat than water. Hence, the effective specific heat of the nanofluid decreases after the dispersion of nanoparticles in the pure water. Moreover, the specific heat is very much dependent on the volume fraction of the nanoparticle due to it decreases gradually with the increasing of the volume fraction. The methanol based nanofluids are a kind of heat transfer fluids used in different heat pipe, heat exchangers. Garner (1996) used copper–methanol heat pipes in application which operated below 0 °C. Electronics cooling is to present a few of the more common examples of demonstrate the heat pipe's application. Dink (1996) used methanol at metal hydride refrigeration system, as a working heat transfer medium for the low-temperature. Recently, Firouzfard et al. (2011) used silver–methanol nanofluid in thermosyphon heat exchanger of an air conditioning system to examine the energy savings compared to pure methanol. Therefore, methanol based nanofluids can potentially enhance the heat transfer rate of heat exchangers and save energy compared to pure methanol. Since then, some experiments have been going on about methanol nanofluids (Arab & Abbas, 2014; Lefèvre et al., 2012; Wong et al., 2012).

1.2 Importance of this study

The energy demand for human civilization is constantly rising which allows it to be one of the “Top Ten” global problems of humanity for next fifty years (Smalley, 2005). Commercial buildings and industries are using 20-50% of the total energy for heating, ventilation and air conditioning (HVAC) systems (Lombard et al., 2008). Heat exchangers are the essential part of HVAC systems and methanol based nanofluids are getting familiar to be used as the working fluid in the system. It is possible to make compact heat exchanger for air conditioning and refrigeration system with methanol based nanofluid due to its enhanced heat transfer capability. The amount of energy required to operate HVAC system can also be reduced by using methanol based nanofluid which is an additional advantage. Therefore, the energy consumption in commercial buildings and industries will decrease and thus the emission, greenhouse effect, and global warming potential will be reduced. However, investigation is required to ensure reliable and accurate performance by determining the fundamental properties such as thermal conductivity, viscosity, density, surface tensions, and heat capacity of methanol based nanofluids with different concentrations.

Few literatures are available on methanol based nanofluids regarding absorption of carbon dioxide (CO₂) in an integrated gasification combined cycle (IGCC) power plants (Lee et al., 2011; Jung et al., 2012; Pineda et al., 2012; Lee and Kang, 2013; Pineda et al., 2014). There are only two available literatures focusing on the enhancement of thermal conductivity (Pang et al., 2012) and (Pang et al., 2013) but the temperature effect was not investigated. Mathematical models of other fluids are being used by several researchers to calculate thermal conductivity (Maxwell model (1891), Hamilton and Crosser (HC) model (1962), etc.), viscosity (Einstein model (1906), Brinkman model (1952), etc.) of methanol based nanofluids. However, the existing models may not be appropriate for methanol based nanofluids as thermophysical properties of base fluids vary for different

fluids. Therefore, in order to analysis accurately the heat transfer, energy performance, lubricity, and so on, calculations using the values of obtained thermophysical properties of methanol based nanofluids are expected to be more appropriate.

1.3 Problem statement

Nanofluid is a very efficient heat transfer fluids due to its enhanced thermophysical properties. Methanol based nanofluids have been used as low temperature working fluids in different types of heat pipes like conventional, vapour-dynamic thermosyphons heat exchanger in HAVAC (heating, ventilation, and air conditioning) system, sorption, micro/miniature heat pipe at temperature range of 200-500K. Methanol is useful in gravity-aided, pool-boiling applications where water heat pipes would be subject to freezing (Dincer & Kanoglu, 2010). This study intends to investigate the thermophysical properties of methanol based nanofluids in order to implement the fluids in low temperature applications (i.e, electronics cooling, HVAC system, refregerator etc.). Specifically, the study seeks to answer:

- (a) What is significance of different type of nanoparticles on methanol based nanofluids preparation?
- (b) How does nanoparticles type and volume concentration affect the stability of nanofluids?
- (c) How does volume concentration and temperature affect thermophysical properties of nanofluids?

1.4 Objectives of this study

To be able to solve the state problems and to answer the research questions, the objectives of the study are considered as follows:

1. To formulate and characterize methanol based nanofluids using selected nanoparticles.
2. To assess the stability of methanol based nanofluids.

3. To determine and validate the thermophysical properties (e.g. thermal conductivity, viscosity and density) of nanofluids.

1.5 Outline of the thesis

This dissertation comprises five chapters. The contents of the individual chapters have been outlined as follows:

Chapter 1: This chapter starts with some background information about methanol based nanofluids as well as describing the importance, aim, objectives, and limitations of the dissertation.

Chapter 2: In this chapter, a review of the literature on preparation, characterization, thermophysical properties (e.g. thermal conductivity, viscosity, and density), and stability of methanol based nanofluids have been addressed.

Chapter 3: It describes the experimental set up, materials, procedures and equipment that have been used during preparation, characterization, and determination of thermophysical properties (e.g. thermal conductivity, viscosity, and density), and stability of methanol based nanofluids.

Chapter 4: This chapter analyzes the outcomes of preparation, characterization, thermophysical properties (e.g. thermal conductivity, viscosity, and density), and stability of methanol based nanofluids.

Chapter 5: This is the last chapter and wraps up the dissertation with some concluding remarks and recommendations for future work.

CHAPTER 2 : LITERATURE REVIEW

2.1 Introduction

The chapter contains an overview of other related studies, their approach development and significance to this study in order to set up the objectives. Study has been conducted through a sound collection related to PhD and Master thesis, journal articles, reports, conference papers, internet sources, and books. It is noteworthy that about 80–90% of the journal papers collected from most relevant and prestigious peer reviewed international referred journals such as International Journal of Refrigeration, International Journal of Heat and Mass Transfer, Applied Thermal Engineering, Energy and Buildings, Energy Conversion and Management, Renewable and Sustainable Energy Reviews, Journal of Nanoparticle Research, International Journal of Thermal Science, etc. Moreover, the substantial amount of relevant information has been collected through personal contact with the key researchers around the world in this research area.

2.2 Nanofluids

Modern technologies are able to produce metallic or non-metallic type of particles. Nanomaterials have its unique properties such as mechanical, electrical, optical, magnetic and thermal properties.

The term “nanofluid” was first introduced by Choi (1995) to describe a colloidal mixture of nanoparticle with size from 1 to 100 nm and a base fluid such as water, oil and ethylene glycol. Nanofluid technology is the new technology where nanoscience, nanotechnology and thermal engineering are directly involved. The main objective of using nanofluid in any purposes is to get maximum possible thermal properties with using minimum possible volume concentrations.

2.2.1 Preparation of nanofluids

Preparation of nanofluid is considered one of the most important steps for improving the thermal conductivity of nanofluid. Generally, there are two methods to prepare nanofluid such as one step method and two step method. However, preparing nanofluid using second step method is easier than one step method.

2.2.1.1 One step method

A simultaneous process of nanoparticle generation and dispersion in a specific fluid is called one step method. This process is able to produce uniformly dispersed particles which make the nanofluid stable. Generally, two methods are involved in preparing nanofluid under these techniques: Physical vapour deposition method and chemical reduction technique.

Single step method is generally applied when metal nanofluid is prepared. However, the main drawback of using one step method is: fluids are incompatible with high vapour pressure and low concentration of nanofluid. This aforementioned draw back actually limits the uses of one step method.

One step method was initially used by few researchers. Zhu et al. (2004) scrutinized one step method involving chemical method to prepare ethylene glycol based Cu nanofluid by reducing copper sulphate penta hydrate with sodium hypophosphate under microwave irradiation. Liu et al. (2006) prepared water based Cu nanofluid through chemical reduction method. One step process forms of simultaneously making and dispersing particles into base fluid and in this process, the agglomeration can be reduced by avoiding the processes of drying, storage, transportation, and dispersion of nanoparticles. Uniformly dispersed nanoparticles can be prepared using one step method and it can be stably suspended into base fluid. Another method is also used to prepare nanofluid using dielectric liquids. The nanoparticles prepared here represent square, polygonal, needle-like and circular morphological shapes. It clearly thwarts the undesired particle from

aggregating. Synthesized nanofluids in large scale are not possible using one step method. Even is not cost-effective as well. However, the one-step chemical method is improving promptly.

2.2.1.2 Two-step method

This method is widely used in preparing nanofluid because it is an economical method. In this method, nanoparticles are suspended into base fluid such as water, engine oil, ethylene glycol etc. by means of external force. Scientist and researchers use two techniques to disperse tiny particles into base fluid which are: Physical technique and chemical technique.

For physical technique method, two types of stabilizing process such as mechanical and ultrasonic can be considered. One way for mechanical dispersion is to apply shear force to pull agglomeration. To create high shear force, high flow rate is required. This is why, a rotor along with a stator is attached to create high shear. This comprises homogenizer, high speed mixer, micro fluidizer and colloid mill. On the other hand, mechanical dispersion means high impact mixing. It uses higher energy to break the tightly bound aggregates apart or to shatter coherent solids into tiny pieces. To disperse particle or to exert an impact on the material, a grinding material of small particle size is used. Nowadays, the most widely used method to prepare nanofluid is Ultrasonication. It is a form of mechanical vibratory energy that disseminates through a liquid medium as elastic waves. The ultrasonic interactions within dispersion might be mechanical, thermal or chemical. The activator inside the ultrasonic machine converts the regular line frequency to a much higher level, which is eventually converted into mechanical vibrations in the tips of various shapes.

A conventional bath type sonication which normally gives less energy density than tip type one. Generally, the tip of the spindle is put into liquid where ultrasonic sonication creates cavitation and which stirs the dispersion or breaks the agglomerates. There are

two kinds of stabilization methods:- which are electrostatic dispersion and physical dispersion method. In electrostatic dispersion, electrostatic charges of sufficient amount are disseminated on the surface of the suspended particles to resist one another and remain in stable suspension. Besides, steric stabilization precludes nanoparticles from getting close enough to merge.

Together with basefluids and nanoparticles, additives are utilized to increase stability of nanofluids and to improve dispersion behavior of them. More common nanoparticles and basefluids exploited in synthesis would be tabulated as below (Li et al., 2009):

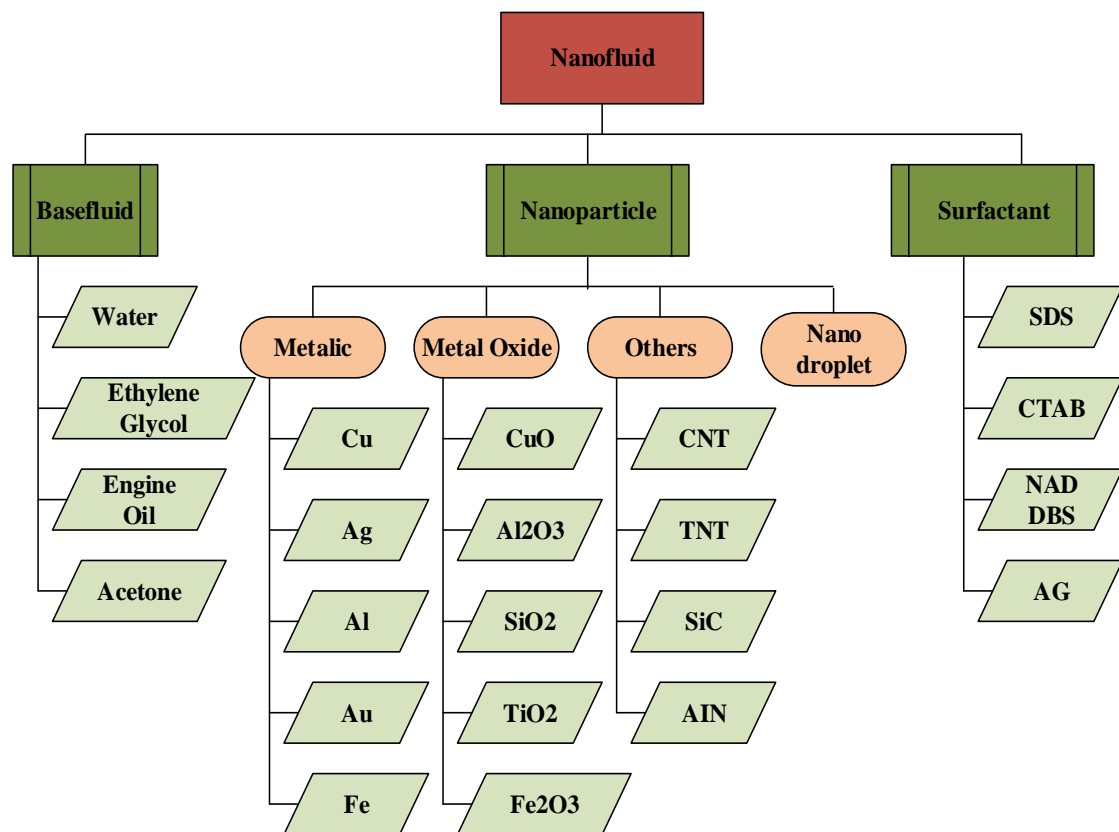


Figure 2.1: Common basefluids, nanoparticles, and surfactants for synthesizing nanofluid

Table 2.1 shows typical synthesis method used by researchers to prepare methanol based nanofluids. From the table it is clear that, researchers used two step method and ultrasonic vibration for proper mixtures. For methanol based nanofluids preparation used ultrasonic vibration for 60-120 min, electrical power 50-750 W and frequency 20 Hz to stabilize the nanofluids.

Table 2.1: Summary of methanol based nanofluids synthesis process that followed by the researchers

Reference	method	particle	Base fluid	Particle size (nm)	Volume fraction	Sonication time (min)	Power (W)	Frequ ency (Hz)
Firouzf ar et al. (2011)	Two-step	Ag	methanol	20	0.1	-	-	-
Kim et al. (2014)	Two-step	Al ₂ O ₃	methanol	40-50	0.001-0.01	60	350	20
Pang et al. (2012)	Two-step	Al ₂ O ₃ SiO ₂	methanol	40-50 10-20	0.005-0.5	120	750	20 @700 rpm
Pang et al. (2013)	Two-step	Al ₂ O ₃	Methanol + NaCl	40-50	0.01-0.1	60	750	20 @700 rpm
Pineda et al. (2012)	Two-step	Al ₂ O ₃ SiO ₂	methanol	40-50 10-20	0.005-0.1	60	-	-
Lee et al. (2011)	Two-step	Al ₂ O ₃ SiO ₂	methanol	40-50 10-20	0.005-0.05	60	750	20
Lee & Kang (2013)	Two-step	Al ₂ O ₃	NaCl aqueous solution	40-50	0.005-0.1	80	750	20
Jung et al. (2012)	Two-step	Al ₂ O ₃	methanol	40-50	0.005-0.1	60	50	20

2.3 Characterization of nanoparticles and nanofluids

X-Ray Diffraction (XRD), Scanning Electron Microscope (SEM) and Transmission Electron Microscope (TEM) are some well-known instruments that have been used to characterize the nanoparticles and nanofluids. Literature about characterization of methanol based nanofluid is limited however there are some studies have been done based on other fluids. However, now a days, these methods are widely used to measure the size and shape of nanoparticles. Throughout this study, both of these types of equipment have been used to measure the nanoparticles size, shape, and elemental composition.

2.3.1 XRD, SEM and TEM

The simplest and most widely used method is XRD for estimating the average nanoparticle grain size. Philip & Shima (2014) used XRD of Ag nanoparticles to characteristic peak match with the standard and the average crystallite size obtained from Debye-Scherrer formula. Figure 2.2 shows the XRD pattern of Ag nanoparticles.

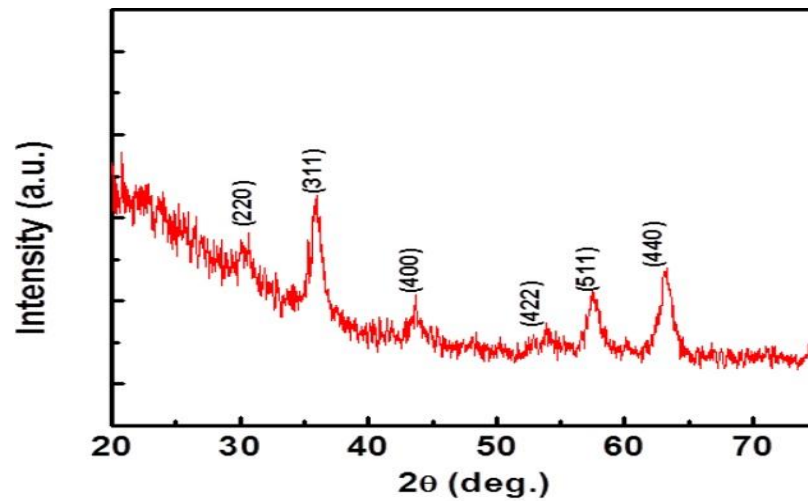


Figure 2.2: XRD pattern of Ag nanoparticles (Philip & Shima, 2014)

SEM and TEM are known as suitable tools for study and determination of microstructures. Shape, size and distribution of nanoparticles can be distinguished using them. Moreover, their aggregation which is related to stability of nanofluid could also be monitored (Yu et al., 2010). They are capable to capture photos in small sizes to reveal suspension situation of nanoparticles inside the fluid after preparation. There are some specialized electron microscopes like Cryogenic electron microscope (Cryo-TEM and Cryo-SEM) that can directly monitor the nanoparticles aggregation state in nanofluids (Wu et al., 2009). Figure 2.3 shows SEM and TEM image of Al_2O_3 -water nanofluids (Shukla et al., 2005).

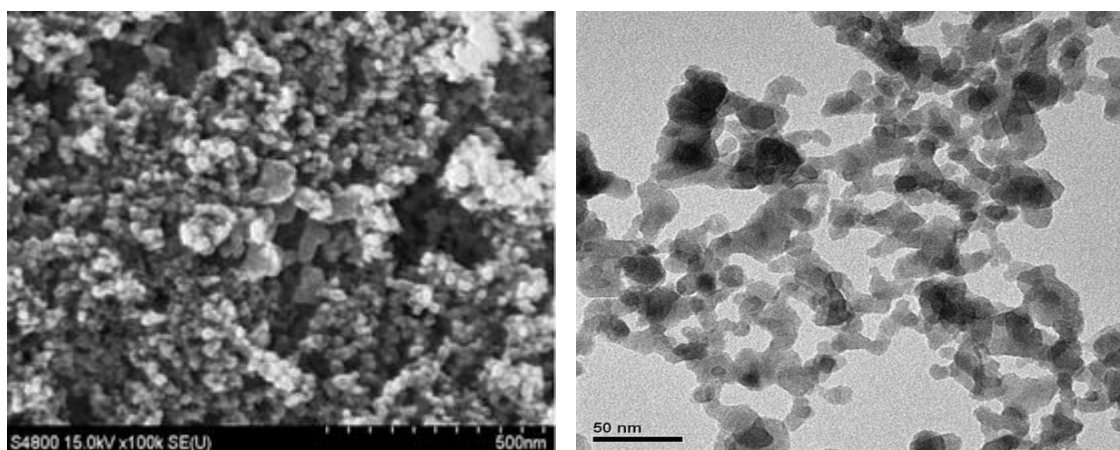


Figure 2.3: SEM (left) and TEM (right) image of Al_2O_3 -water nanofluids (Shukla et al., 2005)

2.4 Stability of nanofluids

Stability of nanofluids is an important phenomenon that needs to be characterized. If nanofluids are not stable, clogging, aggregation and sedimentation would be happened which declines the performance of suspensions via decreasing thermal conductivity and increasing viscosity. Some apparatus and procedures have been introduced in literature that can measure the comparative stability of nano-suspensions. UV-Visible spectrophotometer, Sediment photograph capturing, zeta potential and zetasizer are some well-known instruments those have been used to measure the relative stability of nanofluids

2.4.1 Sediment photograph capturing

This is a basic, easy and cheaper method to find out the sedimentation of suspensions. After the preparation of nanofluids, some percentages of the particles will be inside a test tube or bottle (the bottles need to be clear enough so that the fluid inside could easily be captured by camera). Usually, photos can be captured after certain period of time. From the captured photo, sedimentation of suspension can be compared. Peng et al. (2009) used this method to measure the stability of methanol based nanofluids. In this study, this sediment photograph capturing method has been successfully implemented.

2.4.2 UV-Visible spectrophotometer

Generally, UV–Visible spectrophotometer quantitatively illustrates the colloidal stability of nanofluids. A UV–Visible spectrophotometer exhibits that the light shows different intensity during the absorption and scattering of it during travelling through a fluid. Normally, the stability of nanofluid is determined by measuring the sediment volume versus the sediment time. Nevertheless, this method is not suitable for nanofluids with high concentration of particles. Particularly for the case of nanofluids with CNT nanoparticles, the dispersions are dark enough to distinguish the sediment visibly. For the first time, Jiang et al. (2003) investigated sedimentation estimation for nanofluids using

UV-Visible spectrophotometer. This method was used by Kim et al. (2007) and Lee et al. (2009). To the best of author's knowledge, there is no available literature for the evidence of using UV-Visible spectrophotometer to characterize stability of methanol based nanofluids. Furthermore, the author has used this method to characterize the methanol based nanofluids.

2.4.3 Zeta potential and Zetasizer

Stabilization theory (Kebinski et al., 2005) states that increasing zeta potential, scientific term for electro kinetic potential in colloidal system, results in high stability of the suspension. It is also well known that electrostatic repulsion between the particles would be increased in high absolute value of zeta potential (Yu et al., 2010). Stability of methanol based nanofluids has been inspected by Pang et al. (2012) using zeta potential test. Figure 2.4 shows the zeta potential of methanol based nanofluids as a function of volume fraction and it is clear that the zeta potential value increase with increasing volume fraction except 0.5 vol%. The zeta potential value of Al_2O_3 -methanol nanofluids is over 60 mV and for SiO_2 -methanol is over 30 mV. If the zeta potential value is over 30 mV the nanofluid considered that the fluid becomes stable (Lee et al., 2008).

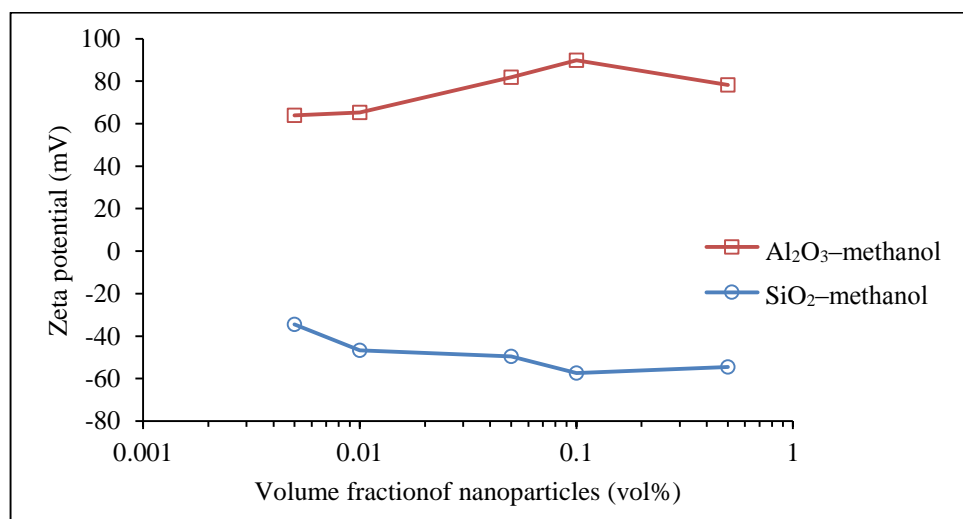


Figure 2.4: Zeta potential of methanol nanofluids as a function of nanoparticle volume fraction (Pang et al., 2012)

Vandsburger (MaïGa et al., 2004) tabulated different values of zeta potential in mV and stated stability situation of the suspension in any specific zeta potential value which can be observed from Table 2.2.

Table 2.2: Zeta potential absolute value and stability

Zeta potential [(Absolute value (mV))]	Stability
0	Little or no stability
15	Some stability but settling lightly
30	Moderate stability
45	Good stability, possible settling
60	Very good stability, little settling likely

Pang et al. (2012) declared that preparation of stable nanofluid would strongly depend on particle size. Moreover, base fluid and particle should be chosen in such a way that density difference of them would be kept as less as possible. Increasing viscosity of base fluid would be another way to increase stability of particle. Figure 2.5 demonstrates that the particle size of methanol based nanofluids as a function of volume fraction. From figure, it can be seen that the particle size of Al₂O₃-methanol keeps at a value range form 120-148 nm and the value from 280-410 nm for SiO₂-methanol nanofluids. In the nanofluids nanoparticle are contracted with each other and make a cluster and the cluster size is larger than the particle size.

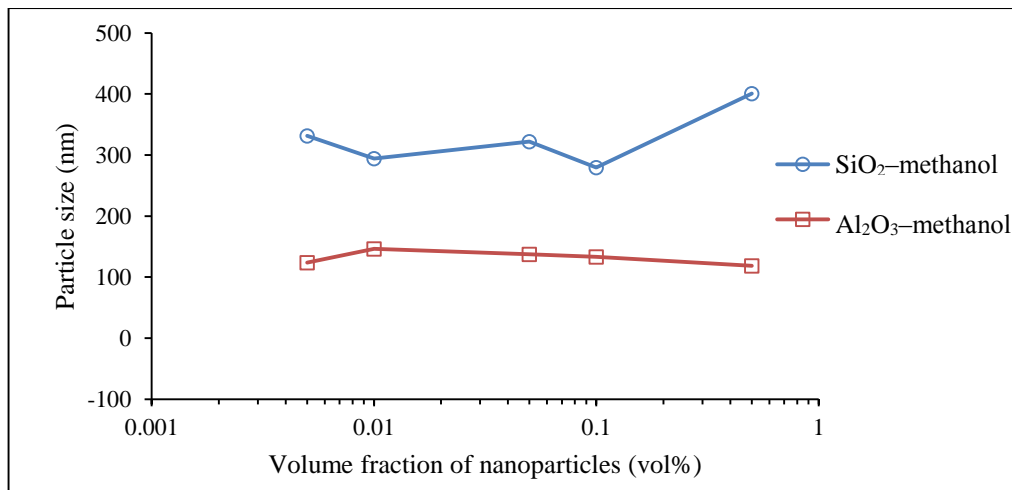


Figure 2.5: Particle size of methanol based nanofluids as a function of nanoparticle volume fraction (Pang et al., 2012)

2.5 Thermophysical properties of nanofluids

This section is divided into three subsections according to the methodology to measure thermal conductivity, viscosity, and density of methanol based nanofluids.

2.5.1 Thermal conductivity of nanofluids

The increment of thermal conductivity by nanofluids compare to the base fluids is one of the major issues which attracts researchers to practice on it. Measuring thermal conductivity is a challenge for a long time since different methods and techniques presented different results. On comparing the effect of nanofluid density and specific heat capacity, thermal conductivity and viscosity on heat transfer play key role in enhancing heat transfer. Therefore, it is important to understand the theoretical studies and experimental studies carried out on nanofluid thermal conductivity and viscosity.

2.5.1.1 Theoretical study on thermal conductivity

In 1873, an equation has been derived by Maxwell (1873) to calculate the effective thermal conductivity of solid-liquid mixtures consisting of spherical particles and showed its dependence on the temperature and pressure. Further, the idea of Maxwell has been utilized to develop the thermal conductivity models. These models are named as Classical models. Many researchers have modified the classical models by incorporating the mechanism for thermal conductivity enhancement such as Brownian

motion, clustering, and shape and size of nanoparticles. These models are named as models derived from classical models. Therefore, the nanofluid thermal conductivity models are classified into two main types: Classical models and Models derived from classical models. The gist of classical thermal conductivity models has been discussed here.

The prediction about the thermal conductivity of a continuum medium with well-dispersed solid-liquid mixtures has been made using the models given by Maxwell (1873), Hamilton-Crosser (HC) (1962), Bruggeman (1935) and Wasp et al. (1977) are the Classical models. For these classical models, some assumptions have been made on nanoparticles having no bulky movement in the basefluids as well as the solid particles are composite in the basefluids. The classical models considered the conduction is the mode for enhanced thermal conductivity. Therefore, classical models are named as static models or structural models. Table 2.3 lists out the classical models developed for determining the nanofluid thermal conductivity.

Table 2.3: List of Classical models for nanofluid thermal conductivity

Researchers	Thermal conductivity model	Factors considered
Maxwell (1873)	$\frac{k_{nf}}{k_{bf}} = \left[\frac{k_{np} + 2k_{bf} + 2\phi(k_{bf} - k_{np})}{k_{np} + 2k_{bf} - \phi(k_{bf} - k_{np})} \right]$	Based on effective Medium theory [EMT], randomly dispersed, and uniform sized spherical particles.
Hamilton – Crosser (HC model) (1962)	$\frac{k_{nf}}{k_{bf}} = \left[\frac{k_{np} + (n-1)k_{bf} - (n-1)\phi(k_{bf} - k_{np})}{k_{np} + (n-1)k_{bf} + \phi(k_{bf} - k_{np})} \right]$	Applicable for spherical and cylindrical particles. Developed by using shape factor, n.
Bruggeman model (1935)	$k_{nf} = \frac{1}{4}[(3\phi-1)k_{np} + (2-3\phi)k_{bf}] + \frac{k_{bf}}{4}\sqrt{\Delta}$ $\Delta = \left[(3\phi-1)\left(\frac{k_{np}}{k_{bf}}\right)^2 + (2-3\phi)^2 + 2(2+9\phi-9\phi^2)\frac{k_{np}}{k_{bf}} \right]$	For a binary mixture of homogeneous spherical and randomly dispersed nanoparticles. Particles interaction taken into account. No limitations for particle volume concentration.

Table 2.3 continued

Researchers	Thermal conductivity model	Factors considered
Wasp model (197)	$\frac{k_{nf}}{k_{bf}} = \left[\frac{k_{np} + 2k_{bf} - 2\phi(k_{bf} - k_{np})}{k_{np} + 2k_{bf} + \phi(k_{bf} - k_{np})} \right]$	Considered shape factor as unity. Not valid for spherical particles.

According to the literature, the prediction cannot be made upon the thermal conductivity of nanofluids by using these classical models. The main reasons behind it exhibit that the effect of temperature and particle size, interfacial layer between particle/fluids, particle distribution and cluster, aggregate and Brownian motion of particles were not considered in the classical models. Consecutively, the thermal conductivity models have been developed by considering the factors which were not considered by Classical models. Few of the thermal conductivity models developed by the researchers have been given in the forthcoming section. Table 2.4 lists out few of the widely used models proposed by modifying the classical models for determining the nanofluid thermal conductivity.

Table 2.4: List of nanofluid thermal conductivity models derived from Classical models

Researchers	Thermal conductivity model	Factors considered
Pak and Cho (1998)	$\frac{k_{nf}}{k_{bf}} = 1 + 7.47\phi$	Under the assumption that the dispersion of suspended nanoparticles cause the enhancement of thermal conductivity.
Yu and Choi (2003)	$\frac{k_{nf}}{k_{bf}} = \frac{k_{np} + 2k_{bf} + 2\phi(k_{np} - k_{nf})(1 + \beta)}{K_{np} + 2k_{nf} - \phi(k_{np} - k_{bf})(1 + \beta)^3}$	Inclusion of interfacial layer and modified Maxwell model
Bhattacharya et al. (2004)	$\frac{k_{nf}}{k_{bf}} = \phi k_{np} + (1 - \phi)k_{bf}$	Inclusion of combined base fluids and nanoparticle thermal conductivities.
Shukla and Dhir (2005)	$\frac{k_{nf}}{k_{bf}} = \left[\frac{k_{np} + 2k_f + 2\phi(k_{np} - k_{bf})}{k_{np} + 2k_f - \phi(k_{np} - k_{bf})} \right] + \frac{C\phi(T - T_o)}{\mu k a^4}$	Based on macroscopic model, Brownian motion and set the lower limit for brown motion.

Table 2.4 continued

Researchers	Thermal conductivity model	Factors considered
Li and Peterson (2006)	$\frac{k_{nf}}{k_{bf}} = 1 + 0.764481\phi + 0.01868867T - 0.4621417$ $\frac{k_{nf}}{k_{bf}} = 1 + 3.6108\phi + 0.01924T - 0.303734$	Temperature dependent model and valid for 27 °C -36°C and valid for Al ₂ O ₃ /water, CuO/water and nanofluids
Timofeeva et al. (2007)	$\frac{k_{nf}}{k_{bf}} = 1 + 3\phi$	Based on effective medium theory for Al ₂ O ₃ nanofluids with the effect of agglomeration.
Chandrasekar et al. (2009)	$\frac{k_{nf}}{k_{bf}} = \left[\frac{k_{np} + (n-1)k_f + (n-1)(1+\beta)^3\phi(k_{np} - k_{bf})}{k_{np} + (n-1)k_f - (1+\beta)^3\phi(k_{np} - k_{bf})} \right]$ $+ \frac{C\phi(T - T_o)}{\mu k a^4}$	Developed by macroscopic model of HC and inclusion of Brownian motion with respect to temperature.
Chandrasekar et al. (2010)	$\frac{k_{nf}}{k_{bf}} = \left[\frac{c_{p,nf}}{c_p} \right]^{-0.023} \left[\frac{\rho_{nf}}{\rho} \right]^{1.35} \left[\frac{M}{M_{nf}} \right]^{0.126}$	Based on the prediction of thermal conductivity of water and the molecular weight of nanoparticle and base fluids.
abbaspoursani et al. (2011)	$\frac{k_{nf}}{k_{bf}} = 1 + m \frac{\phi^\alpha}{(d_{np})^\beta} \left(\frac{T}{T_e} \right)^\delta + R' + R'' + \dots$	Accounts for the interfacial shell, Brownian motion, and aggregation of particles.
Shames et al. (2012)	$\frac{k_{nf}}{k_{bf}} = k_{static} + k_{dynamic}$	By assuming the nanoparticles are st different sizes. Considered the effect of nanolayer.
Mallick et al. (2013)	$\frac{k_{nf}}{k_{bf}} = 0.35\phi^{0.035} Pr_{np}^{0.34} Pr_{bf}^{-0.38} \left(\frac{Re_{np}}{\sqrt{N_{BRnp}}} \right)^{-0.017}$	By employing Prandtl, Reynolds, Brinkman numbers, effects of micro-convection, localized turbulence.

2.5.1.2 Experimental study on thermal conductivity

Many experimental works have been carried out to measure the thermal conductivity. This is because the predicted thermal conductivity results are not consistent for a particular nanofluid. Most of the investigators used Transient Hot Wire (THW) technique to measure the thermal conductivity of nanofluids. Table 2.5 lists out few of the widely referred experimental results of nanofluid thermal conductivity.

Table 2.5: List of experimental studies on nanofluid thermal conductivity

Investigators	Nanoparticles/Base fluids	Particle Volume concentration (%)	Maximum thermal conductivity enhancement (%)	Consideration
Masuda et al. (1993)	Al ₂ O ₃ / Water	1.30–4.30	32.4	31.85°C – 86.85°C
	TiO ₂ /Water	3.10–4.30	10.8	
Lee et al. (1999)	Al ₂ O ₃ /Water	1.00–4.30	10	Room Temperature
	Al ₂ O ₃ / EG	1.00–5.00	18	
	TiO ₂ /Water	0.50–5.00	33	
Xie et al. (2002)	Al ₂ O ₃ /Water/ EG	5.00	23	Room Temperature
	Al ₂ O ₃ / EG	5.00	29	
Das et al. (2003)	Al ₂ O ₃ /Water	1.00–4.00	38.4	24 °C-36 °C
Li and Peterson (2006)	Al ₂ O ₃ /Water	2.00–10.00	29	27.5°C – 34.7°C
Beck et al. (2009)	Al ₂ O ₃ /Water	1.86–4.00	20	Effect of particle size
	Al ₂ O ₃ / EG	2.00–3.01	19	
Mintsa et al. (2009)	Al ₂ O ₃ /Water	0–8	31	20°C – 48°C
Turgut et al. (2009)	TiO ₂ /Water	0.2–3.0	7.4	13°C – 55°C
Chandrasekar et al. (2010)	Al ₂ O ₃ /Water	0.33-5	24	Effect of particle volume fraction
Vajjha and Das, (2009)	Al ₂ O ₃ /Water	1–4	2-16	1 to 40°C
Pang et al. (2012)	Al ₂ O ₃ /methanol	0.005-0.5	10.74	20 °C
	SiO ₂ /methanol		14.29	
Pang et al. (2013)	Al ₂ O ₃ /methanol/NaCl	10wt% NaCl, 40 vol% methanol and 0.1 vol%	6.34	20 °C

However, the authors noted that higher temperatures shows significant discrepancy during thermal conductivity measurements. Natural convection effect in the transient hot-wires method is the main cause of this discrepancy. Ju et al. (2008) showed that the transient hot-wire method can give erroneous results if the measurements are carried out

just after the sonication. This is because the sonication increases temperature of the nanofluid sample. Due to the above mentioned factor, almost same results were found during the thermal conductivity measurement by (Li et al., 2008) and (Ju et al., 2008). Another important reason for discrepancy in experimental data is the clustering of nanoparticles (Hong et al., 2006). There are several parameters on which the level of clustering is dependent. To increase the dispersion and stability along with preventing clustering to some extent, some surfactants can be added as well as the adjustment should be done for the pH value of the nanofluids (Wang et al. 2009). Hence, during experiments, the type as well as the amount of the additives along with the pH value of the samples should be considered.

Many researchers have revealed the factors which increase or decrease the thermal conductivity of nanofluids. Some of the investigations and suggested factors have been discussed in this section. The major factors which affect the nanofluid thermal conductivity are a) Particle volume concentration, b) Particle materials, c) Brownian Motion, d) Nanoparticle size, e) Particle shape/surface area, f) Temperature, g) Basefluid materials, and h) pH value. The summary of important conclusions on nanofluid thermal conductivity proposed by the researchers are: a) the thermal conductivity increases with increasing particle volume concentration, b) the thermal conductivity enhancement of metal nanoparticles is higher than the oxide nanoparticles, c) higher the Brownian motion the higher thermal conductivity enhancement, d) smaller nanoparticles are better for stability and enhancement of thermal conductivity, e) the rod-shaped particles thermal conductivity is higher than the spherical nanoparticles, f) the thermal conductivity increases with increasing temperature g) the nanofluid with water and ethylene glycol mixture have good potential applications in cooling applications, and h) pH value affects the thermal conductivity.

2.5.1.2.(a) Effect of volume fraction on thermal conductivity of nanofluids

It is well known that the thermal conductivity increases with increasing the volume fraction of nano particle. Figure 2.6 shows that thermal conductivity increases with the enhancement of volume fraction. From the figure it is seen that, in most cases experimental thermal conductivity increases abruptly (Murshed et al., 2008; Pang et al., 2012).

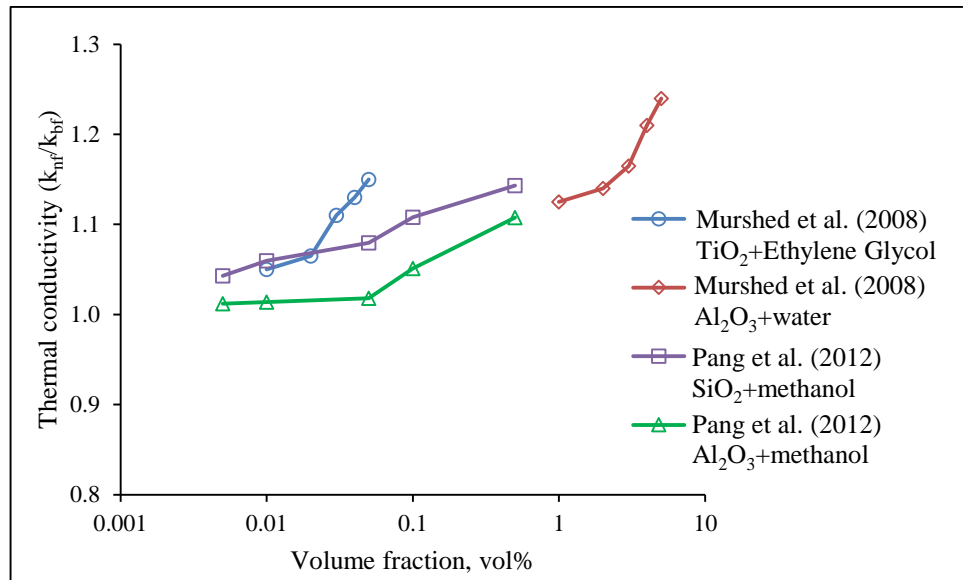


Figure 2.6: Thermal conductivity versus particle volume fraction

2.5.1.2.(b) Influence of temperature on thermal conductivity of nanofluids

Besides, it is found that the thermal conductivity increases accordingly with the temperature of the nanofluids. This would be a good reason to apply nanofluids in heat exchangers. Figure 2.7 shows that thermal conductivity augmented accordingly with the increase of temperatures.

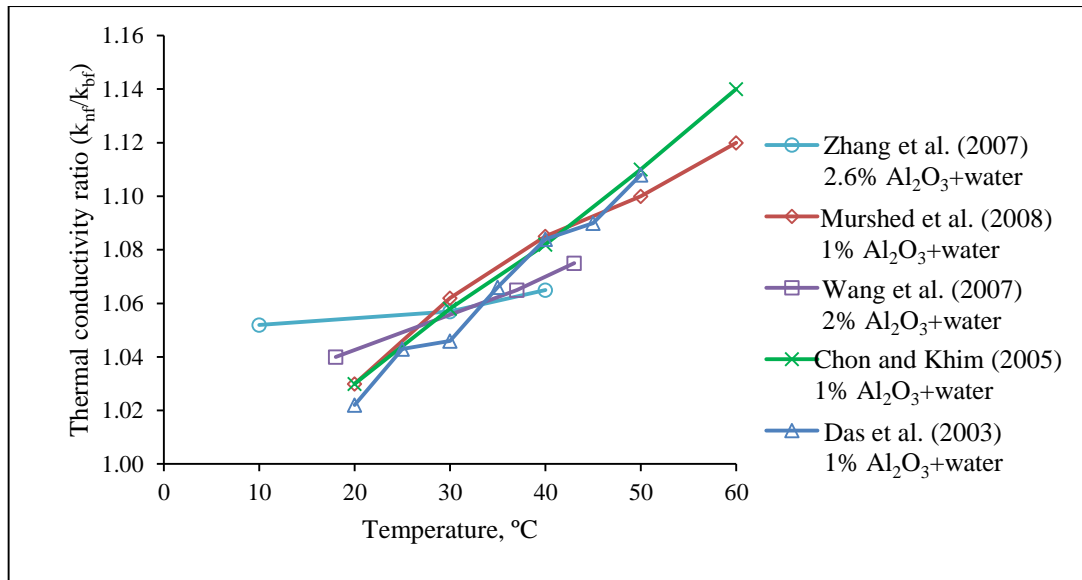


Figure 2.7: Thermal conductivity versus temperature

2.5.2 Viscosity of nanofluids

Considering the practical application, viscosity is one of the important parameters of nanofluids like thermal conductivity. Pressure drop and pumping power in forced convection are the major two problems which are caused by viscosity. Thus from application point of view, ideal nanofluid should not only possess high thermal conductivity but also should have low viscosity. It is suggested that, the particle volume concentration, particle size, temperature, and extent of clustering have great effects on viscosity. Increasing particle volume fraction increases viscosity and this was validated by many studies like Wang et al. (1999), Murshed et al. (2008), Chen et al. (2009) and Chandrasekar et al. (2010). They have revealed the nanofluid viscosity is a function of particle volume concentration and increases with increasing particle volume concentration. They have also reported that the heat transfer increases when particle volume concentration is more and increases the pressure drop.

2.5.2.1 Theoretical study on viscosity

The nanofluid viscosity analytical models are classified into two main types: Classical models and, Models derived from Classical models. Einstein (1906), Krieger (1959), Nielson (1970) and Bachelor (1977) are the first personnel who developed the nanofluid

viscosity model. These models are based on the assumption of dilute, suspended, spherical particles and no interaction between the nanoparticles. These are valid only for relatively low particle volume concentration. This is the motivation for developing nanofluid viscosity model for higher particles volume concentration. Table 2.6 lists out the classical viscosity models proposed by different researchers.

Table 2.6: List of classical models for nanofluid viscosity

Researchers	Nanofluid viscosity model	Factors considered
Einstein (1906)	$\frac{\mu_{nf}}{\mu_{bf}} = 1 + 2.5\phi$	Valid for spherical particles of low particle volume fraction 0.02.
Krieger and Dougherty [K-D]model (1959)	$\frac{\mu_{nf}}{\mu_{bf}} = \left[1 - \frac{\phi_{np}}{\phi_m} \right]^{-\eta\phi_m}$	Based on randomly mono-dispersed spheres. Valid for maximum close packed particles of 0.64.
Nielson (1970)	$\frac{\mu_{nf}}{\mu_{bf}} = (1 + 1.5\phi_{np}) e^{\frac{\phi_{np}}{(1-\phi_m)}}$	Power law model and more appropriate for particle volume fraction more than 0.02.
Bachelor (1977)	$\frac{\mu_{nf}}{\mu_{bf}} = 1 + 2.5\phi + 6.5\phi^2$	Considered the effect of Brownian motion

Many nanofluid viscosity models have been developed by modifying the classical models by different investigators. Few of the widely used models have been listed in Table 2.7.

Table 2.7: List of nanofluid viscosity models derived from classical models

Researchers	Nanofluid viscosity model	Factors considered
Brinkman (1952)	$\frac{\mu_{nf}}{\mu_{bf}} = \frac{1}{(1-\phi)^{2.5}}$	Formulated by two corrections of Einstein's model.
Pak and Cho (1998)	$\frac{\mu_{nf}}{\mu_{bf}} = 1 + 39.11\phi + 533.9\phi^2$	Developed by taking the room temperature as reference.
Wang et al. (1999)	$\frac{\mu_{nf}}{\mu_{bf}} = 1 + 7.3\phi + 123\phi^2$	Particle volume fraction is the key factor for improved viscosity.
Tseng and Li (2003)	$\frac{\mu_{nf}}{\mu_{bf}} = 13.47e^{35.98\phi}$	Developed for TiO ₂ /water nanofluids
Maiga et al. (2004)	$\frac{\mu_{nf}}{\mu_{bf}} = 123\phi^2 + 7.3\phi + 1$	Derived for Al ₂ O ₃ /water nanofluids.

Table 2.7 continued

Researchers	Nanofluid viscosity model	Factors considered
Kulkarni et al. (2006)	$\ln(\mu_{nf}) = -(2.8751 + 53.548\phi - 107.12\phi^2) + (1078.3 + 15857\phi + 20587\phi^2) \left(\frac{1}{T}\right)$	Temperature dependent model and valid for 5°C-50°C.
Nguyen (2007)	$\frac{\mu_{nf}}{\mu_{bf}} = 2.125 - 0.0215T + 0.00027T^2$	Temperature dependent nanofluids viscosity model and valid for 1% - 4%.
Namburu et al. (2008)	$\text{Log}\mu_{nf} = Ae^{BT}$	Temperature dependent model. Valid for 1-10% of Al ₂ O ₃ nanofluids and -35°C to 50°C.
Chandrasekar et al. (2010)	$\frac{\mu_{nf}}{\mu_{bf}} = 1 + b \left(\frac{\phi}{1-\phi}\right)^n$	Contribution of electromagnetic aspects and mechanical –geometrical aspects taken into account.
Shanker et al. (2012)	$\text{Log}\mu_{nf} = \left(1.75 + 16.85\phi + 23.5 \frac{\phi^2}{d_{np}^2}\right) \exp\left(0.015 + 0.15\phi - 31.39\phi^2 + 5.65 \frac{\phi}{d_{np}}\right)$	Correlation developed by taking particle size, concentration, temperature. Valid for 0.0 < ϕ < 0.01 only

Based on the literature review, it is understood that the nanofluid viscosity increases when particle volume fraction is increased and nanofluid viscosity decreases when temperature is increased. The proposed mechanisms are subject to the conditions such as lower/higher particle volume fraction, lower/higher temperature, spherical/non spherical shape, below/above critical size, pH value, and type of base fluids etc. Moreover, the exact mechanism cannot be conceived until the optimum level of particle volume concentration, optimum size for achieving the stability and low agglomeration of nanoparticles. Because the higher particle loading results the more agglomeration and higher the particle size results erosion and easy settling.

Therefore, exact nanofluid analytical viscosity model is to be derived based on the desirable conditions like less agglomeration, low viscosity, without eroding tube wall surfaces, and without lowering thermal conductivity.

2.5.2.2 Experimental study on viscosity

The research groups Pak and Cho (1998), Das et al. (2003), Kulkarni et al. (2006), Liu et al. (2006), and Chandrasekar et al. (2010) experimentally measured the viscosity of different nanofluids. They have suggested that the experimental viscosity data is higher than the predicted viscosity. Nevertheless, the general trend is that the viscosity increases with increasing particle volume concentration. Nguyen et al. (2007) observed increasing viscosity with increasing particle size. Nguyen et al. (2007), and Longo & Zilio (2011) analyzed the effect of temperature on viscosity and observed a decrease in viscosity with increasing temperature.

The researchers have presented that the measured viscosity values slightly deviates from the calculated values. However, at present, it is difficult to obtain a consistent set of experimental data for nanofluids that covers a wide range of particle size and particle volume concentration. Table 2.8 lists out few of the widely referred experimental results of nanofluid viscosity.

Table 2.8: List of experimental studies on nanofluid viscosity

Researchers	Nanoparticles/Base fluids	Particle Volume concentration (%)	Maximum Viscosity increases (%)	Consideration
Masuda et al. (1993)	TiO ₂ /Water	1–4.3	11–60	31.85 °C – 86.85 °C
Wang et al. (1999)	Al ₂ O ₃ /EG	1.2–3.5	7–39	Room temperature
Prasher et al. (2006)	Al ₂ O ₃ /PG	0.5–3	7–29	various shear rates, temperature, nanoparticle diameter, and nanoparticle volume fraction
Chevalier et al. (2007)	SiO ₂ /Ethanol	1.2–5	15–95	Different particle sizes
Murshed et al. (2008a)	Al ₂ O ₃ /DIW	1–5	4–82	20–60 °C.
	TiO ₂ /DIW		24–86	
Nguyen et al. (2008; 2007)	Al ₂ O ₃ /Water	1–13	12–430	Up to 75 °C.
Chen et al. (2009b)	TiO ₂ /Water	0.25–1.2	3–11	20–60 °C

Table 2.8 continued

Researchers	Nanoparticles/Base fluids	Particle Volume concentration (%)	Maximum Viscosity increases (%)	Consideration
Duangthongsuk and Wongwises (2009)	TiO ₂ /Water	0.2 – 2	4 – 15	15 °C to 35 °C
Turgut et al. (2009)	TiO ₂ /Water	0.2 – 3	4 – 135	13 °C – 55 °C
Chandrasekar et al. (2010)	Al ₂ O ₃ /Water	1 – 5	14 – 136	Effect of particle volume fraction
Lee et al. (2011)	SiC/DW	0.001 – 3	1 – 102	pH of 11
Kim et al. (2014)	Al ₂ O ₃ /methanol	0.00– 0.010	11	20 °C

2.5.2.2.(a) Viscosity of nanofluids as a function of volume fraction

Most of the available literatures about viscosity of nanofluids show that viscosity of nanofluids increases accordingly with the augmentation of the volume concentrations. For example, for 12 volume concentration (%) of Al₂O₃ with water, viscosity increased 5.3 times (Nguyen et al., 2008), and for 12 volume concentration (%) of TiO₂ with water viscosity increased 1200 times (Tseng & Lin, 2003). Seemingly, viscosities of metal oxide based nanofluids have been broadly investigated and Al₂O₃ and TiO₂ related literatures are foremost among the accessible literatures on viscosity of nanofluids. The graphical representations of viscosity of nanofluids with Al₂O₃ and TiO₂ nanoparticles have been presented in Figure 2.8.

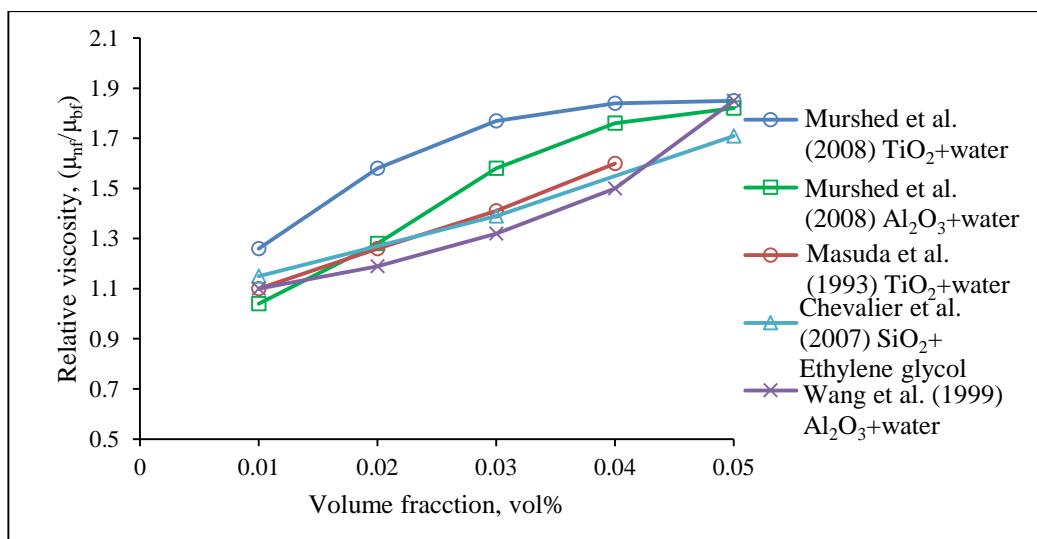


Figure 2.8: Viscosity increases with the increase of particle volume fraction

2.5.2.2.(b) Effect of temperature on viscosity of nanofluids

There are some literatures available on the effect of temperature over viscosity of nanofluids. Available literatures show, the researchers' agreement over the fact that, viscosity of nanofluid increases with the intensification of volume fraction. On the other hand, there are debates about the effect of temperature over viscosity of nanofluids. Most of the researchers showed that, viscosity of nanofluids decreases with the increase of temperature like the viscosity of most of the base fluids decreases with the increase of temperature. However, some of the researchers argued that, viscosity of nanofluids is independent of temperature (Prasher et al., 2006). Figure 2.9 shows viscosity of nanofluids decreases with the increase of temperature.

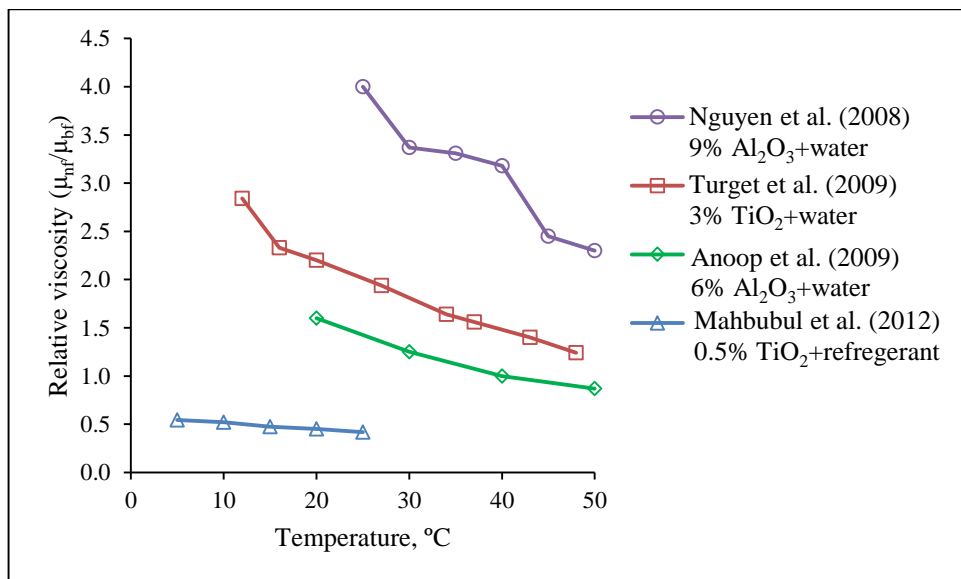


Figure 2.9: Viscosity increases with the increase of temperature

2.5.3 Density of nanofluids

Density of fluid is an important thermophysical property. Like viscosity, density of any fluid also has direct impact over pressure drop and pumping power. There are some literatures available about density of nanofluids. Still, there is no literature available on density of methanol based nanofluids. However, Sommers et al. (2010) observed a linear relationship between density and particle concentration for Al₂O₃–propanol nanofluid. Correspondingly, Teng et al. (2010) found that the density of alumina Al₂O₃–water

nanofluid increased with volume concentrations (0.5–1.5 wt %) and decreased with increase in temperature (10–40 °C). Elias et al. (2014) showed that the density of nanofluids increases with the rising of volume fraction. Ho et al. (2010) compared the measured and predicted density of nanofluid at a constant temperature and different volume fraction with mixing theory. Figure 2.10 shows the relationship among volume fraction and density of nanofluids.

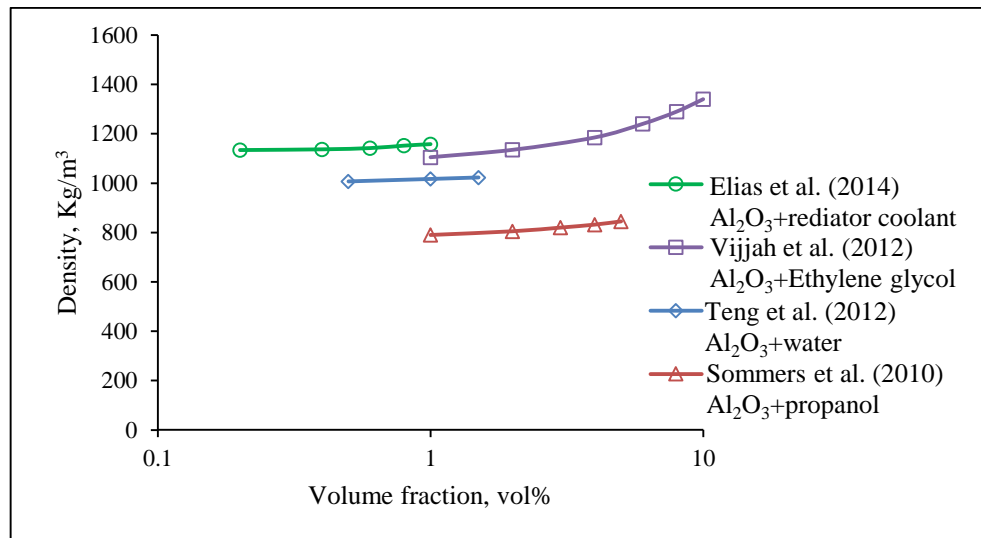


Figure 2.10: Density increases with the increase of particle volume fraction

Mariano et al. (2013) experimented the density of SnO₂-EG nanofluids at different temperature and pressure and described the nanofluids density characterization as, it increases with the increases of particle volume fraction and pressure however decreases in temperature. Figure 2.11 shows the density increases with the increase of temperature.

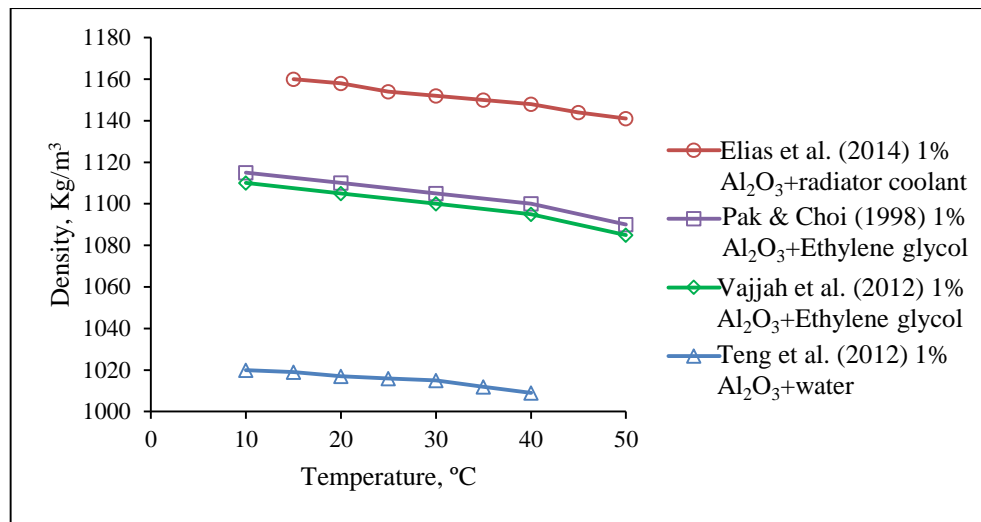


Figure 2.11: Density increases with the increase of temperature

2.6 Summary of literature review

Most of the available literatures about methanol based nanofluids are about CO₂ absorption performance, thermal conductivity measurement and energy performance of HVAC system. This study has mainly focused on the analysis about preparation, characterization, stability, thermal conductivity, viscosity and density of methanol based nanofluids. The summary of available literature about methanol based nanofluids is shown in Table 2.9.

Table 2.9: Summary of the available literature about methanol based nanofluids

Reference	Nanofluids	Findings
Firouzfard et al. (2011)	CH ₃ OH-Ag	Energy saving around 8.8–31.5% for cooling and 18–100% for reheating the supply air stream in HVAC system.
Lee et al. (2011)	CH ₃ OH-SiO ₂ and Al ₂ O ₃	CO ₂ absorption rate enhanced up to 4.5% at 0.01 vol% of Al ₂ O ₃ /methanol at 20 °C, and 5.6% at 0.01 vol% of SiO ₂ /methanol at -20 °C
Jung et al. (2012)	CH ₃ OH-Al ₂ O ₃	CO ₂ absorption rate enhanced up to ~8.3% compare to pure methanol
Pineda et al. (2012)	CH ₃ OH-SiO ₂ and Al ₂ O ₃	CO ₂ maximum enhancement absorption rates of 9.4% and 9.7% for Al ₂ O ₃ and SiO ₂ particles (compare to pure methanol) respectively
Pang et al. (2012)	CH ₃ OH-SiO ₂ and Al ₂ O ₃	Thermal conductivity enhancement up to 10.74% and 14.29% at the volume fraction of 0.05% for Al ₂ O ₃ and SiO ₂ nanoparticles, respectively.
Pang et al. (2013)	CH ₃ OH+ NaCl aqueous solution + Al ₂ O ₃	Thermal conductivity enhancement up to 6.34% for 10 wt% NaCl, 40% vol% CH ₃ OH and 0.1% vol% particle concentration
Kim et al. (2014)	CH ₃ OH-Al ₂ O ₃	Mass transfer coefficient enhancement up to 26 % at 0.01 vol% compared with pure methanol

From the literature- it is evident that, there is very few study regarding methanol based nanofluids. Most of the studies about methanol based nanofluids and nanofluids have been done with metallic and nonmetallic oxide nanoparticles. Moreover, Al_2O_3 , SiO_2 and TiO_2 nanoparticles are most common and widely used in nanofluid. These oxides are comparatively chemically stable. These are cheap and readily available as they are produced industrially in large scale (Chen et al., 2007). Methanol is chosen as base fluid as the freezing temperature of methanol is very low as $-97\text{ }^\circ\text{C}$ in which temperature the water would be freezing (Dincer & Kanoglu, 2010). Thus, methanol as a base fluid is a very good choice for low temperature applications. The methanol also can be operated at higher temperature than boiling point ($64.7\text{ }^\circ\text{C}$, 1atm) and it enhanced the mass transfer (Kim et al., 2014). Therefore, these particles are used to analyze characterization, nanofluids preparation and measure thermophysical properties of methanol based nanofluids. To the best of authors' knowledge, there are only few literatures about thermal conductivity and no literature about viscosity and density of methanol based nanofluids. As there is lack of information regarding methanol based nanofluid, this study aims to minimize the gaps by preparing, characterizing, and analyzing thermal conductivity, viscosity, density, and stability of methanol based nanofluids.

CHAPTER 3 : METHODOLOGY

3.1 Introduction

The aim of this chapter is to designate the materials, equipment, experimental settings and to introduce various parameters that have been used to conduct the research. The equations used in this research are also familiarized. The subsequent sections start with description of the materials and their properties and brief information about the equipment used. The sections are followed by preparation methods, characterization processes, and the measuring procedure of thermophysical properties (e.g. thermal conductivity, viscosity, and density). Flowchart of the experimental steps is presented in Figure 3.1.

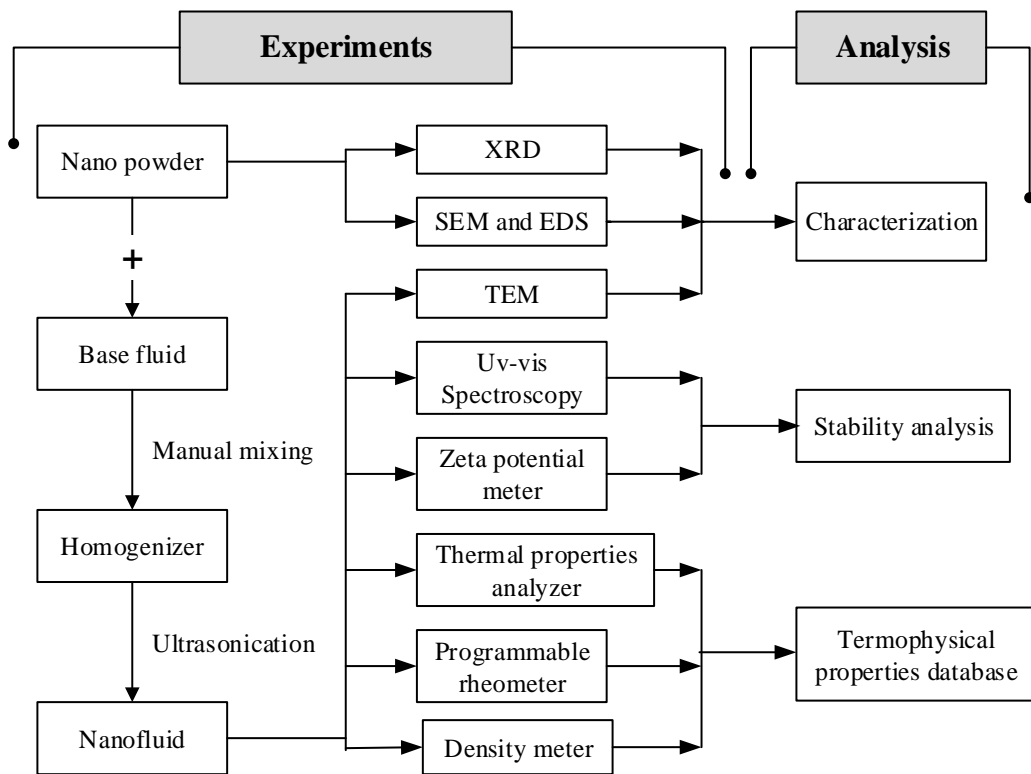


Figure 3.1: Flowchart of experimental analysis

3.2 Experimental setup

This section is divided into materials and equipment that were used throughout this study.

3.2.1 Materials

Three nanoparticles named Al_2O_3 , TiO_2 and SiO_2 have been used in this study for their availability in the market and the sizes of all particles were small enough to apply classical

approach for thermophysical properties analysis. Table 3.1 shows the properties of Al₂O₃, TiO₂ and SiO₂ nanoparticles. Each of the nanoparticles was purchased with different sizes. Manufacturer defined size for Al₂O₃, TiO₂, and SiO₂ are ~13nm, ~21nm and 5~15nm respectively with a purity of 99.5%. All nanoparticles were purchased readily from Sigma Aldrich (Malaysia).

Table 3.1: Properties of nanoparticles

Parameter	Al ₂ O ₃	SiO ₂	TiO ₂
Molecular mass (g/mol)	101.96	60.08	79.87
Average particle diameter (nm)	~13	5~15	~21
Purity (%)	99.5	99.5	99.5
Density (kg/m ³)	4000	2200	4260
Thermal conductivity (W/m K)	40.0	1.2	8.4

Methanol (CH₃OH) with purity of 99.9% was purchased from R & M Chemical and used as the base fluid. Table 3.2 shows the properties methanol at atmospheric pressure.

Table 3.2: Properties of Methanol

Parameter	Methanol (Methyl Alcohol)
Chemical formula	CH ₃ OH
Molecular mass (g/mol)	32.04
Purity (%)	99.8
Acidity (mlN%)	0.02
Alkalinity (mlN%)	0.01
Melting point (°C)	-97.6
Boiling point (°C)	64.7
Flash point (°C)	11-12
Vapor pressure (kPa)	13.02
Parameter	Methanol (Methyl Alcohol)
Density (kg/m ³)	791.8
Viscosity (mPas)	0.59
Thermal conductivity (W/m K)	0.2040

3.2.2 List of equipment

There is quite a lot of equipment used in this research. The equipment with manufacturer name, model number, their purpose and their accuracy are listed at Table 3.3.

Table 3.3: List of equipment used in experiment

Name	Manufacturer	Model	Purpose	Accuracy
Precision analytical balance	AND	GR-200	To measure nanoparticles weight	± 0.1 mg
Orbital shaker incubator	Hottech	718	To prepare nanofluid	
Sonics vibra cell	Madell		To uniformly and evenly distribute nanoparticles into nanofluid	
UV-Visible spectrophotometer	Perkin Elemer	Lambda 35	To characterize nanofluids	
Portable density meter	Kyoto	DA-130	To measure density	± 0.001 g/cm ³
Programmable rheometer	Brookfield	LVDV-III	To measure viscosity	$\pm 1\%$
Thermal properties analyzer	DECAGON	KD2-Pro	To measure thermal conductivity	± 0.01 W/(m·K)
Field Emission Scanning Electron Microscope (FESEM)	Zeiss	AURIGA	To analyze the particle size, shape, and composition	
Transmission Electron Microscope (TEM)	Zeiss	TEM LIBRA 120	To analyze the particle size, shape, and distribution	
Zetasizer	Malvern	ZS	To measure cluster size, distribution and zeta potential	
Refrigerated circulator bath	CPT Inc.	C-DRC 8	To control the temperature	$\pm 0.02^\circ\text{C}$
X-Ray Diffraction (XRD)	PANalytical	Empyrean	determination of crystallinity of a compound	
Scanning Electron Microscopy (SEM)	Phenom	Phenom ProX	To determine particle shape	
Energy dispersive spectrometry (EDS)	Phenom	Phenom ProX	determined elemental composition	

3.3 Preparation of methanol based nanofluids

The experimental procedure to prepare methanol based nanofluids includes the following steps: weighing the desired amount of nanoparticle and place them into a vessel; in the next step adding the required amount of methanol into that vessel. The nanoparticle volume concentration was calculated using Equation 3.1.

$$\text{Volume concentration, } \phi = \left(\frac{\frac{m_{np}}{\rho_{np}}}{\frac{m_{np}}{\rho_{np}} + \frac{m_{bf}}{\rho_{bf}}} \right) \quad (3.1)$$

Firstly, the nanoparticles were suspended into the base fluid (methanol) followed by shaking in the incubator for 30 min 150 rpm. The mixture was disseminated afterwards using an ultra-sonication homogenizer in order to distribute the nanoparticles evenly and homogeneously. The sonication process was maintained at frequency of 20 KHz with power equals to 500W and continued for 2h. Figure 3.2 shows the cluster size of 0.05vol% of Al₂O₃ concentration for different duration of ultrasonication time. The cluster size found to be decreased with longer duration of sonication time. However, a small change in the cluster size is observed after 100 min of total sonication time. Table 3.4 shows the experimental conditions of methanol based nanofluids.

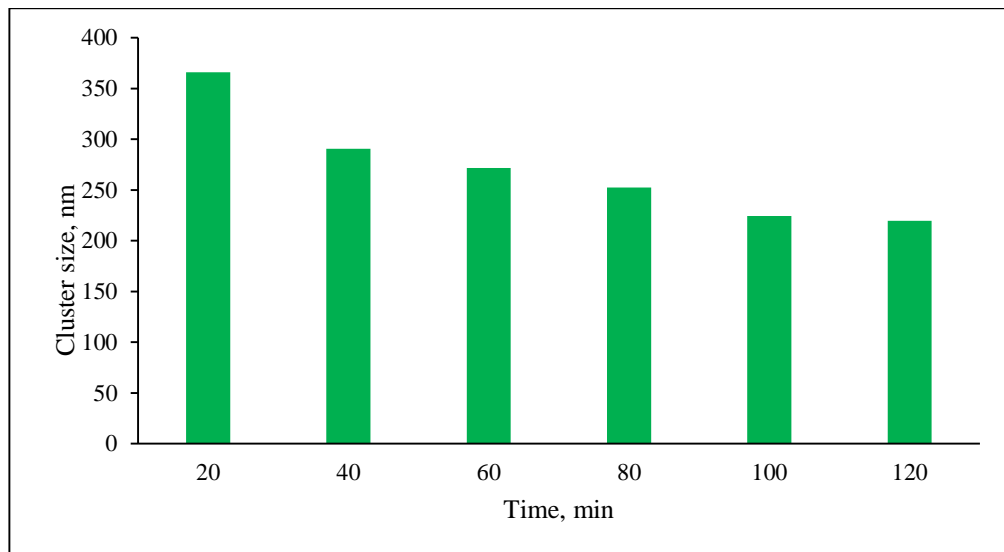


Figure 3.2: Cluster size at different ultrasonication time (0.05vol% of Al₂O₃ concentration)

Table 3.4: Experimental condition

Base fluid	Methanol		
Nanoparticle	Al ₂ O ₃	SiO ₂	TiO ₂
Nanoparticle size (nm)	~13	5~15	~21
Nanoparticle type	Spherical		
Volume concentration (vol%)	0.005, 0.01, 0.05, 0.10 and 0.15		
Shaking (@ 150rpm)	Time [min]	30	
Ultra-sonicator	Time [min]	120	
	Power [W]	500	
	Frequency [kHz]	20	
	Pulse [s]	2	
	Term [s]	2	

The limitation of preparing methanol based nanofluids by ultrasonication method is demonstrated at Figure 3.3. Figure 3.3 (a) shows the beaker is filled with 0.05 volume concentration (%) of Al₂O₃-methanol, just before starting the ultra-sonication process. From the figure it is obvious that, the level of liquid and solid mixture is 100 ml. Figure 3.3 (b) shows the level of mixture after 2h of ultra-sonication which is about 80 ml. Approximately, 20ml of the methanol evaporated with the vibration of ultrasonic amplitude. The same thing happened for SiO₂-methanol and TiO₂-methanol nanofluids. Therefore, temperature control is an important factor for preparation of methanol based nanofluids. In order to avoid evaporation, the temperature was maintained constant at 20 °C using a thermal refrigerated bath during ultrasonication for methanol based nanofluids preparation which is illustrated in Figure 3.4.



(a) Before ultrasonication



(b) After 2h ultrasonication

Figure 3.3: Effect of evaporation on ultrasonication duration of Al_2O_3 -methanol (0.05 vol%) nanofluids (a) before ultrasonication (b) after 2h ultrasonication



Figure 3.4: Using thermal bath to control temperature during ultrasonication time to prepare nanofluids

3.4 Characterization of nanoparticles and methanol based nanofluids

In order to apply nanofluids in practical situations, it is important to understand the behavior of nanoparticles and nanofluids prepared from fundamental point of view in order to apply nanofluids in practical situations. Therefore, the purchased dry

nanopowder and the prepared nanofluids have been characterized by using the following methods. X- Ray Diffraction (XRD), Scanning Electron Microscope (SEM) and Transmission Electron Microscope (TEM) to determine the particle shape, suspension uniformity, and Particle agglomeration.

3.4.1 Determination of particle shape, size and suspension uniformly

The nanopowder was characterized by (X Ray Diffraction) XRD with Empyrean Xray Differatometer and Cu-kal radiation in the range of 20–80°. The X-ray diffraction test was carried out with a scan speed of 3°/minute. The average grain size is estimated by using Debye-Scherrer (Patterson, 1939) equation (3.2). The full width at half maximum (FWHM) is taken from the XRD pattern.

$$d = \frac{k\lambda}{(FWHM)\cos\theta} \quad (3.2)$$

Nanoparticle shapes were measured with the Scanning Electron Microscope (SEM) with a Phenom ProX. Moreover, a LIBRA 120, Transmission Electron Microscope (TEM) manufactured by Zeiss, Germany was used to analyze the particle dispersion. TEM was used to check the particle size, shape, and distribution of 0.05 % particle volume concentration (%) of three solutions. All three combinations were based on methanol with three different nanoparticles. All the samples for TEM test were collected after 24 hours of preparation. A pin point sample of each solution was taken into the fluorescent screen. The solution evaporated naturally during the transfer, i.e. only the particles was in dry form.

3.5 Stability of methanol based nanofluids

This section is divided into three subsections according to the methodology to measure the stability of methanol based nanofluids.

3.5.1 Sediment photograph capturing

A Samsung digital camera was used to capture the photograph of methanol based nanofluids. Photos of all nanofluids prepared by an orbital incubator shaker and sonication were taken just after the preparation, and after seven (7) days to examine the sedimentation and to validate the preparation method. The prepared methanol based nanofluids were kept in closed glass bottle inside normal chamber of the domestic refrigerator at temperature below 20 °C to avoid evaporation.

3.5.2 UV-Visible spectrophotometer

In this investigation, the UV-Vis. spectrophotometer, Lambda 35 model, Perkin Elemer make, absorption range of 190 nm to 1100nm was used to study the stability of nanofluid. The inspection range is from 200 nm to 800nm. The U-V vis. spectrometer works under the principal of Beer –Lamberts law. Beer –Lamberts law relates that an absorbance of light and proportion of material through is passing. The lesser the suspended particles in the solution makes the light absorption lesser.

In this method, the first step is to find the peak absorbance of the dispersed nanoparticles at very dilute suspension by scanning. The relative stability measurement is followed by preparing the desired concentration of nanofluid and keep aside for a couple of days. Whenever it is needed to check the relative stability, the supernatant concentration is measured by UV–Vis spectrophotometer and the absorbance is plotted against wavelength.

3.5.3 Zeta potential and zetasizer

Zetasizer zs from Malvern was used to measure size distribution of nanoparticles in nanofluids with a nanometer to several microns using dynamic light scattering. The same zetasizer was also used to measure the zeta potential of nanofluids at different concentrations of all methanol nanofluids using electrophoretic light scattering. To

evaluate the stability of nanoparticles inside the base fluid, Stokes law, suggesting an equation for sedimentation velocity calculation of small spherical particles, states that:

$$v = \frac{r^2}{9\mu}(\rho_{np} - \rho_{bf}) \quad (3.3)$$

Buoyancy force, drag force and body force are acting on the suspended nanoparticles. Among these three forces, buoyancy and drag forces are acting upward and resisting against body force acting downwards resulting from gravitational attraction. As it was mentioned earlier, higher suspension time is desired in nanofluids. Therefore, some remedies can be offered extracting from Stokes law to improve the stability of nanofluids. In order to decrease sedimentation velocity as much as possible, radius of particles should be kept as small as possible. Since sedimentation velocity is proportional to square of radius, reducing size of nanoparticles will lessen it dramatically.

3.6 Thermophysical properties of methanol based nanofluids

This section is divided into three subsections according to the methodology to measure thermal conductivity, viscosity, and density of methanol based nanofluids.

3.6.1 Thermal conductivity measurement

The thermal conductivity measurement by steady-state methods is not suitable for liquids, because it needs a longer time and the heat loss during this period cannot be quantified, which may lead to large errors in results. Moreover, natural convection might take place during this period causing an additional error in the results. In this study, thermal conductivity was measured by using a KD₂ pro thermal conductivity meter (Made by Decagon, USA). This device measures thermal conductivity by transient hot wire method over the range of 0.02–2.00 W/m K. The accuracy of the equipment is ±0.001% for measurement within the mentioned range. Thermal conductivity of Al₂O₃–methanol, SiO₂–methanol and TiO₂–methanol at various volume fractions (0.005%, 0.01%, 0.05%, 0.1% and 0.15%) was measured at temperatures of 1, 5, 10, 15 and 20 °C, respectively.

All the data were recorded for three times and the corresponding average values were analyzed for result. Figure 3.5 shows the schematic diagram of KD₂ pro thermal properties analyzer. The measured values of methanol-based nanofluids were then compared with those obtained by the existing models. One of the most common models for the thermal conductivity measurement had been proposed by Hamilton and Crosser model (1962), Bruggeman model (1935), Wasp model (1999) and Patel et al. (2010).

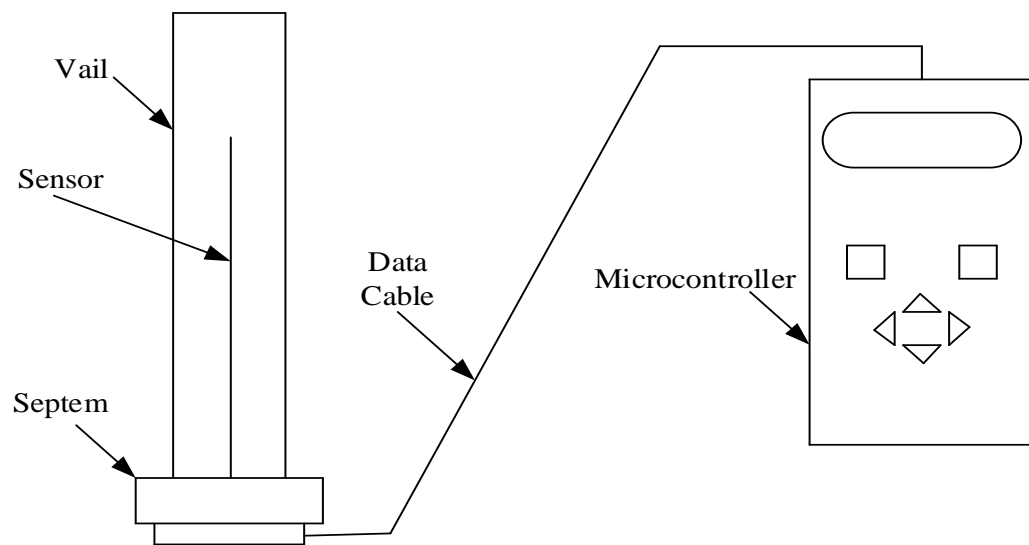


Figure 3.5: Schematic diagram of KD₂ pro thermal properties analyzer

A KD₂ pro thermal conductivity meter was calibrated using water and pure methanol at 1°C, 5°C, 10°C, 15°C and 20°C to compare the results with the reference data ("Thermophysical Properties - Methanol "). Figure 3.6 illustrates the comparison between the experimental values obtained in the current study with the existing literature data. The results show relatively acceptable consensus with the existing data. The uncertainties in the measurements of thermal conductivity are approximately 1.27% for DI water and 2.78% for pure methanol.

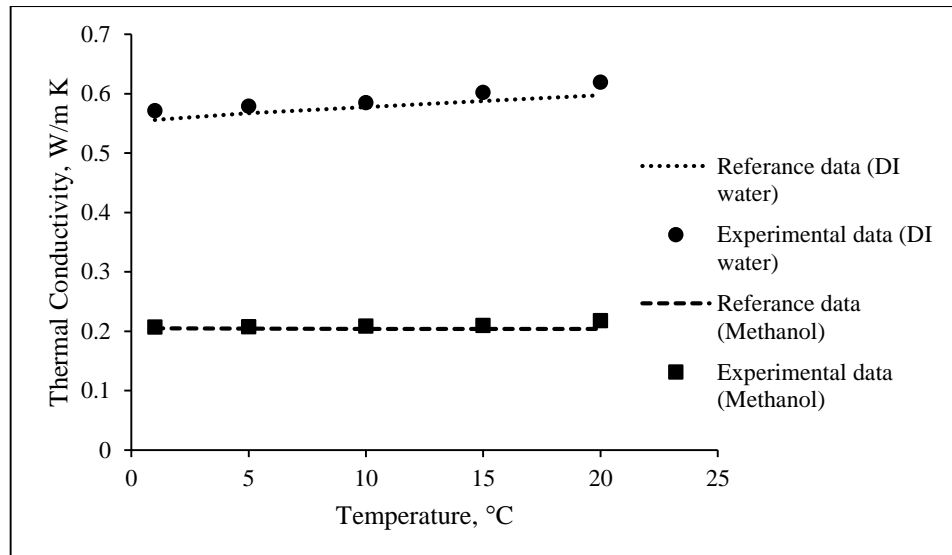


Figure 3.6: Thermal conductivity comparison with measured and reference data

3.6.2 Viscosity measurement

The viscosity of nanofluids was measured by the most widely used LVDV series-(LVDV II, LVDV III and LVDV III ultra-programmable) Viscometer. To measure the viscosity of low viscous fluids, these LV series are very suitable.

In this experiment, several parameters such as the viscosity and shear stress at different shear rates, volume fractions and temperatures were measured by Brookfield (LVDV III ultra-programmable) rheometer. In order to collect and store the measured data, a computer was connected with the viscometer. The spindle of the viscometer was submerged into the nanofluids. The viscous effect was developed against the spindle due to deflection of calibrated spring with the help of Ultra Low Adapter (ULA). The viscosity measurement range of this equipment is 0.1–6,000,000 mPa.s. In this experiment, the viscosity and shear stress data of all samples were measured within a shear rate range of 61.15s^{-1} while the spindle rotation was 60 rpm.

The viscosity of Al_2O_3 -methanol, SiO_2 -methanol and TiO_2 -methanol at various volume fractions (0.005%, 0.01%, 0.05%, 0.1% and 0.15%) was measured at temperatures of 1, 5, 10, 15 and 20 °C, respectively. All data were recorded for three times and the corresponding averaged values were plotted. The temperature was controlled by

connecting a refrigerated circulating bath to the ULA attached with the rheometer. The rheometer was connected with a computer where rheocalc 32 software had been installed to obtain the rheological data of methanol based nanofluids. Schematic diagram of the experimental set up is shown in Figure 3.7. After recording the all the data at least for three times, the corresponding averages are plotted. Then the measured value of viscosities for 0.01 to 0.15 vol.% of methanol based nanofluids at 20 °C were compared with the existing familiar models as well as some previous experimental studies Einstein, (1906), Brinkman (1952), Batchelor (1977) and Song et al. (2005).

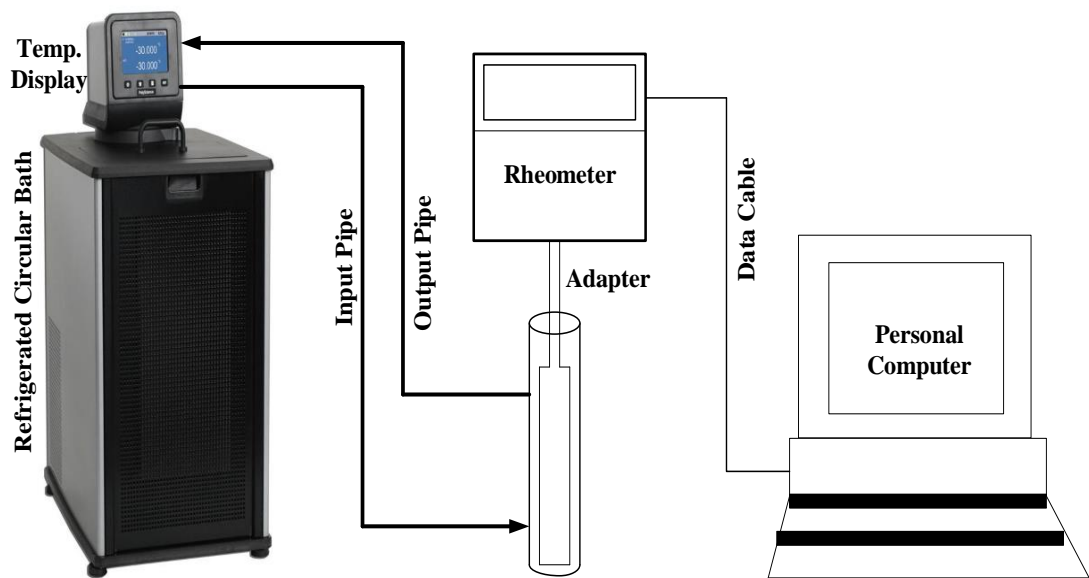


Figure 3.7: Schematic diagram of viscosity measurement

The viscosity of methanol was first measured to calibrate the experimental apparatus. The viscosity was measured at temperature 1, 5, 10, 15 and 20 °C and then compared with reference data ("Thermophysical Properties - Methanol "). Figure 3.8 shows the comparison between measured data obtained from experiment in this study with existing literature data. The results show relatively acceptable consensus with the existing data. The uncertainty in the measurement of viscosity is approximately 2.98%.

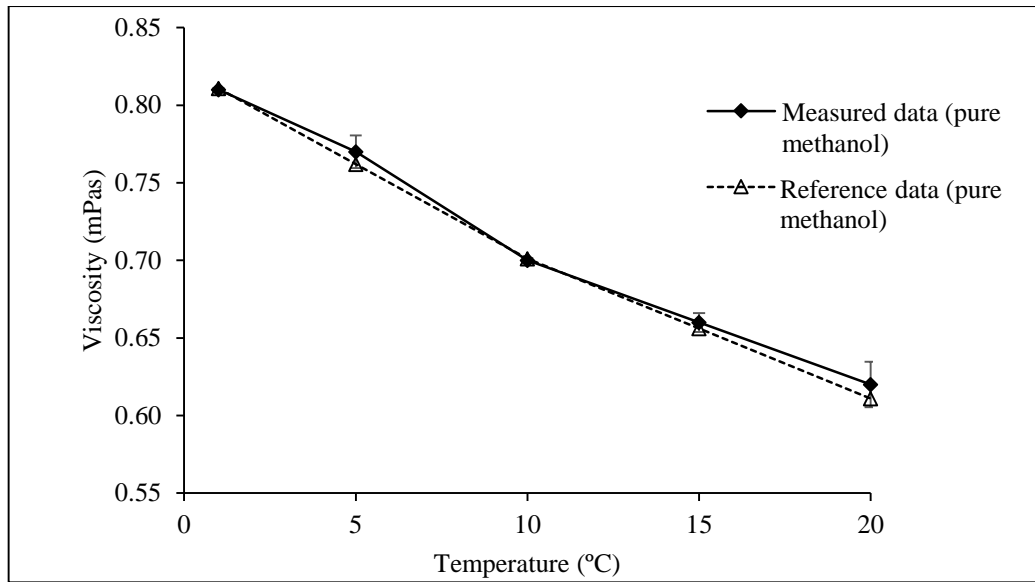


Figure 3.8: Viscosity comparison with measured and reference data

3.6.3 Density measurement

The density of methanol based nanofluids was measured by using a density meter, KEM-DA 130N (Kyoto, Japan). This device measures a density in a range of 0 to 2000 kg/m³. The accuracy of the equipment is $\pm 0.001\%$ kg/m³. The density was measured at different temperatures and volume concentrations in this study. All data were recorded for three times and the mean values were considered to be plotted against temperature. There are no experimental data available in the literature. Then the experimental results compared with equation (3.13).

$$\rho_{nf} = (1 - \varphi)\rho_{bf} + \rho_{np}\varphi \quad (3.13)$$

The density meter was calibrated using water and pure methanol at 1°C, 5°C, 10°C, 15°C and 20°C comparing the results with the reference data ("Thermophysical Properties - Methanol"). Figure 3.9 shows the comparison between the experimental values obtained in the current study with the existing data in literature. The results show relatively acceptable consensus with the existing data. The uncertainties in the measurements of density are approximately 3.30% for pure methanol.

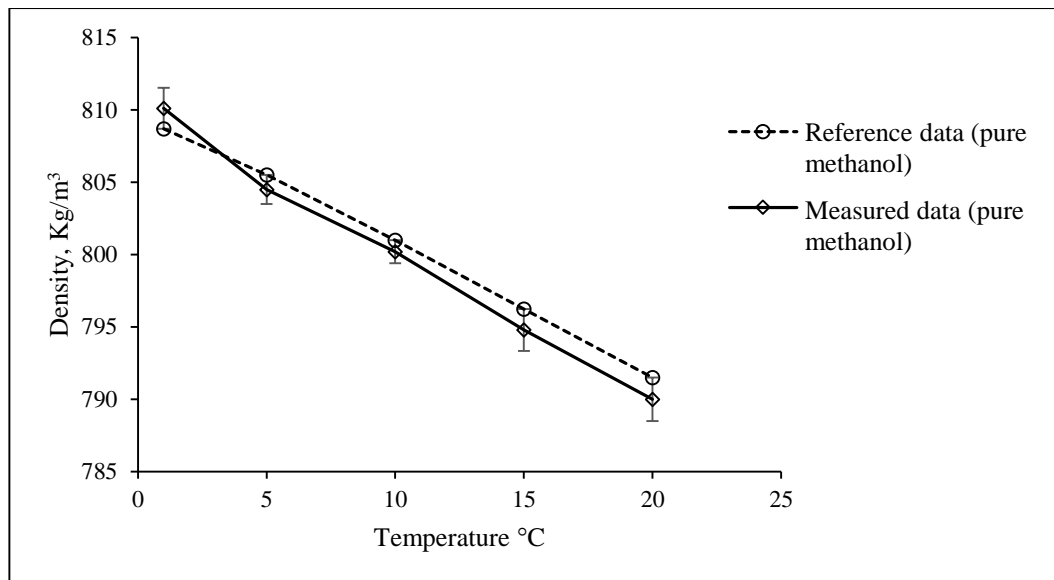


Figure 3.9: Density comparison with measured and reference data

CHAPTER 4 : RESULTS AND DISCUSSIONS

4.1 Introduction

This chapter focuses on the presentation of results of the experiments and analysis that were obtained based on the methodology described in Chapter Three. The data obtained throughout the investigation are interpreted and presented. This chapter is divided into three sections and several subsection based on the objectives of the study.

4.2 Characterization of nanoparticles and methanol based nanofluids

The results and discussions about characterization of nanoparticles and methanol based nanofluid section are divided into three subsections which are presented below.

4.2.1 X-ray Diffraction (XRD) image analysis

The characterization of Al_2O_3 , SiO_2 and TiO_2 nanoparticles was performed by XDR for phase identification, crystallite size and crystal structure determination. Figures 4.1, 4.2 and 4.3 show XRD pattern of Al_2O_3 , SiO_2 and TiO_2 nanoparticles respectively. The diffraction peaks of (302), (217), (317) and (442) have been indexed to tetragonal phase of Al_2O_3 nanoparticles shows in the Figure 4.1 which is the result match with Cava et al. (2007) results. The characteristic peaks match with the standard Joint Committee on Powder Diffraction Standards (JCPDS) card no. 00-047-1770. The average crystallite size obtained from the most intense peak of (302) by using Debye-Scherrer formula (equation 3.2) and is found to be ~11nm. Similarly, the diffraction peaks of (201), (020) and (231) have been indexed to anorthic phase for SiO_2 nanoparticle and (101), (103), (200), (211) and (220) have been indexed to tetragonal phase for TiO_2 nanoparticle. The characteristic peaks match with the JCPDS card no. 98-000-1440 and 03-065-5714 and the average particle size 5~15 nm and 20~25nm for SiO_2 and TiO_2 nanoparticles, respectively. The XRD pattern results ware match for SiO_2 and TiO_2 nanoparticles with (Murshed, 2005; "SiO₂ XRD pattern ").

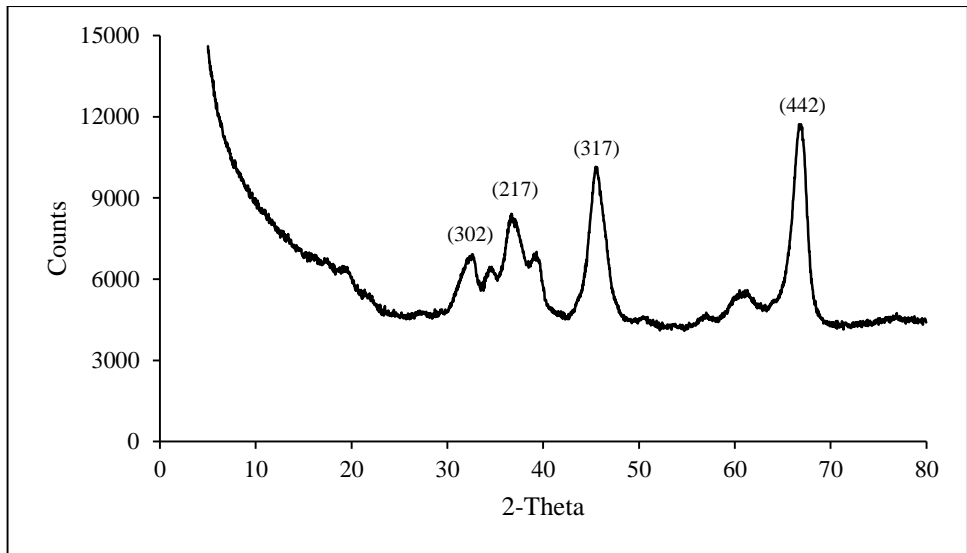


Figure 4.1: XRD pattern of Al₂O₃ nanoparticles

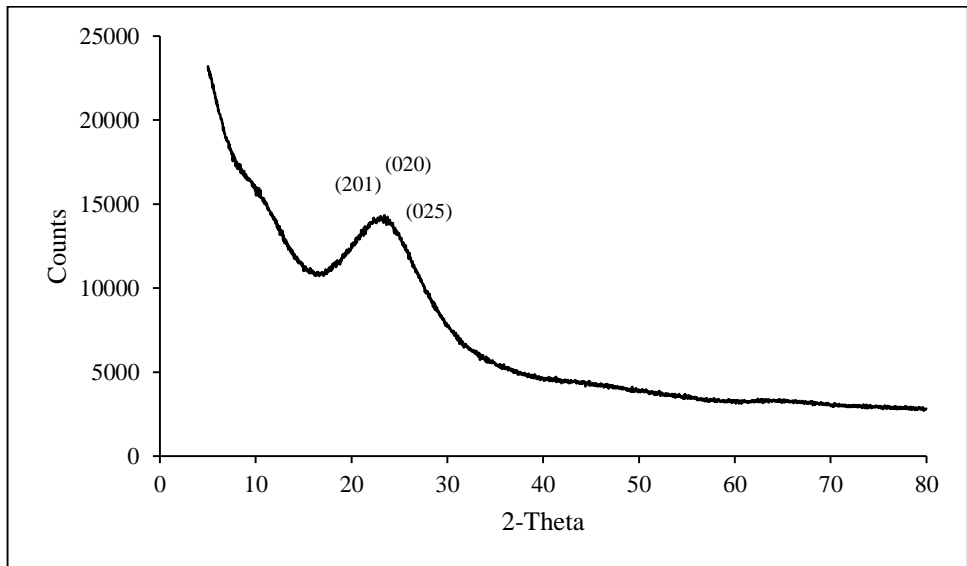


Figure 4.2: XRD pattern of SiO₂ nanoparticles

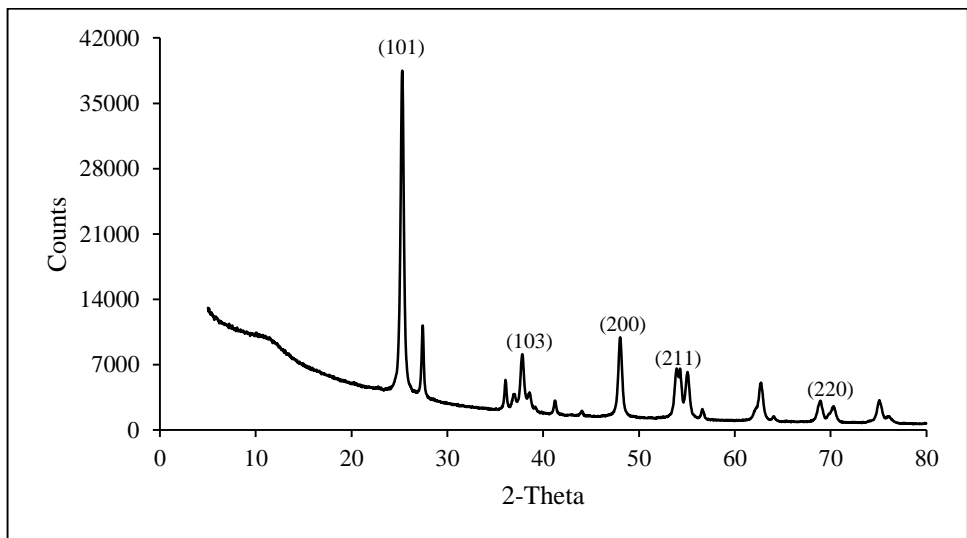


Figure 4.3: XRD pattern of TiO₂ nanoparticles

4.2.2 Scanning electron microscope (SEM) image Analysis

The particle shape is an important characterization to analyze the fundamental properties. Wu et al. (2009) suggested the SEM is the powerful tool to study the shape, and suspension uniformity. Xie et al. (2002) reported that particles shape and suspension uniformity as spherical shape particles gives higher thermal conductivity enhancement than cylindrical particles. Figures 4.4, 4.5 and 4.6 exhibit SEM micrograph of Al_2O_3 , SiO_2 and TiO_2 , respectively. Primarily all nanoparticles are approximately spherical. However, due to strong Van der Waals attractive force, nearly all three nanoparticles are in the form of dried agglomerates with larger dimensions than the primary particles. In order to break down the large agglomerates, ultrasonication is applied. The percentage of chemical components in three nanoparticles are analysed by Energy dispersive spectrometry (EDS) and have been presented in Appendix A.

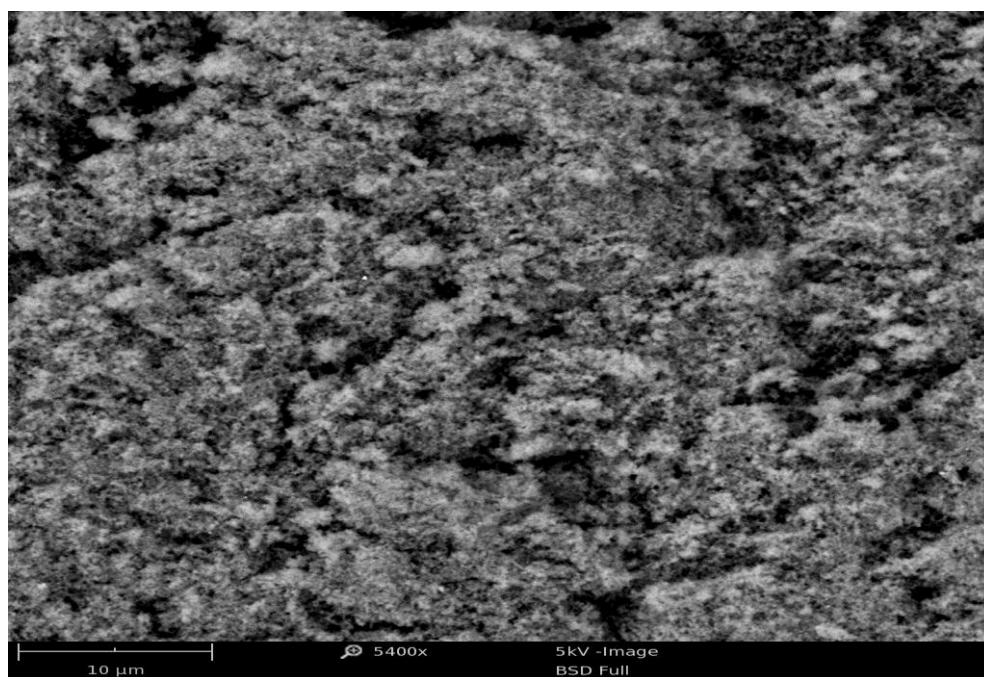


Figure 4.4: SEM image of Al_2O_3 nanoparticles

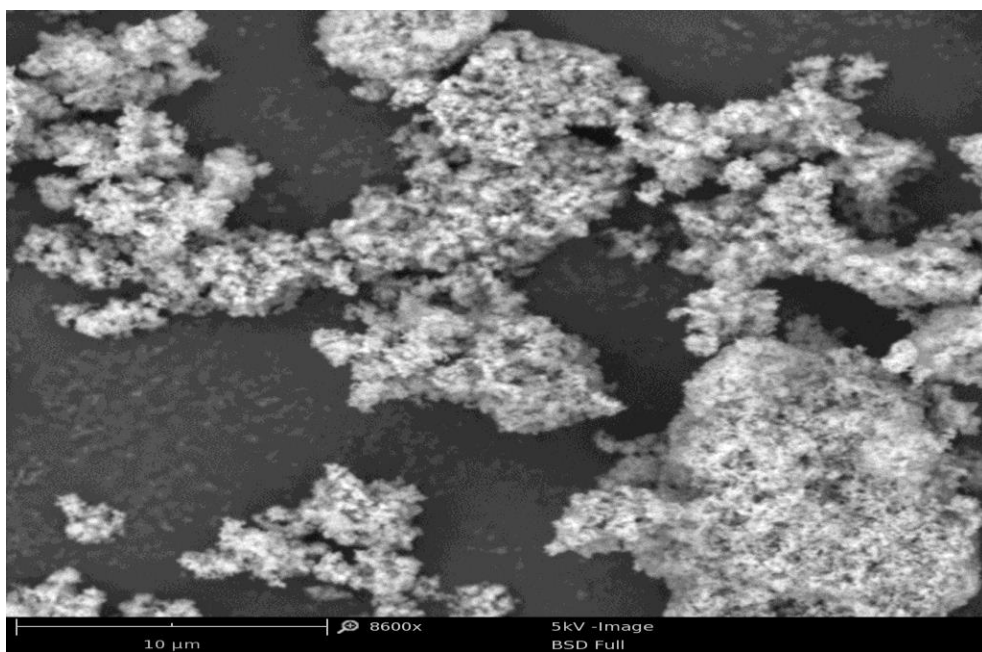


Figure 4.5: SEM image of SiO₂ nanoparticles

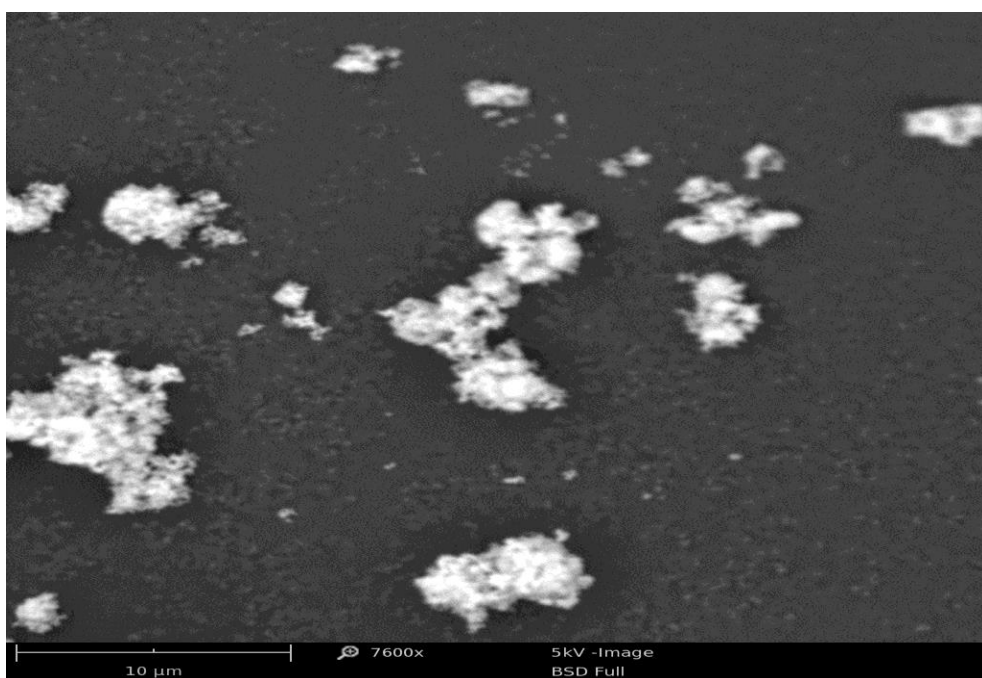


Figure 4.6: SEM image of TiO₂ nanoparticles

4.2.3 TEM image analysis

Transmission Electron Microscope (TEM) is reckoned as the most important tool to determine the size distribution and the morphology of the synthesized nanoparticles. It uses electron beam to create the image of samples.

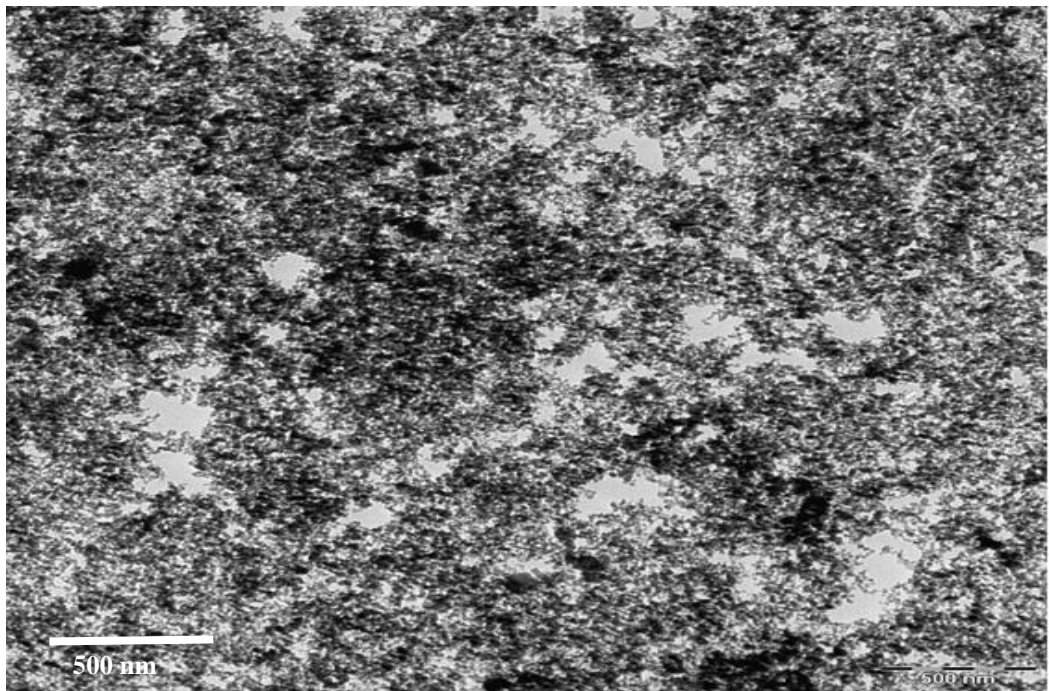


Figure 4.7: TEM image of Al_2O_3 -methanol nanofluid (0.05 vol%)

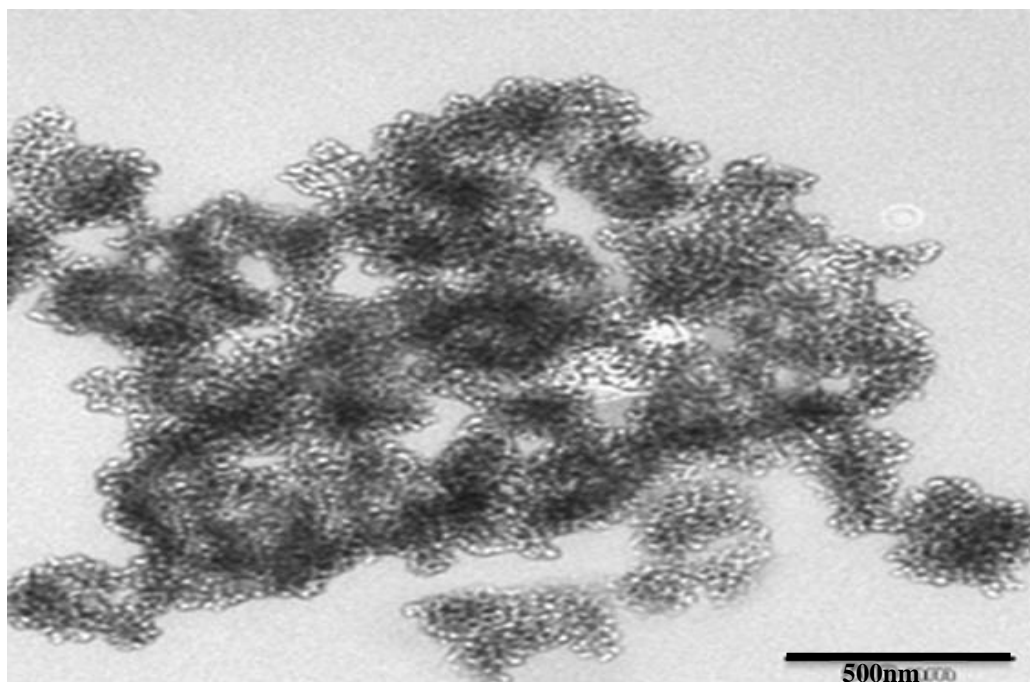


Figure 4.8: TEM image of SiO_2 -methanol nanofluid (0.05 vol%)

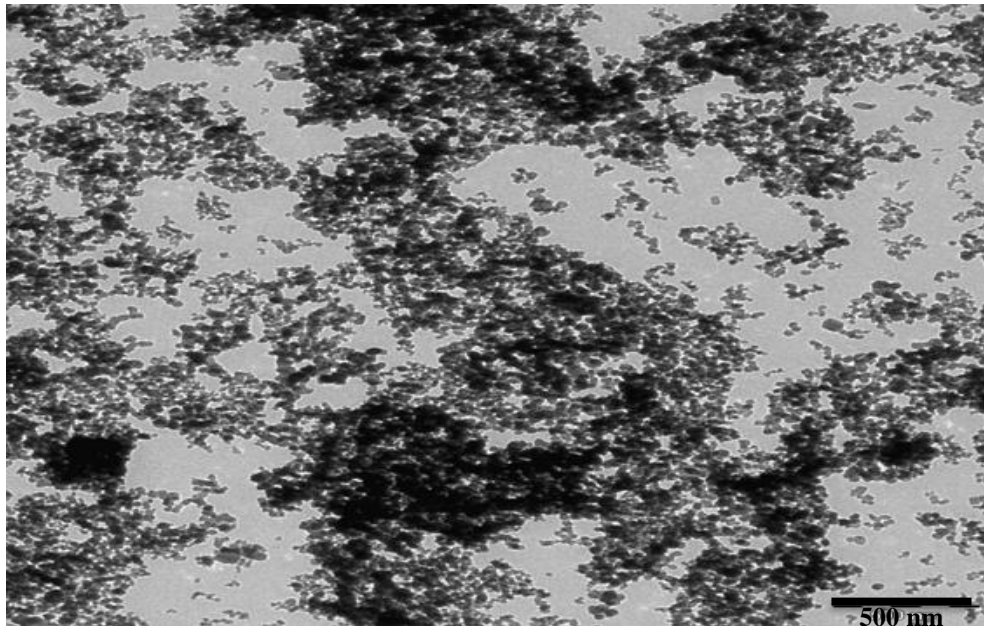


Figure 4.9: TEM image of TiO₂-methanol nanofluid (0.05 vol%)

Figures 4.7, 4.8 and 4.9 demonstrate the TEM image of Al₂O₃-methanol, SiO₂-methanol and TiO₂-methanol nanofluids at 0.05 vol%, respectively. As indicated in the TEM images three nanoparticles are spherical in shape. The TEM image shows less agglomeration for this solution even after 24 hours of preparation. Some area of TEM image have the most severe agglomeration this is because the over loading of dispersant which agglomerates the particles. The particle size measurement by TEM has been presented in Appendix B.

4.3 Stability of methanol based nanofluids

The agglomeration of nanoparticles results in clogging and settlement and thus reduces the thermal conductivity of nanofluids. So, stability analysis is a crucial circumstance in context to its application. In order to evaluate the stability of nanofluids, sedimentation, Uv-vis spectrometer, and zeta potential analysis are the three basic reliable methods.

4.3.1 Sedimentation image analysis

Figure 4.10 demonstrates the picture of five volume concentrations (0.005, 0.01, 0.05, 0.10 and 0.15 vol(%)) of Al₂O₃-methanol, SiO₂-methanol and TiO₂-methanol nanofluids just after preparation and after seven (7) days of preparation. From Figure 4.10, it is

observed that, not much sedimentation occurs in Al₂O₃-methanol nanofluids after seven days but for other two nanofluids, there is sedimentation at the bottom of the bottles. Generally, the sedimentation of mixtures is measured from the bottom of the specimen. It could be possible when there are slurries obvious at the bottom of the sample. From figures it is also obvious that low concentration suspension has low sedimentation compare to high concentration. From the visualization Al₂O₃-methanol nanofluid is more stable compare to SiO₂-methanol and TiO₂-methanol nanofluids.

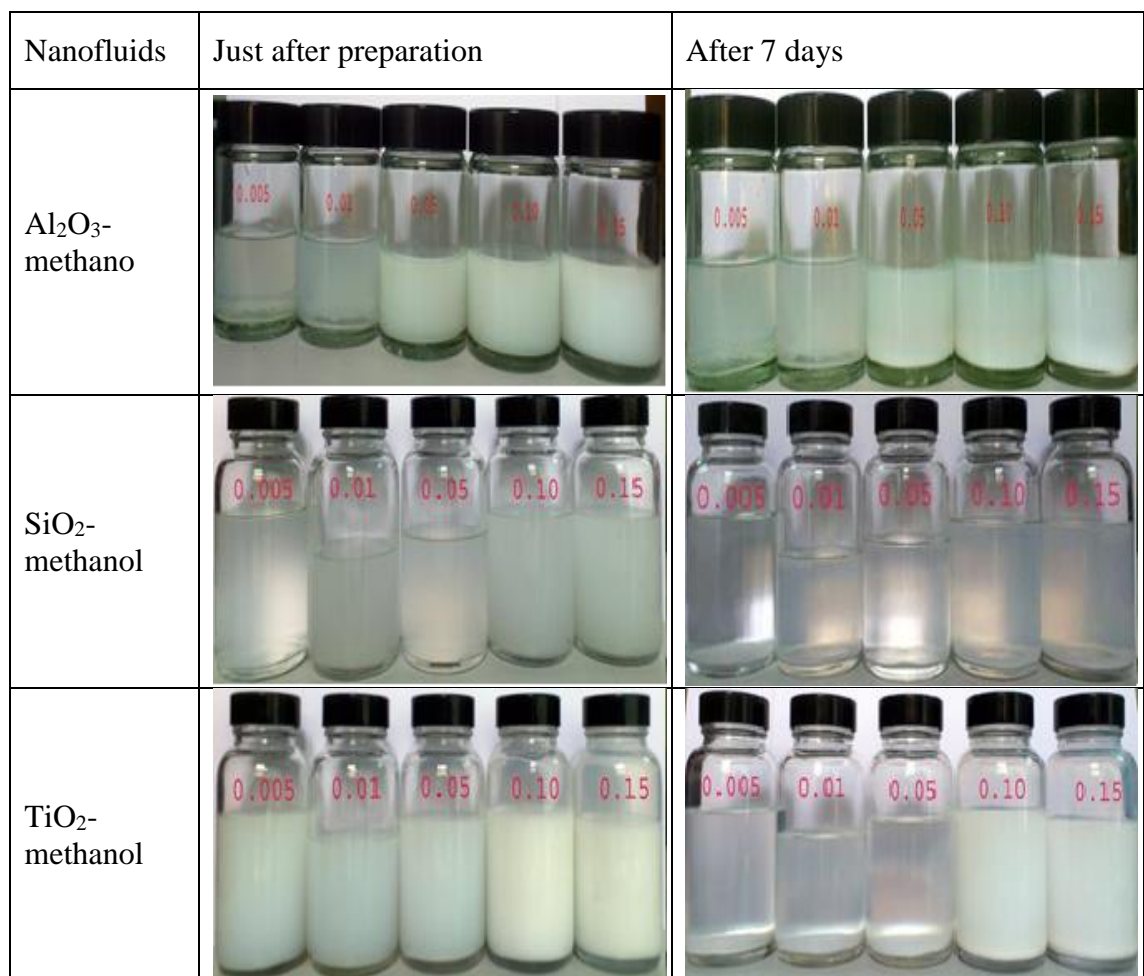


Figure 4.10: Photograph of methanol based nanofluids just after preparation and after 7 days preparation

4.3.2 Inspection stability by Uv-Visible spectrophotometer

Characterization for stability of methanol based nanofluids was analyzed with the UV-Visible spectrophotometer. Figures 4.11, 4.12 and 4.13 show the spectrum image of 0.005 vol% of Al₂O₃-methanol, SiO₂-methanol and TiO₂-methanol just after preparation by

using ultrasonic agitation. It is also shows that the peak absorbance of Al_2O_3 , SiO_2 and TiO_2 nanoparticle suspension on methanol appear at 217.9 nm, 220.98 nm and 226 nm respectively. The absorption suspended range of nanofluid is 1, 0.8 and 1.6 respectively. For others volume fraction the absorption peak are not found only noise found. Furthermore, the absorption strength of 0.005 vol% nanofluid is lower. This is because the 0.005% nanofluid leaves more ‘particle free region’ in base fluids. The other volume fraction nanofluids absorption strength is relatively higher than 0.005% nanofluid. The nanofluids are stable just after preparation.

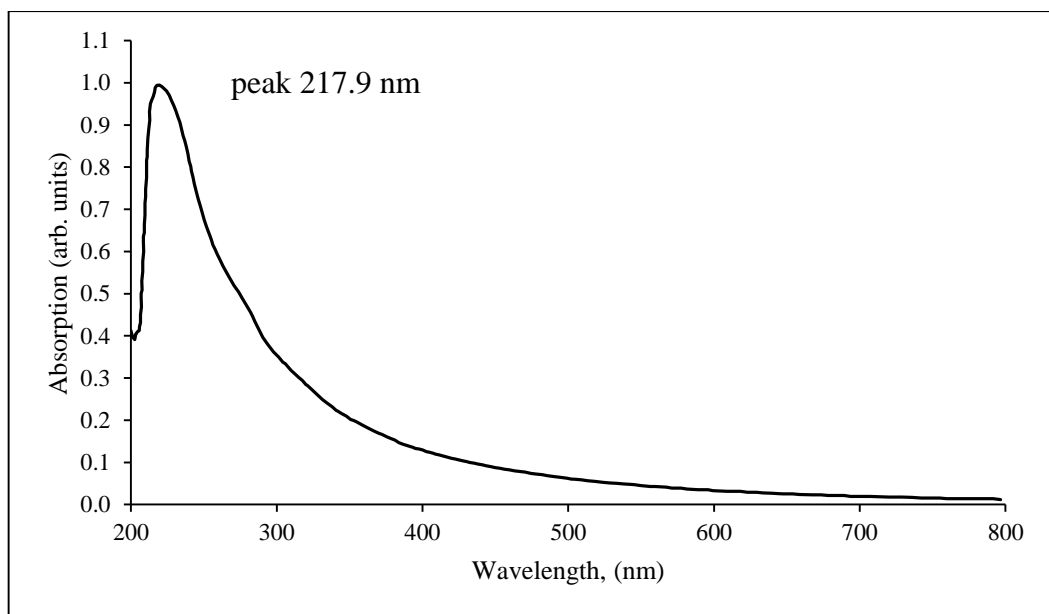


Figure 4.11: UV-Vis spectrum of Al_2O_3 -methanol nanofluids

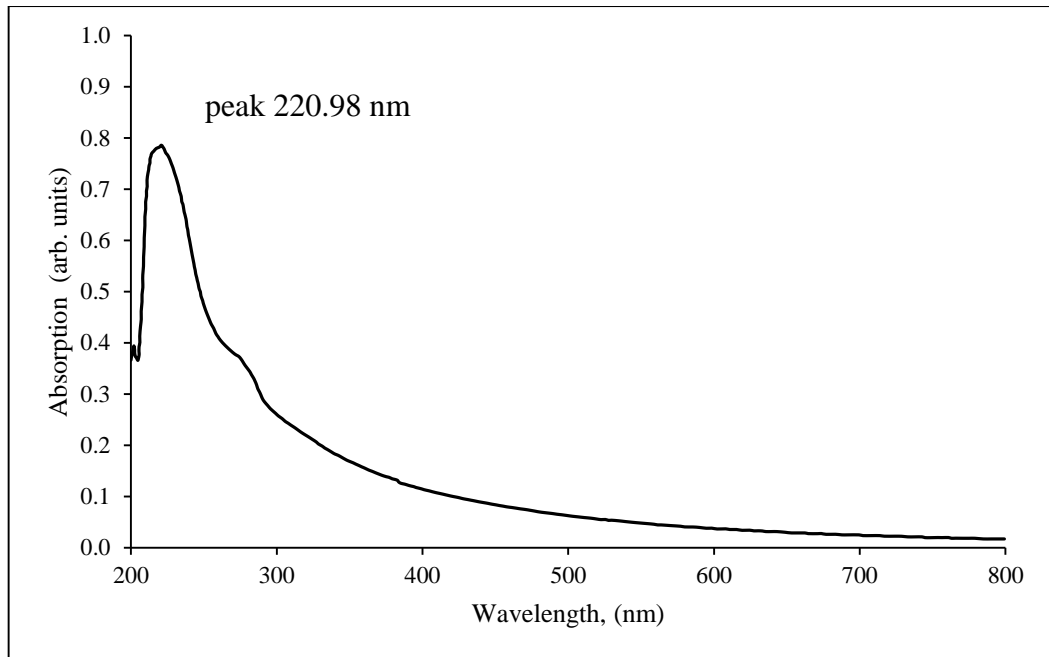


Figure 4.12: UV-Vis spectrum of SiO₂-methanol nanofluids.

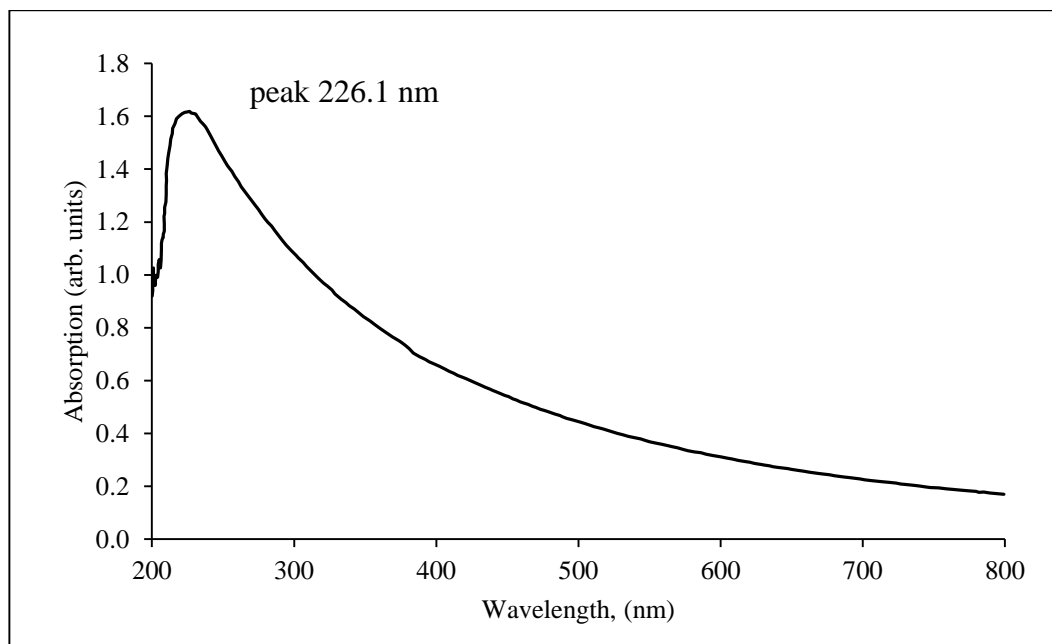


Figure 4.13: UV-Vis spectrum of TiO₂-methanol nanofluids

4.3.3 Stability inspection by Zeta potential and Zetasizer test

The stability of methanol based nanofluids is analyzed with zeta potential test result. Figure 4.14 demonstrates the zeta potential result as a function of nanoparticle volume concentrations. It is seen that the absolute zeta potential value for Al₂O₃-methano nanofluids increases with increasing volume concentration accept 0.15 vol% but other two nanofluids increases or decreases arbitrary. The absolute zeta potential value for

Al₂O₃-methanol nanofluids varies from 18 to 27 mV which is moderately stable. For SiO₂-methanol and TiO₂-methanol nanofluids, the absolute zeta potential value varies 11 to 18 mV and 10 to 17 mV respectively which is almost stable but settling lightly. In table 2.2 the range of absolute zeta potential values for stability are well described. When the zeta potential values are high, the particles are stable in nanofluids due to high electrostatic repulsion force between particles.

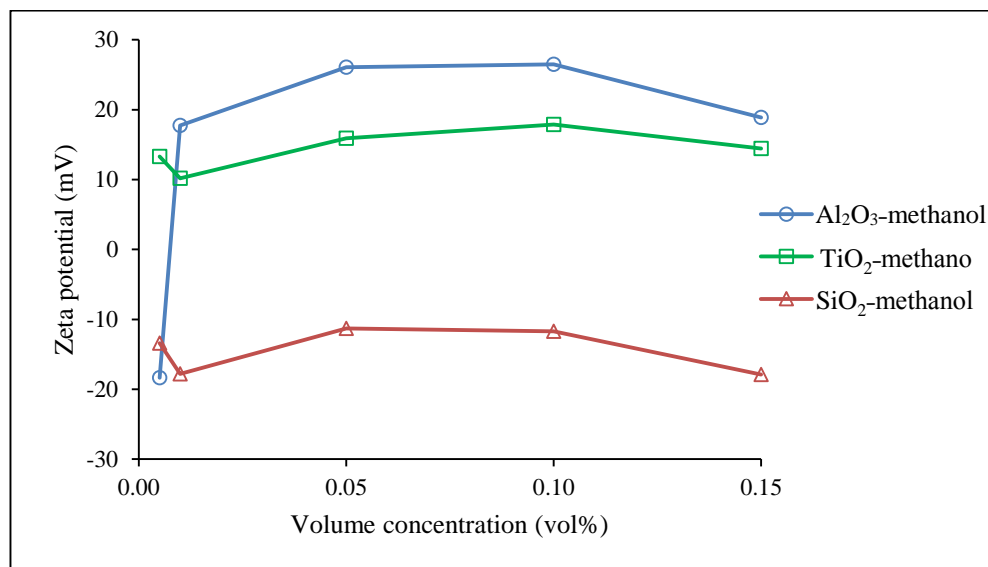


Figure 4.14: Zeta potential of methanol based nanofluids as a function of nanoparticle volume concentration

The suspension of small particle distribution is analyzed with Zetasizer technique. Figure 4.15 illustrates the particle size of methanol nanofluids as a function of volume concentration. From the figure, the Al₂O₃ particle size keeps a range from 244 to 263nm and the SiO₂ and TiO₂ nanoparticle size remains 212 to 238 nm and 225 to 240 nm respectively. The comparison between powder size and cluster particle size of three methanol based nanofluids, it can be observed that the nanoparticles in nanofluids contact each other and forms some cluster. The cluster size of Al₂O₃ nanoparticle is higher than the others two SiO₂ and TiO₂ nanoparticles (powder size and cluster size of Al₂O₃: 13 nm and 244 -263nm; powder size and cluster size of SiO₂: 5~15 nm and 212 -238 nm; powder size and cluster size of TiO₂: 21 nm and 225 -240nm).

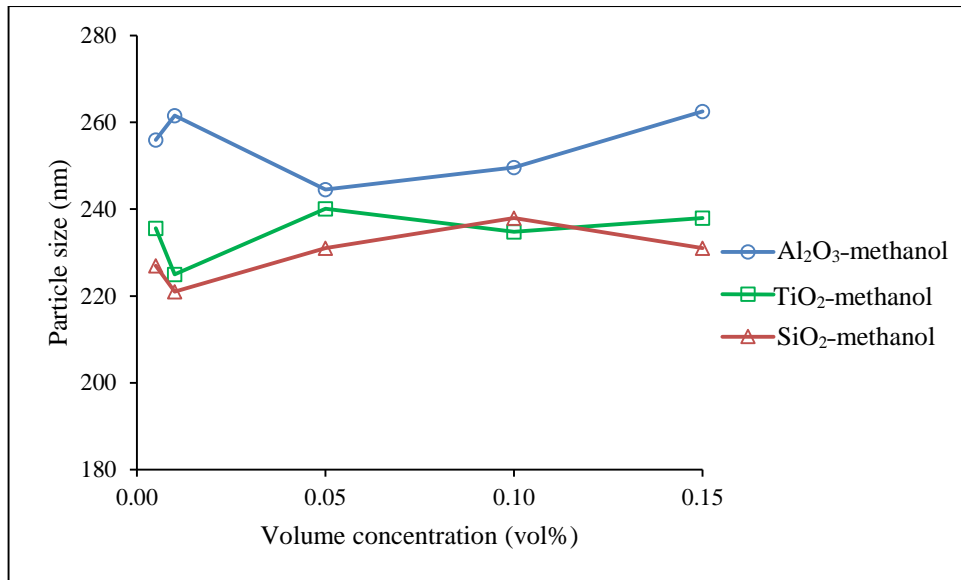


Figure 4.15: Particle size in methanol based nanofluids as a function of volume concentration

The dispersion stability of nanofluids evaluate with hydrodynamic diameter of the particles measured by Zetasizer zs. The volume distribution of particle size within the methanol nanofluids were shown in the Appendix C.

4.4 Thermophysical properties of methanol based nanofluids

This section is divided into three subsections according to the results and discussions of thermal conductivity, viscosity, and density of methanol based nanofluids. Each of the subsection firstly, describes the effect of volume concentrations and finally, describes the effect of temperature.

4.4.1 Thermal conductivity of methanol based nanofluids

Figures 4.16, 4.17 and 4.18 show the thermal conductivity of Al₂O₃-methanol, SiO₂-methanol and TiO₂-methanol nanofluids as a function of temperature and particles volume fraction. The results indicate that the thermal conductivity of methanol-based nanofluids increases with the increase of particle volume fraction and temperature compared with that of the base fluids. For example, at 20 °C temperature, the thermal conductivity value 0.264 W/mK for 0.15 vol% and 0.245 W/mK for 0.005 vol%. The difference of thermal conductivity is 0.019W/mK for 0.145 vol%. Similarly, the

difference of thermal conductivity is 0.018W/mK and 0.023 W/mK for SiO₂-methanol and TiO₂-methanol nanofluids. For all cases, the maximum thermal conductivity enhancement was found at 0.15 vol% and 20°C. The results also show that thermal conductivity improved from 1.47 to 8.33%, 0.98 to 7.35% and 1.47 to 6.86% for Al₂O₃-methanol, SiO₂-methanol and TiO₂-methanol, respectively with every 0.05 vol% increase in nanoparticles volume fraction. This is because of more particles loading has higher particle surface to volume ratio. The mechanism for this enhancement may be because of particle to particle interactions, nanoparticle cluster and Brownian motion. It is also noted that the thermal conductivity increased with every 5°C increase in temperature (0.49 to 3.92%, 0.49 to 3.43% and 0.49 to 3.92% for Al₂O₃-methanol, SiO₂-methanol and TiO₂-methanol, respectively). It was because increased temperature decreased viscosity which intensified the Brownian motion and the effects of nanoconvection. Thermal conductivity increases due to the rotational motion of spherical nanoparticles according to nanoconvection model (Hojjat et al., 2009). These results agree well with the measured thermal conductivity data suggested by Das et al. (2003), and Chandrasekar et al. (2010) for Al₂O₃ water nanofluid at low particle volume concentration.

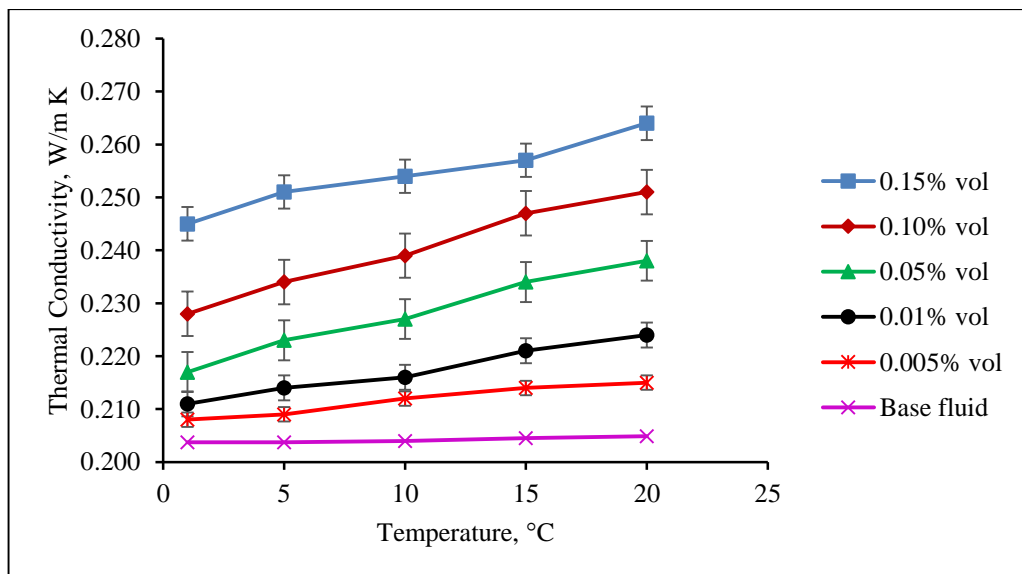


Figure 4.16: Thermal conductivity of Al₂O₃-methanol as a function of temperature and particle volume concentration.

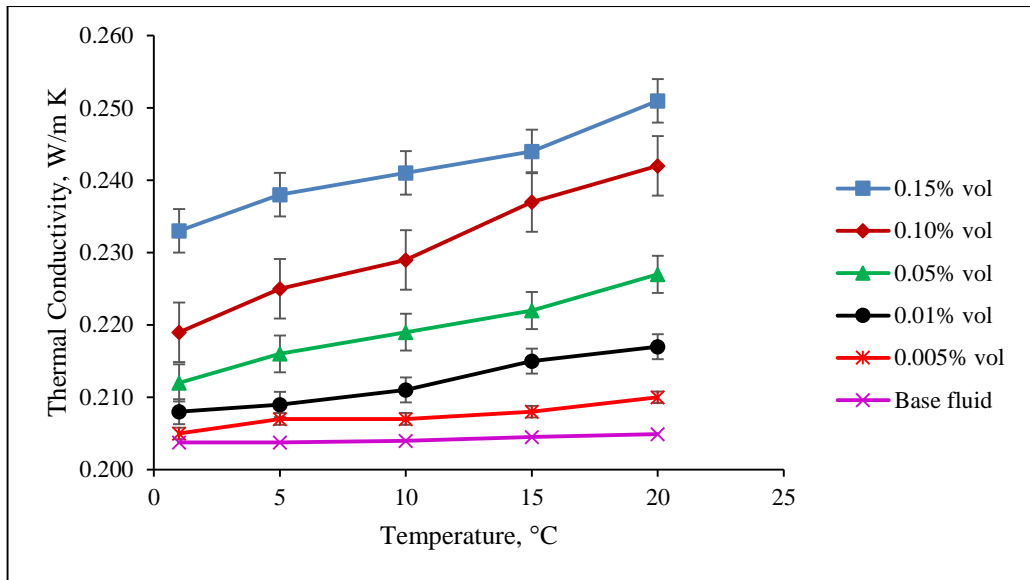


Figure 4.17: Thermal conductivity of SiO₂-methanol as a function of temperature and particle volume concentration.

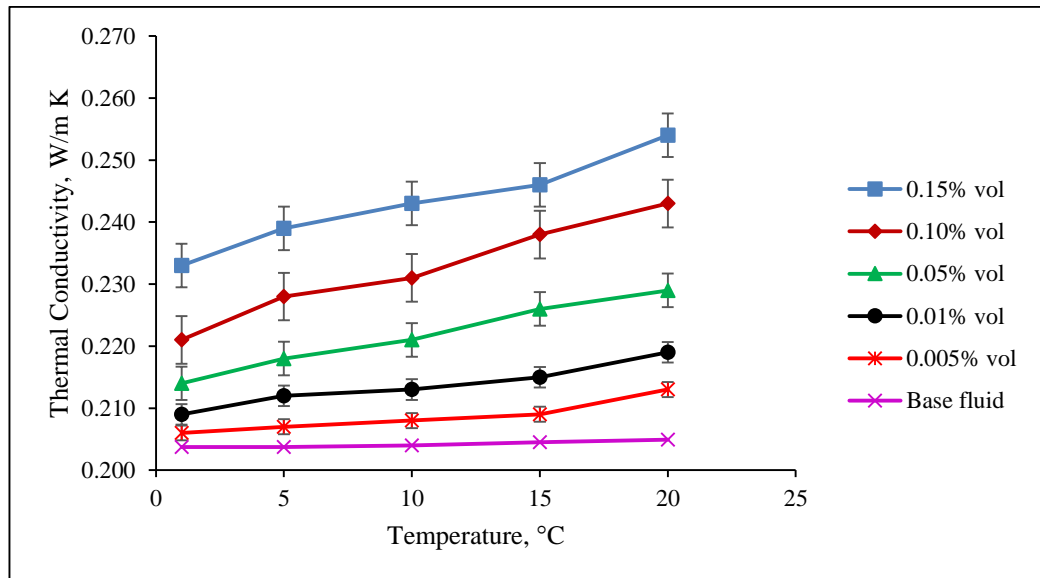


Figure 4.18: Thermal conductivity of TiO₂-methanol as a function of temperature and particle volume concentration.

Figures 4.19, 4.20 and 4.21 represent comparisons between the measured data and the predicted values using existing correlations for the three nanofluids. The results are presented for the measured values of thermal conductivity measured at 20 °C with some existing model for Al₂O₃-methanol, SiO₂-methanol and TiO₂-methanol. The figures show that the thermal conductivity of methanol based nanofluids increases with nanoparticle volume concentration enhancement. The increment rate with the augmentation of concentration expected to be linear. The experimental values for this

study were found to be higher than all other models such as: Patel et al. (2010), Hamilton and Crosser (1962), Wasp et al. (199), Yu and Choi (2003), and Bruggeman (1935). The mean deviation of this experimental value was around 22 % and 20 % with Patel et al. (2010) and Bruggeman (1835), respectively. Most of these developed models depended on water based suspensions. This happens because these model were developed with base fluid water and different type of particle, size and shape (Timofeeva et al., 2007). However, at high concentration of methanol based nanofluids high clustering of nanoparticles have been observed which increase abnormal and nonlinear thermal conductivity tremendously. Another reason may be nanoparticle alignments that also cause abnormal increment of thermal conductivity (Zhu et al., 2006).

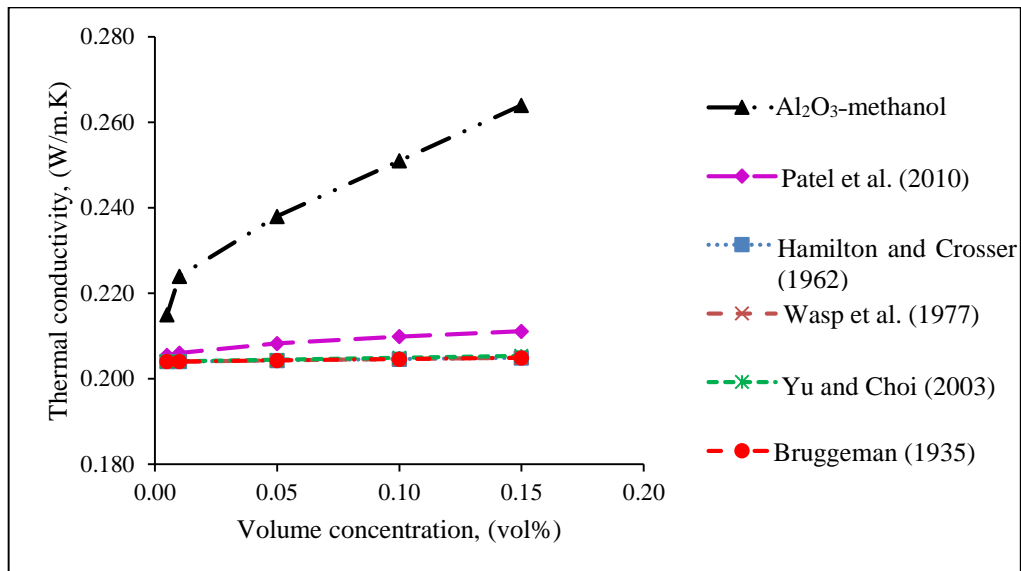


Figure 4.19: Experimental values of thermal conductivity (Al₂O₃-methanol) compared with the values from existing correlation

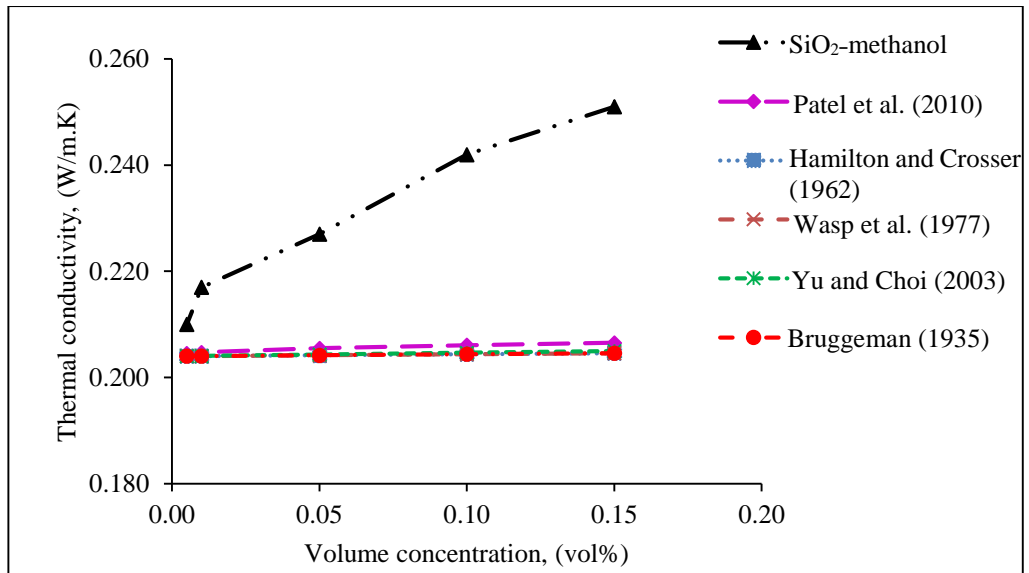


Figure 4.20: Experimental values of thermal conductivity (SiO₂–methanol) compared with the values from existing correlation

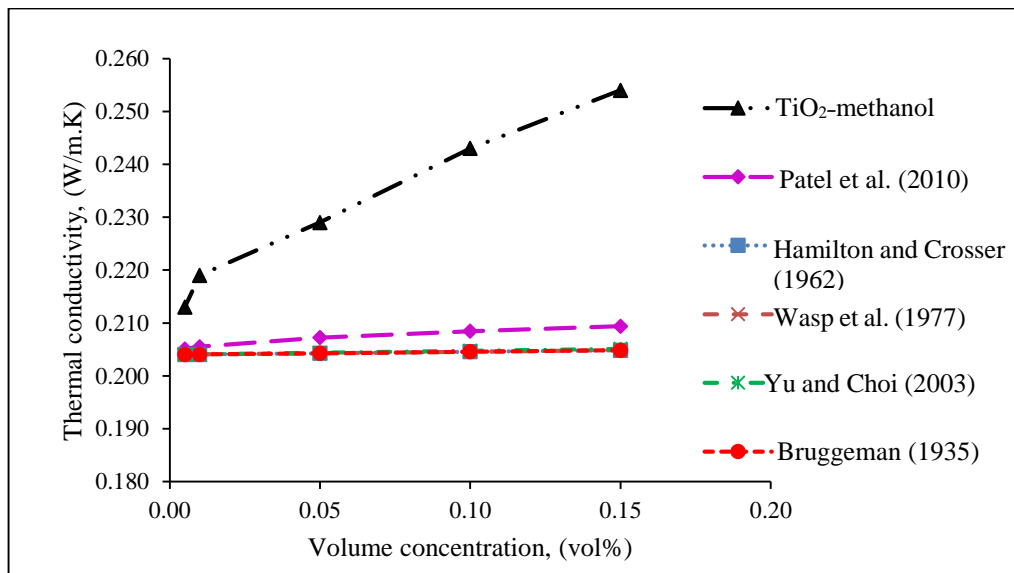


Figure 4.21: Experimental values of thermal conductivity (TiO₂–methanol) compared with the data from existing correlation

Figure 4.22 shows the enhancement in thermal conductivity of different nanoparticle volume fractions at 20°C for methanol-based nanofluids. The results show that the thermal conductivity augmented compared with the pure base fluid. It is observed from Figure 4.22 that thermal conductivities improved up to 29.41%, 23.03% and 24.51% at volume concentrations of 0.15vol% for the three nanoparticles. It is also clear that Al₂O₃-methanol owns higher values of thermal conductivity compared with the other two

nanofluids as Al_2O_3 nanoparticles have higher thermal conductivity compared to SiO_2 and TiO_2 nanoparticles. Moreover, the nanoparticles in the fluid are moving due to the Brownian motion of these nanoparticle suspensions. This motion resulting from the fundamental thermal properties of the nanoparticles and hence arise the effective thermal conductivity of these nanoparticle suspensions. The nanoparticles thermal conductivity influenced the enhancement of nanofluids thermal conductivity (Hojjat et al., 2009) and (C. H. Li and Peterson, 2006). Another reason may have the clustering effect of nanoparticle. Gao et al. (2009) suggested that clustering size held the key to enhance the thermal conductivity. In Figure 4.15 describe the cluster size of methanol based nanofluids. The comparison between measured data from the current study and those from the experiments done by Pang et al. (2012) at the same operating temperature are shown in Figure 4.22. The difference between these results may vary for various factors such as a difference in particle size, preparation method, source, as well as measurement techniques (Duangthongsuk and Wongwises, 2009).

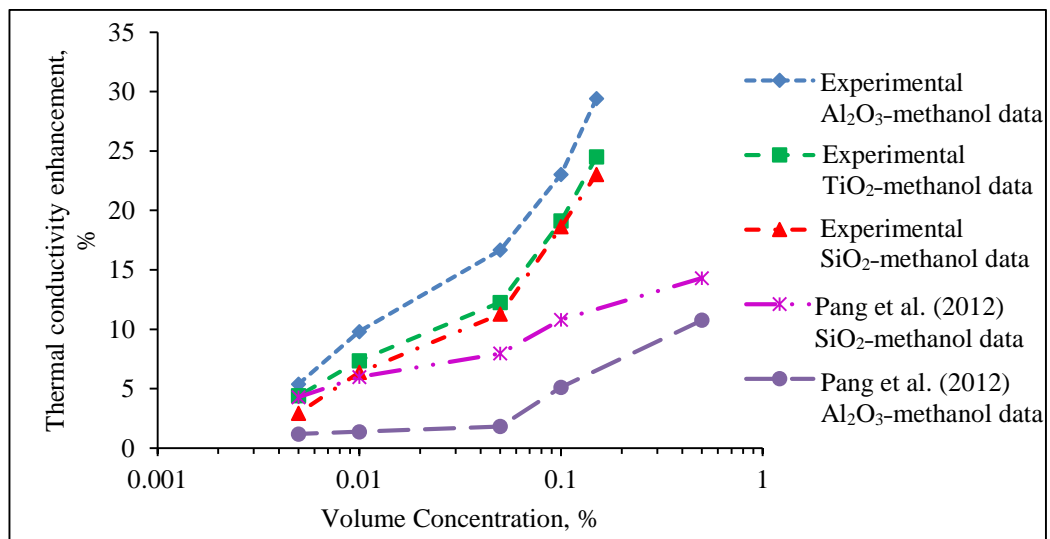


Figure 4.22: Comparison of thermal conductivity enhancement with reference data.

Thermal conductivity of methanol based nanofluids depends on nanoparticles volume fraction and temperature. The similar trend was also observed by Pang et al. (2012) for methanol-based Al_2O_3 and SiO_2 nanofluids. Thus, it is obvious that relative thermal conductivity of methanol based nanofluids is a function of particle volume fraction and

temperature. It was observed from the experimental values that the existing correlations are inappropriate for predicting the thermal conductivity of methanol-based nanofluids. Thus, a new linear correlation has been proposed hereby based on the experimental results for measuring thermal conductivity of methanol based nanofluids:

$$\frac{k_{nf}}{k_{bf}} = x + y\phi \quad (4.1)$$

Where the constant values of x and y are described as follows:

Nanofluids	X	y	Correlation coefficient (R ²)
Al ₂ O ₃ -methanol	1.0712	1.546	0.9685
SiO ₂ -methanol	1.0405	1.3342	0.9749
TiO ₂ -methanol	1.0514	1.3317	0.9864

This type of correlation had been proposed by (Duangthongsuk and Wongwises, 2009) for measurement of water-TiO₂ nanofluids thermal conductivity at different volume fraction and temperature. The correlation is valid for a particle volume fraction of 0.05% to 0.15% and temperature of 20°C. Figure 4.23 shows comparison between the measured value and value obtained from proposed new correlation. The results show that the correlation coefficient (R²) value of this present correlation is about 0.97 which is close to 1.

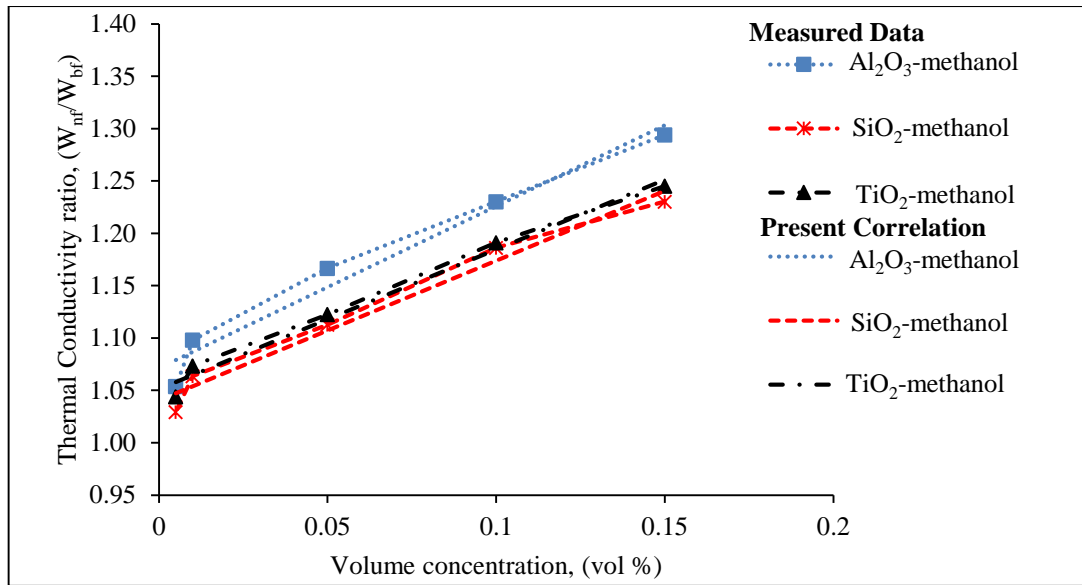


Figure 4.23: Comparison of thermal conductivity ratio measured data with proposed correlation

4.4.2 Viscosity of methanol based nanofluids

The effects of nanoparticles volume fraction and temperature on rheological behavior of methanol based nanofluids were studied. The experimental data were measured based on the shear stress and viscosity with respect to shear rate. Figures 4.24, 4.25 and 4.26 illustrate the shear stress and viscosity vs. shear rate at 0.05 vol% for Al₂O₃-methanol, SiO₂-methanol and TiO₂-methanol nanofluids. The solid line represents the relationship between shear stress and shear rate. The figures indicate that shear stress increased with an increase of shear rate and decrease with temperature accordingly. The increasing trend of shear stress of all types of methanol based nanofluids was almost similar for every volume concentration. The increasing trend was nonlinear and the phenomenon of shear stress vs. shear rate behaves like a non-Newtonian fluid with a shear thickening or dilatant behavior. The decreasing rate of shear stress was more prominent at higher shear rate. For example, at shear rate of 61.15 s^{-1} , shear stress of 0.01 vol% was 0.56 and 0.46 D/cm^2 (a difference of 0.10 D/cm^2) at 1 and 20 °C, respectively; while the shear stress was 5.69 and 5.06 D/cm^2 (a difference of 0.59 D/cm^2) respectively at shear rate of 305.8 s^{-1} . Shear stress also depends on particle volume concentration as with increasing particle volume concentration, shear stress increased at the same shear rate. For example, the shear stress

values were 5.06 and 5.48 D/cm² for 0.01 and 0.10 vol% respectively at shear rate of 305.80 s⁻¹. The shear stress value for TiO₂-methanol nanofluids was higher than Al₂O₃-methanol, and SiO₂-methanol nanofluids at the same shear rate, volume fraction and temperature. For example, the shear stress values were 5.24 and 5.06 D/cm² for TiO₂-methanol and Al₂O₃-methanol nanofluids respectively at shear rate of 305.80 s⁻¹, concentration of 0.01 vol% and temperature of 20 °C. Similar results were obtained for SiO₂-methanol nanofluids at different volume fractions and temperatures.

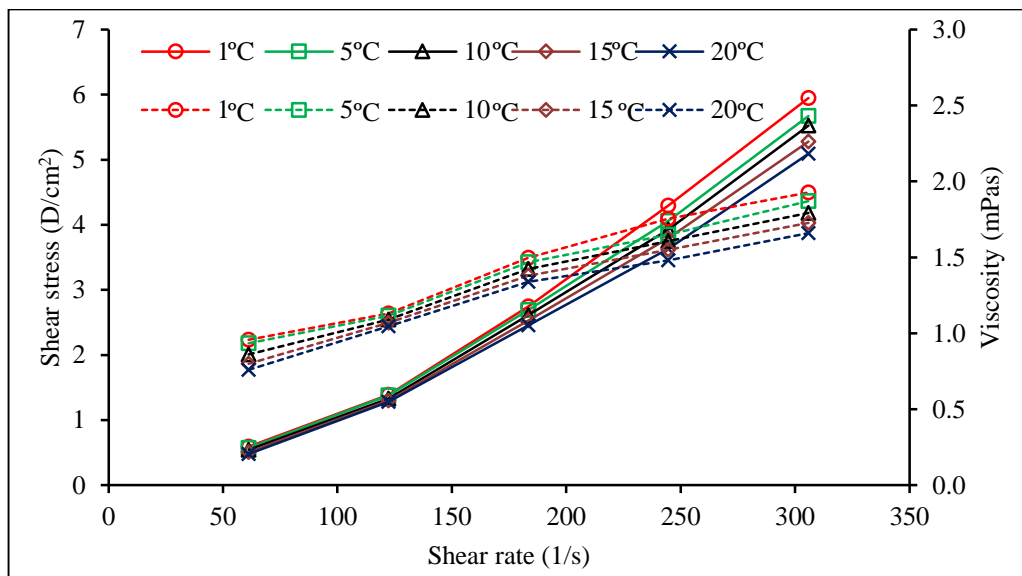


Figure 4.24: Shear stress and viscosity of Al₂O₃-methanol nanofluids for 0.05 vol% as a function of shear rate and temperature.

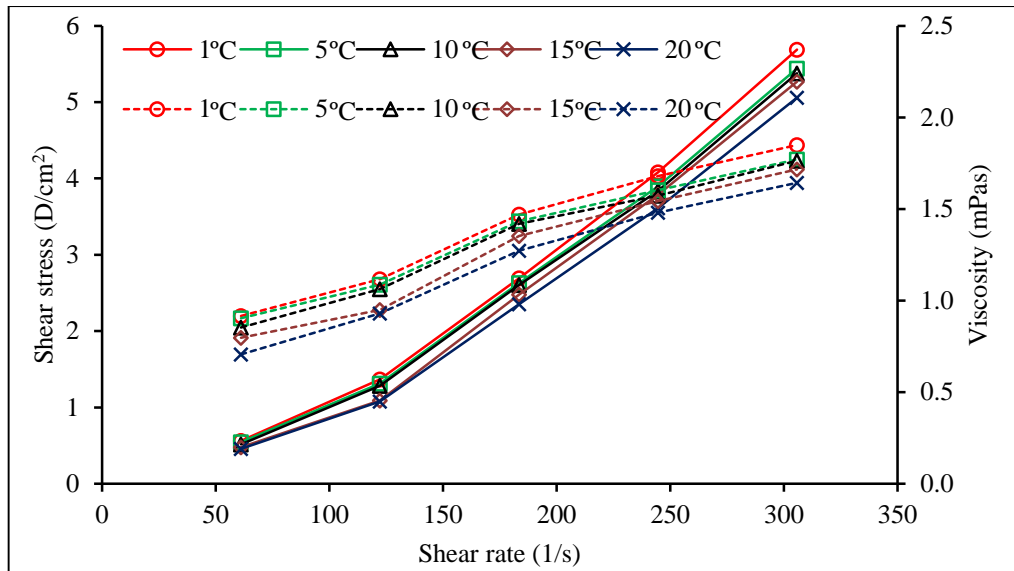


Figure 4.25: Shear stress and viscosity of SiO₂-methanol nanofluids for 0.05 vol% as a function of shear rate and temperature.

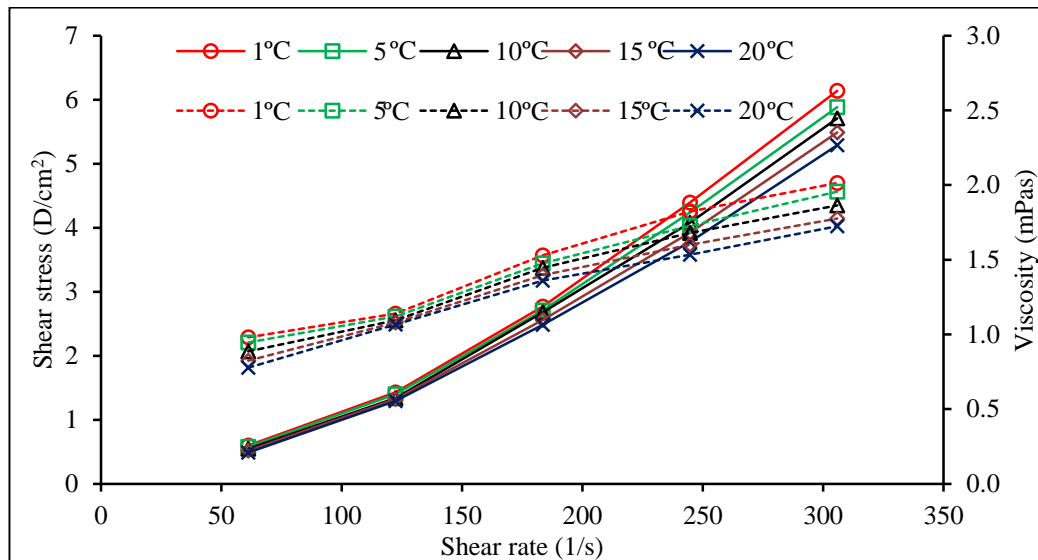


Figure 4.26: Shear stress and viscosity of TiO₂-methanol nanofluids for 0.05 vol% as a function of shear rate and temperature.

The viscosity of Al₂O₃-methanol, SiO₂-methanol and TiO₂-methanol at various volume concentration and temperatures is shown in Figure 4.27, 4.28 and 4.29, respectively. According to this figures, the viscosity increases with increasing volume concentration and decreases with rising temperatures in all cases. The increasing and decreasing trend are nonlinear. For Al₂O₃-methanol based nanofluid, at 0.15 vol% the viscosity vale 0.90 mPas and 0.72 mPas at 1°C and 20°C temperature respectively. Similar results were found for SiO₂-methano and TiO₂-methano nanofluids. The same trend for decrease of viscosity

with the increase of temperature were found by some other researchers (Kulkarni et al., 2006; Namburu et al., 2007) It is also demonstrated that the viscosity decreased with an increase in volume fraction and temperature for both nanofluids due to the weakening adhesion force of the particle. When the temperature increases, the interaction time between neighboring molecules of a fluid decreases due to increased velocities of individual molecules. High temperature also influences the Brownian motion of nanoparticles and hence decreases the viscosity of nanofluids. The present viscosity results hold good agreement with the experimental data presented by Choi (1999), Wang et al. (1999) Murshed et al. (2008), Kulkarni et al. (2002), Das et al. (2003), Maiga et al. (2004), Chen et al. (2009), Nguyen et al. (2007), and Chandrasekar et al. (2010). Therefore, it is expected that the higher the particle concentration may increase the pressure drop and pumping power.

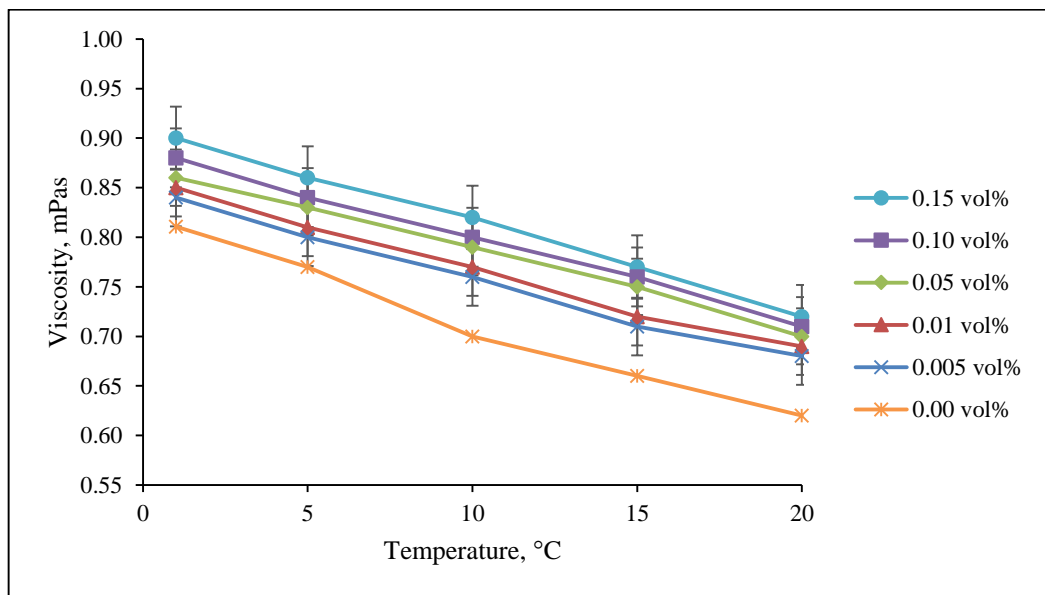


Figure 4.27: Viscosity of Al₂O₃-methanol as a function of temperature and particle volume concentration.

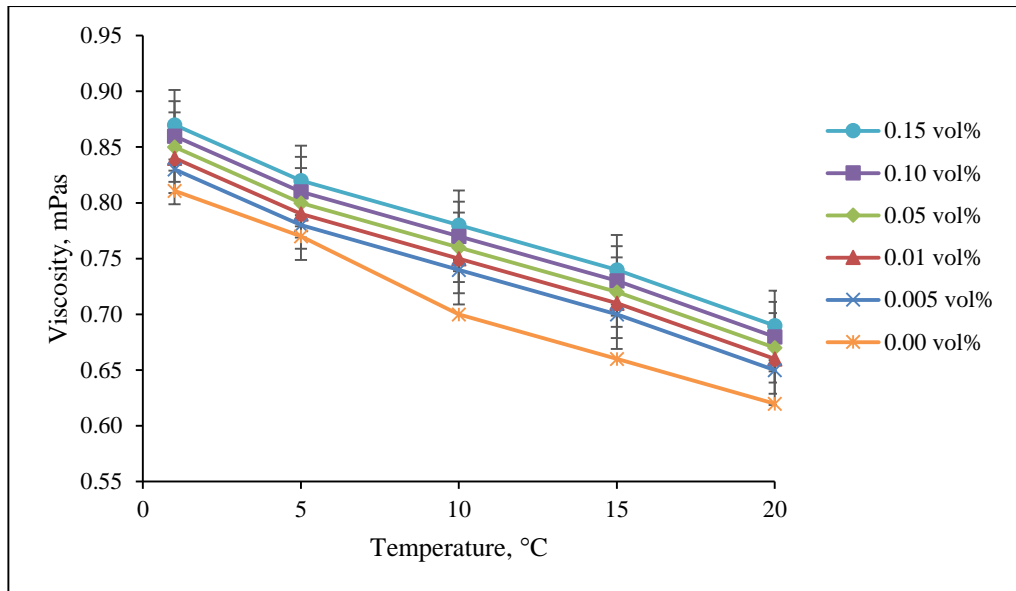


Figure 4.28: Viscosity of SiO₂-methanol as a function of temperature and particle volume concentration.

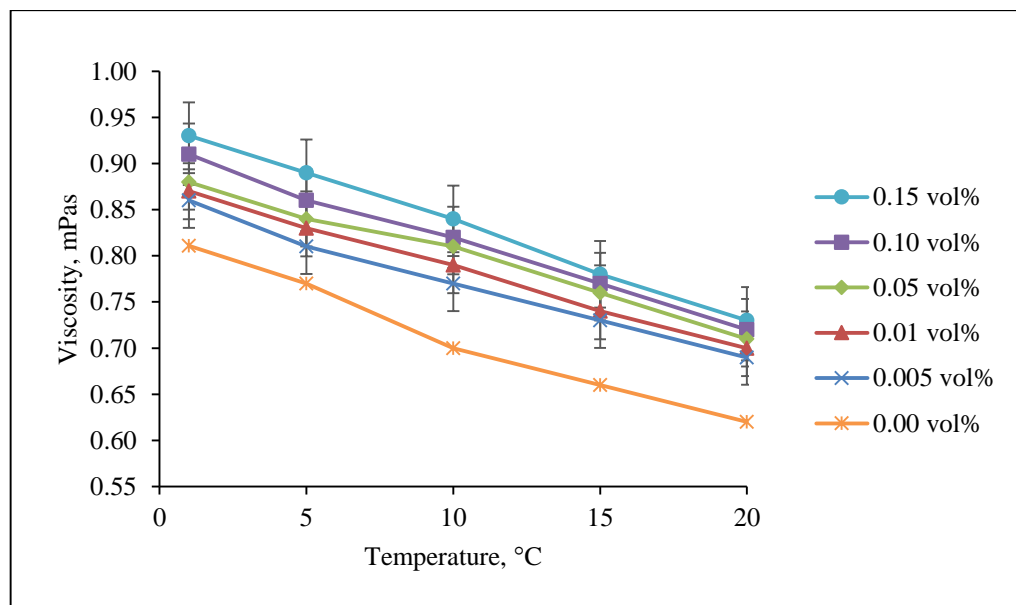


Figure 4.29: Viscosity of TiO₂-methanol as a function of temperature and particle volume concentration.

Figure 4.30 show the comparison of measured viscosity compared with some existing equation at 20°C temperature. The increasing trend of viscosity for all fluids was nonlinear. It was also observed that the measured viscosity of three nanofluids showed higher value than the value obtained from correlations. Thus, the model are not suitable for evaluating the viscosity of methanol based nanofluids (Mahbubul et al., 2012) because these models were generalized models developed to estimate the viscosity of a

suspension. Therefore, agglomeration cluster of nanoparticles can be considered as one of the reasons for higher viscosity.

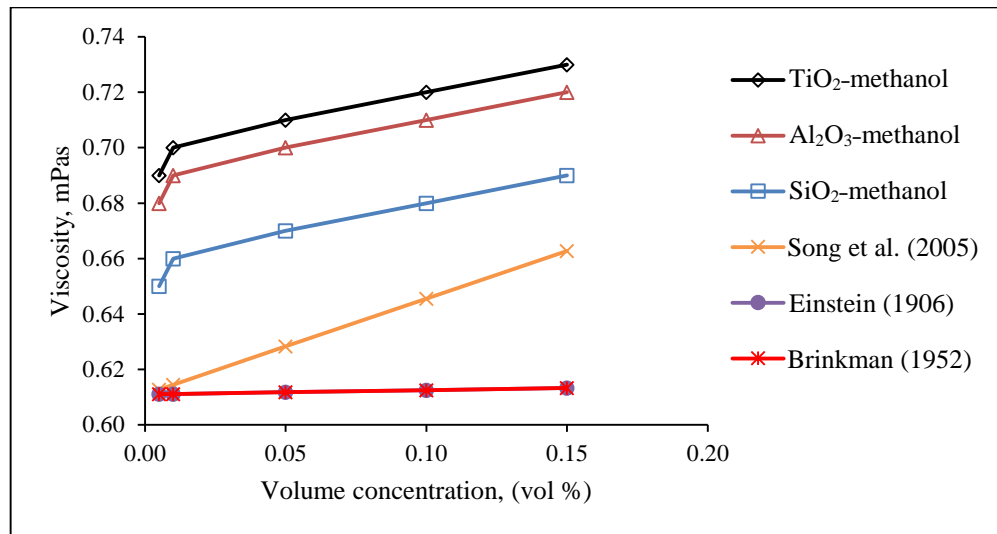


Figure 4.30: Comparison of measured viscosity with the values from existing correlation

Figure 4.31 shows the effective viscosity ratio of methanol based nanofluids at 20 °C. It is observed that the viscosity TiO₂-methanol is higher than the Al₂O₃-methanol and SiO₂-methanol nanofluids. The maximum viscosity increases is found to be 17.8%, 16.1% and 11.1% for TiO₂-methanol, Al₂O₃-methanol and SiO₂-methanol nanofluids respectively. Mahbubul et al. (2013) observed 214 times greater than base fluid for 5°C and 2 volume concentration (%) of particles. Tseng and Lin (2003) found a higher relative viscosity compared to that in this experimental value. They observed that the viscosity increased up to 1200 times more than the base fluid for 12 volume concentration (%) of TiO₂ with water.

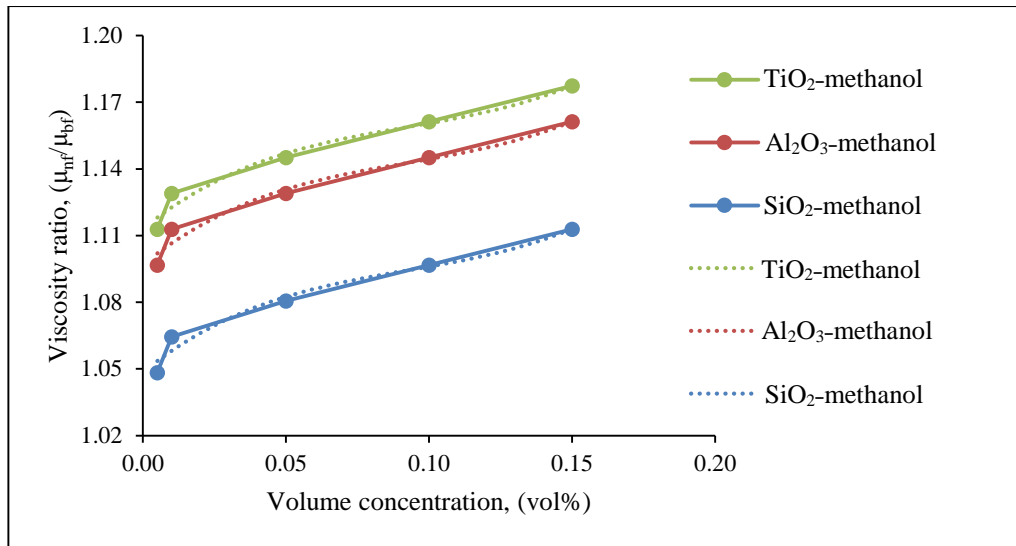


Figure 4.31: Comparison of viscosity ratio measured values with proposed correlation. Theoretically, these are classical models established to estimate the viscosity of a suspension that the agglomeration cluster of nanoparticles had not been taken into consideration. So it is reasonable that these models are not suitable for the nanofluids. However, it appears difficult to build a perfect equation with obtained results due to various factors such as the variation of the nanoparticles or base liquid as well as the differences in the shape of nanoparticles. For computing purpose, the following correlations (Eq. 4.2) have been proposed for methanol-based Al₂O₃, SiO₂ and TiO₂ nanoparticles for a particle volume fraction of 0.05% to 0.15% and temperature of 20°C:

$$\frac{\mu_{nf}}{\mu_{bf}} = 31.581\phi^3 - 8.7839\phi^2 + 1.0367\phi + C \quad (4.2)$$

Nanofluids	Constant
Al ₂ O ₃ -methanol	1.0970
SiO ₂ -methanol	1.0486
TiO ₂ -methanol	1.1131

4.4.3 Density of methanol based nanofluids

The density of Al₂O₃-methanol, SiO₂-methanol and TiO₂-methanol nanofluids as a function of different temperatures and different volume concentration are shown in

Figures 4.32, 4.33 and 4.34, respectively. The results indicate the density of methanol based nanofluids increases in volume concentration. The density of nanofluids shows higher values than the base fluids. For example, at temperature 1 °C the value of density is 809.29 kg/m³ for 0.005 vol% and 818.42 kg/m³ for 0.15 vol% for Al₂O₃–methanol. At volume concentration 0.15 vol% the density value 807.45 kg/m³ for 20 °C and 818.42 kg/m³ for 1 °C. Similar results were found in all volume concentration and SiO₂-methanol and TiO₂-methanol nanofluids due to higher density of nanoparticles dispersed in base fluids. From Figures 4.32, 4.33 and 4.34, the density of methanol nanofluids decrease with increase in temperature. For example, the density of Al₂O₃-methanol nanofluids at 0.15 vol% is 818.56 kg/m³ at 01°C and 807.12 kg/m³ at 20 °C. The difference in density is 11.44 kg/m³ for Al₂O₃-methanol nanofluids. Similar results were found for SiO₂-methanol and TiO₂-methanol nanofluids. This is because, when the temperature decreases, the viscosity as well as the density of base fluids also decreases.

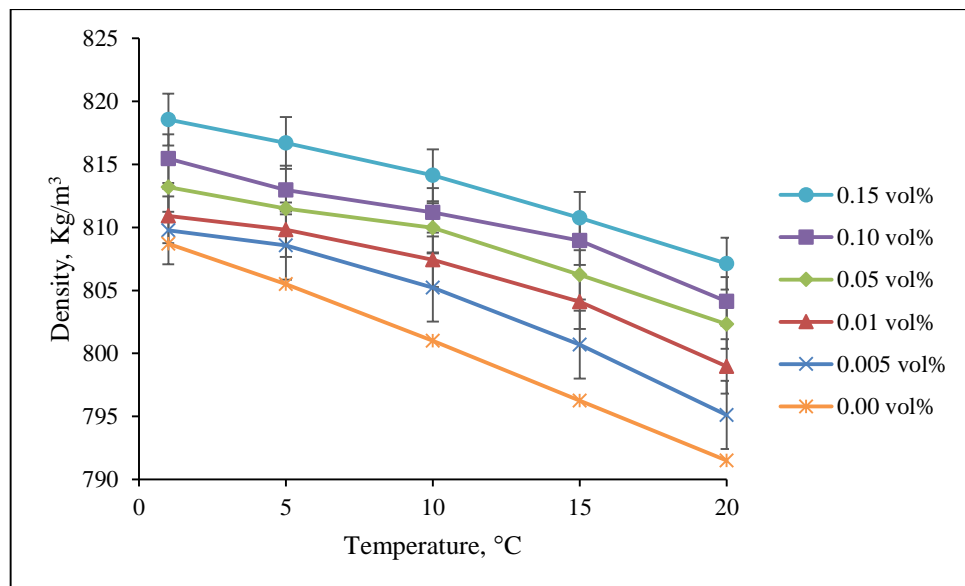


Figure 4.32: Density of Al₂O₃–methanol as a function of temperature and particle volume concentration.

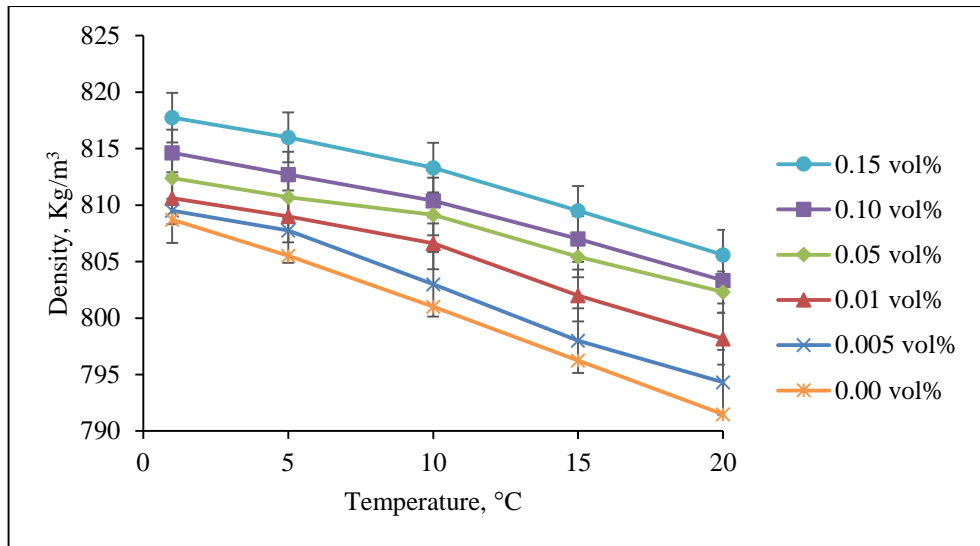


Figure 4.33: Density of SiO₂-methanol as a function of temperature and particle volume concentration.

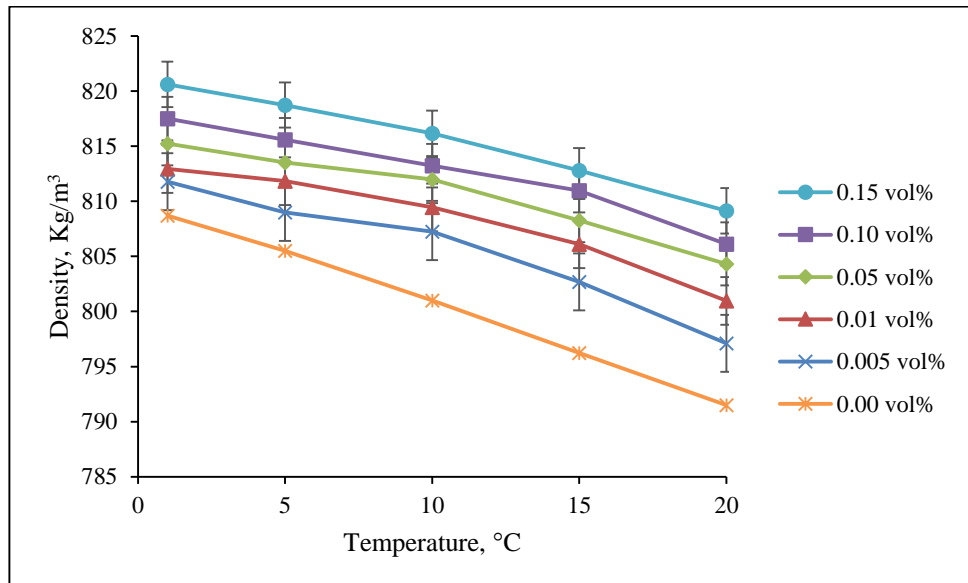


Figure 4.34: Density of TiO₂-methanol as a function of temperature and particle volume concentration.

The experimental value of density increases of methanol based nanofluids at 20 °C was compared with the model given by Pak and Choi (1998) shown in Figure 4.35. The experimental value was slightly higher than the existing correlation due to the difference in the density of the base fluids and water based nanofluids whereas Pak and Cho's model was proposed for the latter. The highest increases observed for TiO₂-methanol then Al₂O₃-methanol and SiO₂-methanol nanofluids. It may happen due to nanoparticles density difference.

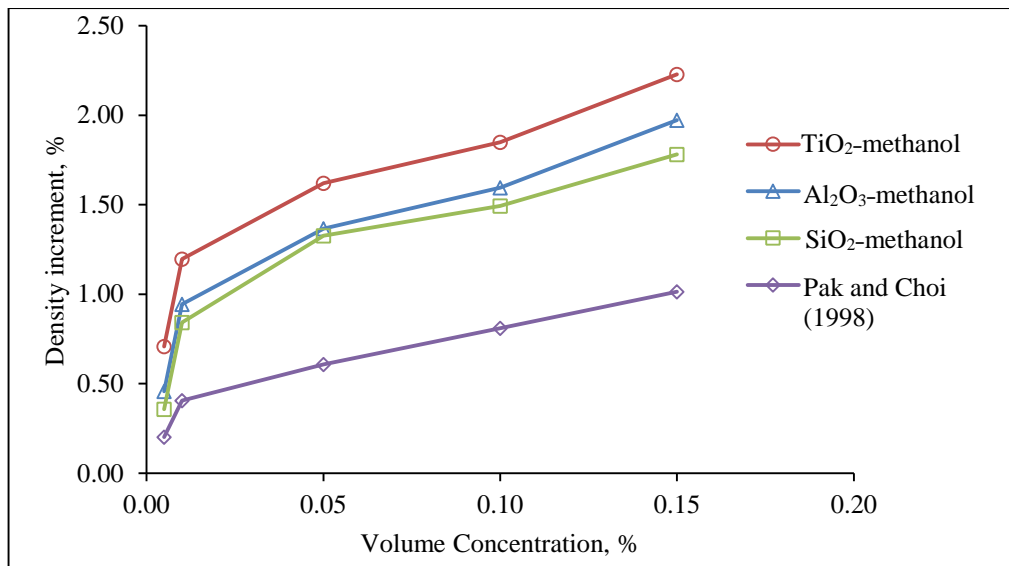


Figure 4.35: Comparison of density increment with the values from existing correlation.

4.5 Implication of this study

The findings of this study demonstrated an enhanced thermophysical properties of methanol based nanofluids compared with base fluids. Thus, the enhanced experimental values of thermophysical properties would allow methanol based nanofluids to be used in low temperature applications to avoid the freezing of working fluids. Methanol based working fluids can be applied in gravity aided and pool boiling applications in various heat pipe, electronics cooling, refrigeration and HVAC system.

CHAPTER 5 : CONCLUSIONS AND RECOMMENDATIONS

5.1 Introduction

The study was set out to explore the characterization of nanoparticles and thermophysical properties of methanol based nanofluids. Experiments were conducted to characterize Al_2O_3 , SiO_2 and TiO_2 nanoparticles, formulation of methanol based nanofluids, observe the stability and measure the thermal conductivity, viscosity and density of methanol based nanofluids. The section starts with some concluding remarks and finally concludes with some recommendations for future work.

5.2 Conclusions

From the comparative analysis and evaluation, the conclusions can be drawn as follows:

First of all, the characteristic peak of XRD results match with Joint committee on Powder Diffraction Standards (JCPDS) of Al_2O_3 , SiO_2 and TiO_2 nanoparticles and the particle size are almost as supplier mentioned.

The nanoparticles dispersed well and less agglomeration were found from Transmission Electron Microscope (TEM) viewing. TEM was also used to check the suspension uniformity, particle agglomeration and confirm the size distribution of particle in nanofluids.

In the second part, Al_2O_3 -methanol nanofluids found to be more stable compared to SiO_2 -methanol and TiO_2 -methanol nanofluids from sedimentation photograph captured to observe the sediment of suspension. UV-Visible spectrophotometer test and zeta potential test are also used to check the stability of methanol based nanofluids. The results shows, the absolute zeta potential value of Al_2O_3 -methanol nanofluids found higher compared to SiO_2 -methano and TiO_2 -methanol nanofluids.

Finally, the thermophysical properties of methanol based nanofluids is investigated. The thermal conductivity of methanol based nanofluids has increased with the increase of

nanoparticle volume fraction and temperature. Thermal conductivity enhancement was about 29.41%, 23.03% and 24.51% compared to base fluids for Al₂O₃, SiO₂ and TiO₂ nanoparticles, respectively with nanoparticles volume fraction of 0.15vol% and at temperature of 20°C. The values for thermal conductivity enhancement of Al₂O₃-methanol were approximately 6% and 5% higher compared to SiO₂ and TiO₂ nanoparticles for the same volume concentration and operating temperature. The experimental results show that, methanol based nanofluids is a non-Newtonian fluid. Volume fractions and temperature have significant effects over viscosity of methanol based nanofluids. Results indicate that viscosity increases with the increase of the particle volume fractions. However, viscosity decreases when temperature increases. The maximum viscosity increases is found to be 1.78%, 1.61% and 1.11% higher over the base fluids for TiO₂-methanol, Al₂O₃-methanol and SiO₂-methanol nanofluids respectively. Like viscosity, the density of methanol based nanofluids also increases with the enhancement of volume fraction. Similarly, it decreases with the increase of temperature. The highest increment observed for TiO₂-methanol than Al₂O₃-methanol and SiO₂-methanol nanofluids and the enhancement is 2.2%.

Finally, it can be concluded that Al₂O₃-methanol nanofluids have comparative good stability and good thermophysical properties. The types of nanoparticles, variation of temperature and volume concentrations have significant effect on thermophysical properties of methanol based nanofluids.

5.3 Recommendations for future work

The stability of methanol based nanofluids is not in satisfactory level. There are several techniques to improve the stability of the nanofluids for instance, addition of surfactant and pH control. Sodium dodecyl sulfate (SDS), Sodium dodecyl benzene sulphonate (SDBS), Dodecyl trimethyl ammonium bromide (DTAB), Sodium octanoate (SOCT), Hexadecyl trimethyl ammonium bromide (HCTAB), Polyvinylpyrrolidone (PVP) and

Arabic gum (AG) are the common surfactants used to improve stability of nanofluids. Therefore, the effect of surfactant on stability and thermophysical properties of methanol based nanofluids need to be investigated.

According to literature, pH value of 7-9 for Alumina (Huang et al., 2009) and pH 1-4 for Titania (Penkavova et al., 2011) provide good stability and the pH value are important for explaining the thermal conductivity of nanofluids (Prasher et al., 2006). Therefore, the variation of pH value of methanol based nanofluids need to be investigated.

Specific heat capacity, surface tension and latent heat of vaporization are the important properties of nanofluids. These properties need to be determined experimentally for methanol based nanofluids as they are directly related to the heat transfer performance analysis.

REFERENCES

- Arab, M., & Abbas, A. (2014). A model-based approach for analysis of working fluids in heat pipes. *Applied Thermal Engineering*, 73(1), 749-761.
- Aravind, S. J., Baskar, P., Baby, T. T., Sabareesh, R. K., Das, S., & Ramaprabhu, S. (2011). Investigation of structural stability, dispersion, viscosity, and conductive heat transfer properties of functionalized carbon nanotube based nanofluids. *The Journal of Physical Chemistry C*, 115(34), 16737-16744.
- Batchelor, G. (1977). The effect of Brownian motion on the bulk stress in a suspension of spherical particles. *Journal of Fluid Mechanics*, 83(01), 97-117.
- Beck, M. P., Yuan, Y., Warriar, P., & Teja, A. S. (2009). The effect of particle size on the thermal conductivity of alumina nanofluids. *Journal of Nanoparticle Research*, 11(5), 1129-1136.
- Bhattacharya, P., Saha, S., Yadav, A., Phelan, P., & Prasher, R. (2004). Brownian dynamics simulation to determine the effective thermal conductivity of nanofluids. *Journal of Applied Physics*, 95(11), 6492-6494.
- Brinkman, H. (1952). The viscosity of concentrated suspensions and solutions. *The Journal of Chemical Physics*, 20, 571.
- Bruggeman, D. A. G., (1935). Calculation of various physics constants in heterogenous substances I-dielectricity constants and conductivity of mixed bodies from isotropic substances. *Annalen der Physik, Leipzig*, 24, (7), 636-679.
- Cava, S., Tebcherani, S., Souza, I., Pianaro, S., Paskocimas, C., Longo, E., & Varela, J. (2007). Structural characterization of phase transition of Al₂O₃ nanopowders obtained by polymeric precursor method. *Materials Chemistry and Physics*, 103(2), 394-399.
- Chandrasekar, M., & Suresh, S. (2009). A review on the mechanisms of heat transport in nanofluids. *Heat Transfer Engineering*, 30(14), 1136-1150.
- Chandrasekar, M., Suresh, S., & Chandra Bose, A. (2010). Experimental investigations and theoretical determination of thermal conductivity and viscosity of Al₂O₃/water nanofluid. *Experimental Thermal and Fluid Science*, 34(2), 210-216.
- Chandrasekar, M., Suresh, S., Srinivasan, R., & Bose, A. C. (2009). New analytical models to investigate thermal conductivity of nanofluids. *Journal of nanoscience and nanotechnology*, 9(1), 533-538.

- Chen, H., Ding, Y., Lapkin, A., & Fan, X. (2009). Rheological behaviour of ethylene glycol-titanate nanotube nanofluids. *Journal of nanoparticle research*, 11(6), 1513-1520.
- Chen, H., Ding, Y., & Tan, C. (2007). Rheological behaviour of nanofluids. *New Journal of Physics*, 9(10), 367.
- Chen, H., Witharana, S., Jin, Y., Kim, C., & Ding, Y. (2009). Predicting thermal conductivity of liquid suspensions of nanoparticles (nanofluids) based on rheology. *Particuology*, 7(2), 151-157.
- Chevalier, J., Tillement, O., & Ayela, F. (2007). Rheological properties of nanofluids flowing through microchannels. *Applied physics letters*, 91(23), 233103-233103-233103.
- Choi, S. U., & Eastman, J. (1995). Enhancing thermal conductivity of fluids with nanoparticles: Argonne National Lab., IL (United States).
- Chon, C.H., Kihm, K.D., Lee, S. P., & Choi, S. U. S. (2005). Empirical correlation finding the role of temperature and particle size for nanofluid (Al_2O_3) thermal conductivity enhancement *Applied physics letters*, 87 (15)
- Clerk Maxwell, J. (1873). A treatise on electricity and magnetism. *Also available on enwikisource.org/wiki/A_Treatise_on_Electricity_and_Magnetism.*
- Das, S. K., Choi, S. U., Yu, W., & Pradeep, T. (2008). *Nanofluids: science and technology*: Wiley-Interscience Hoboken, NJ.
- Das, S. K., Putra, N., & Roetzel, W. (2003). Pool boiling characteristics of nano-fluids. *International Journal of Heat and Mass Transfer*, 46(5), 851-862.
- Dincer, I., & Kanoglu, M. (2010). *Refrigeration Systems and Applications*: Wiley.
- Dinh, K (1996) Heat pipe in HVAC, in Heat Pipe Technology. Pergamon, London. Pp 357-363.
- Duangthongsuk, W., & Wongwises, S. (2009). Measurement of temperature-dependent thermal conductivity and viscosity of TiO_2 -water nanofluids. *Experimental Thermal and Fluid Science*, 33(4), 706-714.
- Einstein, A. (1906). A new determination of molecular dimensions. *Annalen der Physik*, 19 (4), 289-306.

- Elias, M. M., Mahbubul, I. M., Saidur, R., Sohel, M. R., Shahrul, I. M., Khaleduzzaman, S. S., & Sadeghipour, S. (2014). Experimental investigation on the thermo-physical properties of Al₂O₃ nanoparticles suspended in car radiator coolant. *International Communications in Heat and Mass Transfer*, 54(0), 48-53.
- Feng, Y., Yu, B., Xu, P., & Zou, M. (2007). The effective thermal conductivity of nanofluids based on the nanolayer and the aggregation of nanoparticles. *Journal of Physics D: Applied Physics*, 40(10), 3164.
- Firouzfard, E., Soltanieh, M., Noie, S. H., & Saidi, S. H. (2011). Energy saving in HVAC systems using nanofluid. *Applied Thermal Engineering*, 31(8–9), 1543-1545.
- Gamer, S. D. (1996) Heat pipe for electronics cooling application. *Electronics cooling* Spetember 1-9.
- Gao, J., Zheng, R., Ohtani, H., Zhu, D., & Chen, G. (2009). Experimental investigation of heat conduction mechanisms in nanofluids. Clue on clustering. *Nano letters*, 9(12), 4128-4132.
- H. Masuda, A. E., K. Terama, N. Hishinuma,. (1993). Alteration of thermal conductivity and viscosity of liquid by dispersing ultra-fine particles (Dispersion of Al₂O₃, SiO₂ and TiO₂ ultra-fine particles). *Netsu Bussei (Japan)*, 7, 227-233.
- Hamilton, R., & Crosser, O. (1962). Thermal conductivity of heterogeneous two-component systems. *Industrial & Engineering chemistry fundamentals*, 1(3), 187-191.
- Herold, K. E., & Rasooly, A. (2009). *Lab on a Chip Technology: Fabrication and microfluidics* (Vol. 1): Horizon Scientific Press.
- Ho, C., Liu, W., Chang, Y., & Lin, C. (2010). Natural convection heat transfer of alumina-water nanofluid in vertical square enclosures: an experimental study. *International Journal of Thermal Sciences*, 49(8), 1345-1353.
- Hojjat, M., Etemad, S. G., Bagheri, R., & Thibault, J. (2009). *The thermal conductivity of non-Newtonian nanofluids*. Paper presented at the 8th World Congress of Chemical Engineering, Montreal, Canada.
- Hong, K., Hong, T.-K., & Yang, H.-S. (2006). Thermal conductivity of Fe nanofluids depending on the cluster size of nanoparticles. *Applied Physics Letters*, 88(3), 031901.

- Huang, J., Wang, X., Long, Q., Wen, X., Zhou, Y., & Li, L. (2009). *Influence of pH on the stability characteristics of nanofluids*. Paper presented at the Photonics and Optoelectronics, 2009. SOPO 2009. Symposium on.
- Jiang, L., Gao, L., & Sun, J. (2003). Production of aqueous colloidal dispersions of carbon nanotubes. *Journal of Colloid and Interface Science*, 260(1), 89-94.
- Ju, Y. S., Kim, J., & Hung, M.-T. (2008). Experimental study of heat conduction in aqueous suspensions of aluminum oxide nanoparticles. *Journal of Heat Transfer*, 130(9), 092403.
- Jung, J.-Y., Lee, J. W., & Kang, Y. T. (2012). CO₂ absorption characteristics of nanoparticle suspensions in methanol. *Journal of mechanical science and technology*, 26(8), 2285-2290.
- Kebllinski, P., Eastman, J. A., & Cahill, D. G. (2005). Nanofluids for thermal transport. *Materials Today*, 8(6), 36-44.
- Kim, J.-K., Jung, J. Y., & Kang, Y. T. (2007). Absorption performance enhancement by nano-particles and chemical surfactants in binary nanofluids. *International Journal of Refrigeration*, 30(1), 50-57.
- Kim, J. H., Jung, C. W., & Kang, Y. T. (2014). Mass transfer enhancement during CO₂ absorption process in methanol/Al₂O₃ nanofluids. *International Journal of Heat and Mass Transfer*, 76(0), 484-491.
- Krieger, I. M., & Dougherty, T. J. (1959). A Mechanism for Non-Newtonian Flow in Suspensions of Rigid Spheres. *Transactions of The Society of Rheology (1957-1977)*, 3(1), 137-152.
- Krishnamurthy, S., Bhattacharya, P., Phelan, P., & Prasher, R. (2006). Enhanced mass transport in nanofluids. *Nano Letters*, 6(3), 419-423.
- Kulkarni, D. P., Das, D. K., & Chukwu, G. A. (2006). Temperature dependent rheological property of copper oxide nanoparticles suspension (nanofluid). *Journal of nanoscience and nanotechnology*, 6(4), 1150-1154.
- Lee, J.-H., Hwang, K. S., Jang, S. P., Lee, B. H., Kim, J. H., Choi, S. U., & Choi, C. J. (2008). Effective viscosities and thermal conductivities of aqueous nanofluids containing low volume concentrations of Al₂O₃ nanoparticles. *International Journal of Heat and Mass Transfer*, 51(11), 2651-2656.

- Lee, J. W., Jung, J.-Y., Lee, S.-G., & Kang, Y. T. (2011). CO₂ bubble absorption enhancement in methanol-based nanofluids. *International Journal of Refrigeration*, 34(8), 1727-1733.
- Lee, J. W., & Kang, Y. T. (2013). CO₂ absorption enhancement by Al₂O₃ nanoparticles in NaCl aqueous solution. *Energy*, 53(0), 206-211.
- Lee, K., Hwang, Y., Cheong, S., Kwon, L., Kim, S., & Lee, J. (2009). Performance evaluation of nano-lubricants of fullerene nanoparticles in refrigeration mineral oil. *Current Applied Physics*, 9(2), e128-e131.
- Lee, S., Choi, S. U., Li, S., and, & Eastman, J. (1999). Measuring thermal conductivity of fluids containing oxide nanoparticles. *Journal of Heat Transfer*, 121(2).
- Lee, S. W., Park, S. D., Kang, S., Bang, I. C., & Kim, J. H. (2011). Investigation of viscosity and thermal conductivity of SiC nanofluids for heat transfer applications. *International Journal of Heat and Mass Transfer*, 54(1-3), 433-438.
- Lefèvre, F., Conrardy, J.-B., Raynaud, M., & Bonjour, J. (2012). Experimental investigations of flat plate heat pipes with screen meshes or grooves covered with screen meshes as capillary structure. *Applied Thermal Engineering*, 37(0), 95-102.
- Li, C. H., & Peterson, G. (2006). Experimental investigation of temperature and volume fraction variations on the effective thermal conductivity of nanoparticle suspensions (nanofluids). *Journal of Applied Physics*, 99(8), 084314.
- Li, X., Zhu, D., Wang, X., Wang, N., Gao, J., & Li, H. (2008). Thermal conductivity enhancement dependent pH and chemical surfactant for Cu-H₂O nanofluids. *Thermochimica Acta*, 469(1), 98-103.
- Li, Y., Zhou, J. e., Tung, S., Schneider, E., & Xi, S. (2009). A review on development of nanofluid preparation and characterization. *Powder Technology*, 196(2), 89-101.
- Liu, M.-S., Lin, M. C.-C., Tsai, C., & Wang, C.-C. (2006). Enhancement of thermal conductivity with Cu for nanofluids using chemical reduction method. *International Journal of Heat and Mass Transfer*, 49(17), 3028-3033.
- Longo, G. A., & Zilio, C. (2011). Experimental measurement of thermophysical properties of oxide-water nano-fluids down to ice-point. *Experimental Thermal and Fluid Science*, 35(7), 1313-1324.

- Lu, W.-Q., & Fan, Q.-M. (2008). Study for the particle's scale effect on some thermophysical properties of nanofluids by a simplified molecular dynamics method. *Engineering analysis with boundary elements*, 32(4), 282-289.
- Mahbubul, I., Saidur, R., & Amalina, M. (2012). Investigation of viscosity of R123-TiO₂ nanorefrigerant. *Int. J. Mech. Mater. Eng*, 7(2), 146-151.
- Mahbubul, I. M., Saidur, R., & Amalina, M. A. (2012). Latest developments on the viscosity of nanofluids. *International Journal of Heat and Mass Transfer*, 55(4), 874-885.
- Mahbubul, I. M., Saidur, R., & Amalina, M. A. (2013). Influence of particle concentration and temperature on thermal conductivity and viscosity of Al₂O₃/R141b nanorefrigerant. *International Communications in Heat and Mass Transfer*, 43(0), 100-104.
- Maïga, S. E. B., Nguyen, C. T., Galanis, N., & Roy, G. (2004). Heat transfer behaviours of nanofluids in a uniformly heated tube. *Superlattices and Microstructures*, 35(3), 543-557.
- Mallick, K., Jarvis, A., Fisher, J. B., Tu, K. P., Boegh, E., & Niyogi, D. (2013). Latent Heat Flux and Canopy Conductance Based on Penman–Monteith, Priestley–Taylor Equation, and Bouchet's Complementary Hypothesis. *Journal of Hydrometeorology*, 14(2), 419-442.
- Mariano, A., Pastoriza-Gallego, M. J., Lugo, L., Camacho, A., Canzonieri, S., & Piñeiro, M. M. (2013). Thermal conductivity, rheological behaviour and density of non-Newtonian ethylene glycol-based SnO₂ nanofluids. *Fluid Phase Equilibria*, 337, 119-124.
- Mintsa, H. A., Roy, G., Nguyen, C. T., & Doucet, D. (2009). New temperature dependent thermal conductivity data for water-based nanofluids. *International Journal of Thermal Sciences*, 48(2), 363-371.
- Murshed, S. M. S., Leong, K. C., & Yang, C. (2008). Investigations of thermal conductivity and viscosity of nanofluids. *International Journal of Thermal Sciences*, 47(5), 560-568.
- Namburu, P. K., Kulkarni, D. P., Misra, D., & Das, D. K. (2007). Viscosity of copper oxide nanoparticles dispersed in ethylene glycol and water mixture. *Experimental Thermal and Fluid Science*, 32(2), 397-402.
- Nguyen, C. T., Desgranges, F., Galanis, N., Roy, G., Maré, T., Boucher, S., & Angue Mintsa, H. (2008). Viscosity data for Al₂O₃–water nanofluid—hysteresis: is heat

transfer enhancement using nanofluids reliable? *International Journal of Thermal Sciences*, 47(2), 103-111.

Nguyen, C. T., Desgranges, F., Roy, G., Galanis, N., Maré, T., Boucher, S., & Angue Mintsa, H. (2007). Temperature and particle-size dependent viscosity data for water-based nanofluids – Hysteresis phenomenon. *International Journal of Heat and Fluid Flow*, 28(6), 1492-1506.

Nielsen, L. E. (1970). Generalized equation for the elastic moduli of composite materials. *Journal of Applied Physics*, 41(11), 4626-4627.

Pak, B. C., & Cho, Y. I. (1998). Hydrodynamic and heat transfer study of dispersed fluids with submicron metallic oxide particles. *Experimental Heat Transfer an International Journal*, 11(2), 151-170.

Pang, C., Jung, J.-Y., & Kang, Y. T. (2013). Thermal conductivity enhancement of Al₂O₃ nanofluids based on the mixtures of aqueous NaCl solution and CH₃OH. *International Journal of Heat and Mass Transfer*, 56(1–2), 94-100.

Pang, C., Jung, J.-Y., Lee, J. W., & Kang, Y. T. (2012). Thermal conductivity measurement of methanol-based nanofluids with Al₂O₃ and SiO₂ nanoparticles. *International Journal of Heat and Mass Transfer*, 55(21–22), 5597-5602. doi:

Perez-Lombard, L., Ortiz, J., & Pout, C. (2008). A review on building energy consumption information *Energy and buildings*, 40(3), 394-398.

Patel, H. E., Sundararajan, T., & Das, S. K. (2010). An experimental investigation into the thermal conductivity enhancement in oxide and metallic nanofluids. *Journal of Nanoparticle Research*, 12(3), 1015-1031.

Peng, H., Ding, G., Jiang, W., Hu, H., & Gao, Y. (2009). Heat transfer characteristics of refrigerant-based nanofluid flow boiling inside a horizontal smooth tube. *International journal of refrigeration*, 32(6), 1259-1270.

Penkavova, V., Tihon, J., & Wein, O. (2011). Stability and rheology of dilute TiO₂-water nanofluids. *Nanoscale research letters*, 6(1), 1-7.

Philip, J., & Shima, P. D. (2014). Role of Thermal Conductivity of Dispersed Nanoparticle on Heat Transfer Properties of Nanofluids. *Industrial & Engineering Chemistry Research*.

Pineda, I. T., Choi, C. K., & Kang, Y. T. (2014). CO₂ gas absorption by CH₃OH based nanofluids in an annular contactor at low rotational speeds. *International Journal of Greenhouse Gas Control*, 23(0), 105-112.

- Prasher, R., Phelan, P. E., & Bhattacharya, P. (2006). Effect of aggregation kinetics on the thermal conductivity of nanoscale colloidal solutions (nanofluid). *Nano Letters*, 6(7), 1529-1534.
- S.M.S. Murshed, K. C. L., C. Yang. (2005). Enhanced thermal conductivity of TiO₂-water based nanofluids. *International Journal of Thermal Sciences*, 44, 367.
- Saidur, R., Leong, K. Y., & Mohammad, H. A. (2011). A review on applications and challenges of nanofluids. *Renewable and Sustainable Energy Reviews*, 15(3), 1646-1668.
- Shames, A., Osipov, V. Y., Von Bardeleben, H., & Vul, A. Y. (2012). Spin S= 1 centers: a universal type of paramagnetic defects in nanodiamonds of dynamic synthesis. *Journal of Physics: Condensed Matter*, 24(22), 225302.
- Shanker, N. S., Reddy, M. C. S., & Rao, V. B. (2012). *On prediction of viscosity of nanofluids for low volume fractions of nanoparticles*. Paper presented at the International Journal of Engineering Research and Technology.
- Shukla, R., Bansal, V., Chaudhary, M., Basu, A., Bhonde, R. R., & Sastry, M. (2005). Biocompatibility of gold nanoparticles and their endocytotic fate inside the cellular compartment: a microscopic overview. *Langmuir*, 21(23), 10644-10654.
- Shukla, R. K., & Dhir, V. K. (2005). *Study of the effective thermal conductivity of nanofluids*. Paper presented at the ASME 2005 International Mechanical Engineering Congress and Exposition.
- SiO₂ XRD pattern). Retrieved 12.01.2015, from <http://www.sigmaaldrich.com>
- Smalley, R. E. (2005). Future global energy prosperity: the terawatt challenge. *Mrs Bulletin*, 30(06), 412-417.
- Song, S., Peng, C., Gonzalez-Olivares, M. A., Lopez-Valdivieso, A., & Fort, T. (2005). Study on hydration layers near nanoscale silica dispersed in aqueous solutions through viscosity measurement. *Journal of Colloid and Interface Science*, 287(1), 114-120..
- Sommers, A. D., & Yerkes, K. L. (2010). Experimental investigation into the convective heat transfer and system-level effects of Al₂O₃-propanol nanofluid. *Journal of Nanoparticle Research*, 12(3), 1003-1014.
- Thermophysical Properties - Methanol). Retrieved 11.09.2013, from <http://www.engineeringtoolbox.com>

- Timofeeva, E. V., Gavrilov, A. N., McCloskey, J. M., Tolmachev, Y. V., Sprunt, S., Lopatina, L. M., & Selinger, J. V. (2007). Thermal conductivity and particle agglomeration in alumina nanofluids: experiment and theory. *Physical Review E*, 76(6), 061203.
- Torres Pineda, I., Lee, J. W., Jung, I., & Kang, Y. T. (2012). CO₂ absorption enhancement by methanol-based Al₂O₃ and SiO₂ nanofluids in a tray column absorber. *International Journal of Refrigeration*, 35(5), 1402-1409.
- Tseng, W. J., & Lin, K.-C. (2003). Rheology and colloidal structure of aqueous TiO₂ nanoparticle suspensions. *Materials Science and Engineering: A*, 355(1–2), 186-192.
- Turgut, A., Tavman, I., Chirtoc, M., Schuchmann, H., Sauter, C., & Tavman, S. (2009). Thermal conductivity and viscosity measurements of water-based TiO₂ nanofluids. *International Journal of Thermophysics*, 30(4), 1213-1226.
- Vajjha, R. S., & Das, D. K. (2009). Experimental determination of thermal conductivity of three nanofluids and development of new correlations. *International Journal of Heat and Mass Transfer*, 52(21–22), 4675-4682.
- Wang, X.-j., & Zhu, D.-s. (2009). Investigation of pH and SDBS on enhancement of thermal conductivity in nanofluids. *Chemical Physics Letters*, 470(1), 107-111.
- Wang, X.-Q., & Mujumdar, A. S. (2007). Heat transfer characteristics of nanofluids: a review. *International Journal of Thermal Sciences*, 46(1), 1-19.
- Wasp, E. J., Kenny, J. P., & Gandhi, R. L. (1977). Solid--liquid flow: slurry pipeline transportation.[Pumps, valves, mechanical equipment, economics]. *Ser. Bulk Mater. Handl.:(United States)*, 1(4).
- Wong, S.-C., Lin, Y.-C., & Liou, J.-H. (2012). Visualization and evaporator resistance measurement in heat pipes charged with water, methanol or acetone. *International Journal of Thermal Sciences*, 52(0), 154-160.
- Wu, D., Zhu, H., Wang, L., & Liu, L. (2009). Critical issues in nanofluids preparation, characterization and thermal conductivity. *Current Nanoscience*, 5(1), 103-112.
- Xia, G., Jiang, H., Liu, R., & Zhai, Y. (2014). Effects of surfactant on the stability and thermal conductivity of Al₂O₃/de-ionized water nanofluids. *International Journal of Thermal Sciences*, 84(0), 118-124.

- Xie, H., Wang, J., Xi, T., Liu, Y., Ai, F., & Wu, Q. (2002). Thermal conductivity enhancement of suspensions containing nanosized alumina particles. *Journal of Applied Physics*, 91(7), 4568-4572.
- Yu, W., & Choi, S. (2003). The role of interfacial layers in the enhanced thermal conductivity of nanofluids: a renovated Maxwell model. *Journal of Nanoparticle Research*, 5(1-2), 167-171.
- Yu, W., Xie, H., Chen, L., & Li, Y. (2010). Enhancement of thermal conductivity of kerosene-based Fe₃O₄ nanofluids prepared via phase-transfer method. *Colloids and Surfaces A: Physicochemical and Engineering Aspects*, 355(1), 109-113.
- Zhang, X., Gu, H., & Fujii, M. (2007). Effective thermal conductivity and thermal diffusivity of nanofluids containing spherical and cylindrical nanoparticles. *Experimental Thermal and Fluid Science*, 31(6), 593-599.
- Zhu, H.-t., Lin, Y.-s., & Yin, Y.-s. (2004). A novel one-step chemical method for preparation of copper nanofluids. *Journal of colloid and interface science*, 277(1), 100-103.
- Zhu, H., Zhang, C., Liu, S., Tang, Y., & Yin, Y. (2006). Effects of nanoparticle clustering and alignment on thermal conductivities of Fe₃O₄ aqueous nanofluids. *Applied Physics Letters*, 89(2), 023123.

LIST OF PUBLICATION AND PRESENTATION

Journal paper:

1. **R.M. Mostafizur**, M.H.U. Bhuiyan, R. Saidur, A.R. Abdul Aziz, Thermal conductivity variation for methanol based nanofluids, International Journal of Heat and Mass Transfer, 76(0) (2014) 350-356. **(Q1, IF: 2.38)**
2. **R.M. Mostafizur**, A.R. Abdul Aziz, R. Saidur, M.H.U. Bhuiyan, I.M. Mahbubul, Effect of temperature and volume fraction on rheology of methanol based nanofluids, International Journal of Heat and Mass Transfer, 77(0) (2014) 765-769. **(Q1, IF: 2.38)**
3. **R.M. Mostafizur**, R. Saidur, A.R. Abdul Aziz, M.H.U. Bhuiyan, Thermophysical properties of methanol based Al₂O₃ nanofluids, International Journal of Heat and Mass Transfer, 85 (0) (2015) 414-419. **(Q1, IF: 2.38)**

Conference paper:

1. **R.M. Mostafizur**, R. Saidur, A.R. Abdul Aziz, M.H.U. Bhuiyan, Investigation on stability and density of methanol based TiO₂ nanofluids, 7th International Conference on Cooling & Heating Technologies (ICCHT 2014), 4th – 6th November 2014, Subang Jaya, Selangor, Malaysia.
2. **R.M. Mostafizur**, R. Saidur, A.R. Abdul Aziz, M.H.U. Bhuiyan, Viscosity measurement of methanol based SiO₂ nanofluids, 6th BSME International Conference on Thermal Engineering (ICTE 2014) December 19-21, 2014, Dhaka, Bangladesh.

APPENDIXES

APPENDIX A: CHEMICAL ELEMENTS COMPOSITION OF NANOPARTICLES

The element composition of Al_2O_3 , SiO_2 and TiO_2 nanoparticles are analyzed using Energy dispersive spectrometry (EDS) system.

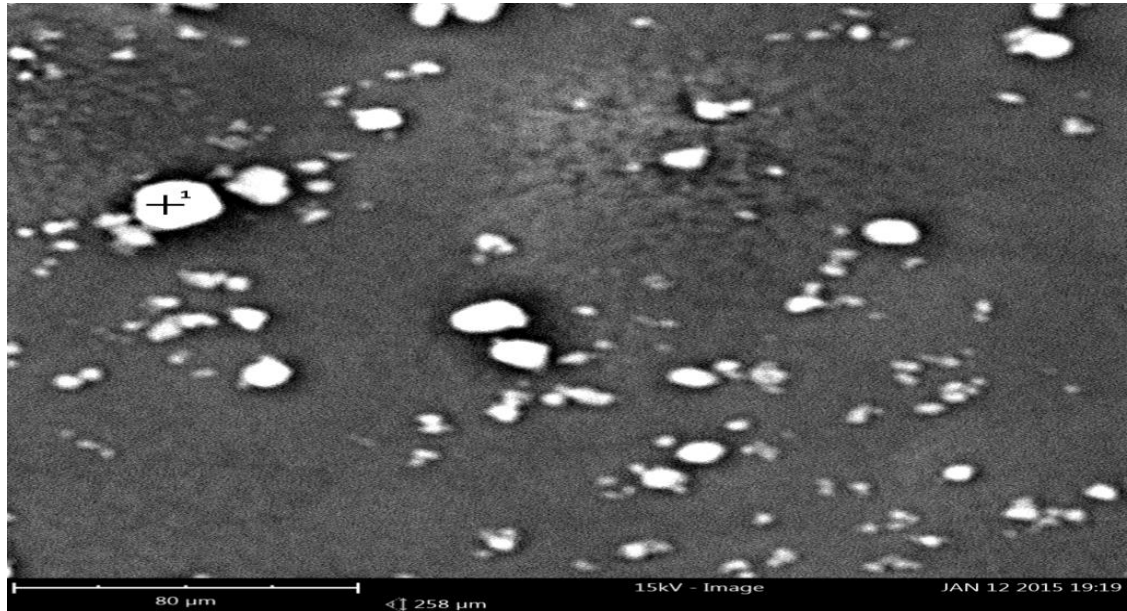


Figure A.1: SEM image of Al_2O_3 nanoparticles during EDS analysis with the marking of point 1

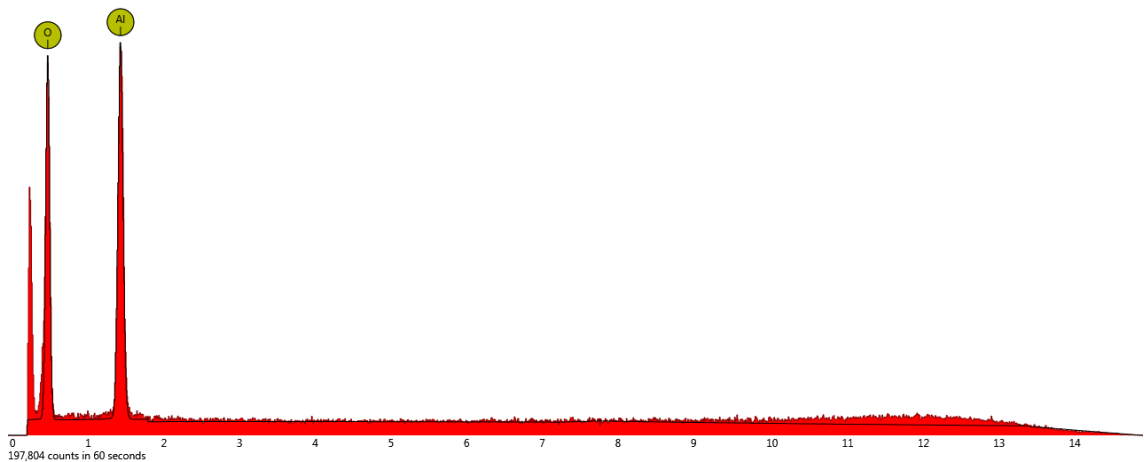


Figure A.2: EDS analysis of Al_2O_3 nanoparticles at point 1.

Table A.1: Chemical Elemental composition of Al₂O₃ nanoparticles by EDS analysis at point 1.

Element	Atomic (%)	Weight (%)
Al	22.9	33.4
O	77.1	66.6

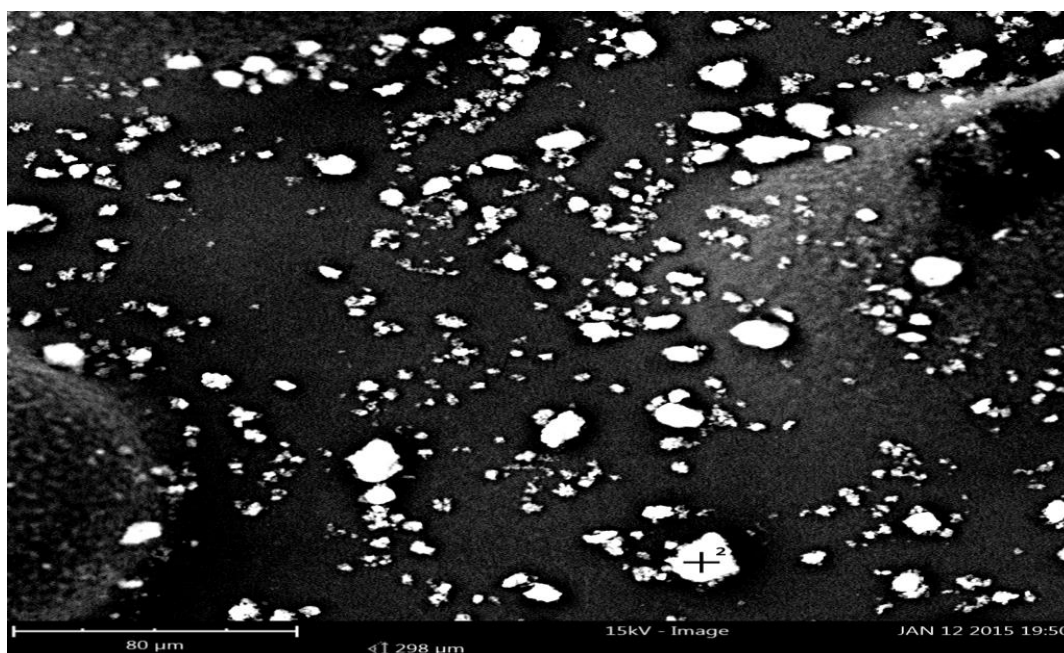


Figure A.3: SEM image of SiO₂ nanoparticles during EDS analysis with the marking of point 2.

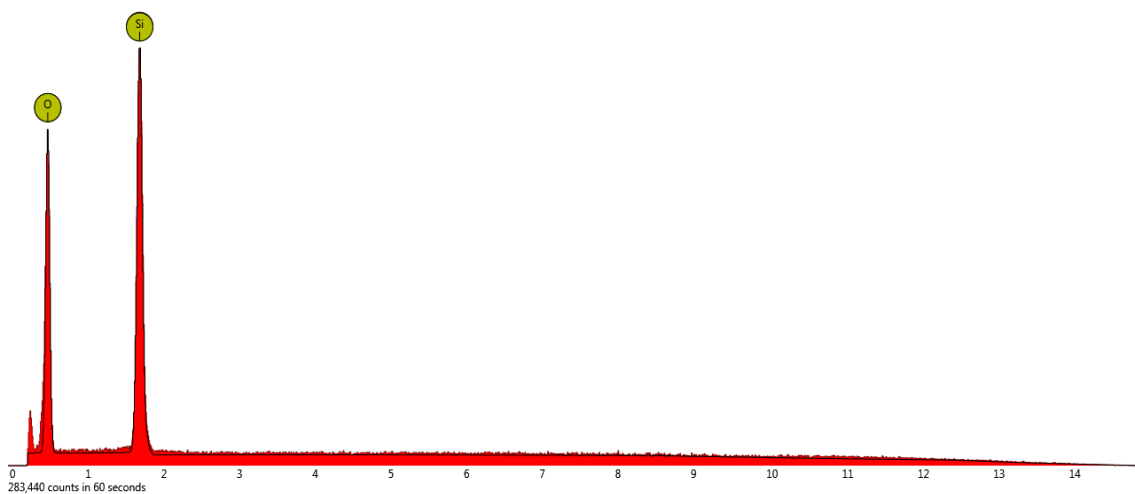


Figure A.4: EDS analysis of SiO₂ nanoparticles at point 2.

Table A.2: Chemical Elemental composition of SiO₂ nanoparticles by EDS analysis at point 2.

Element	Atomic (%)	Weight (%)
Si	19.8	30.3
O	80.2	69.7

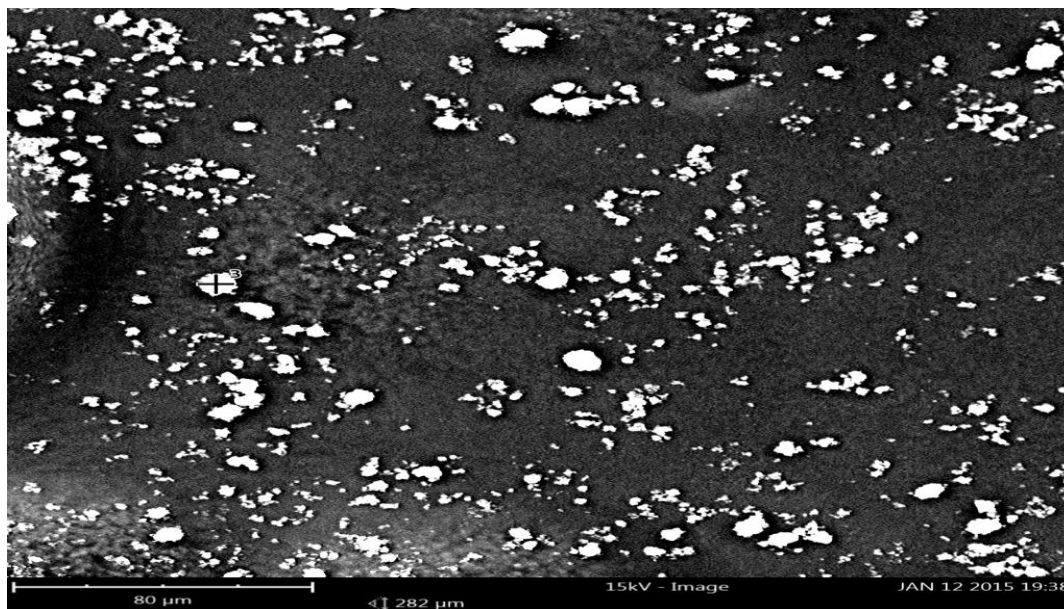


Figure A.5: SEM image of TiO₂ nanoparticles during EDS analysis with the marking of point 3.

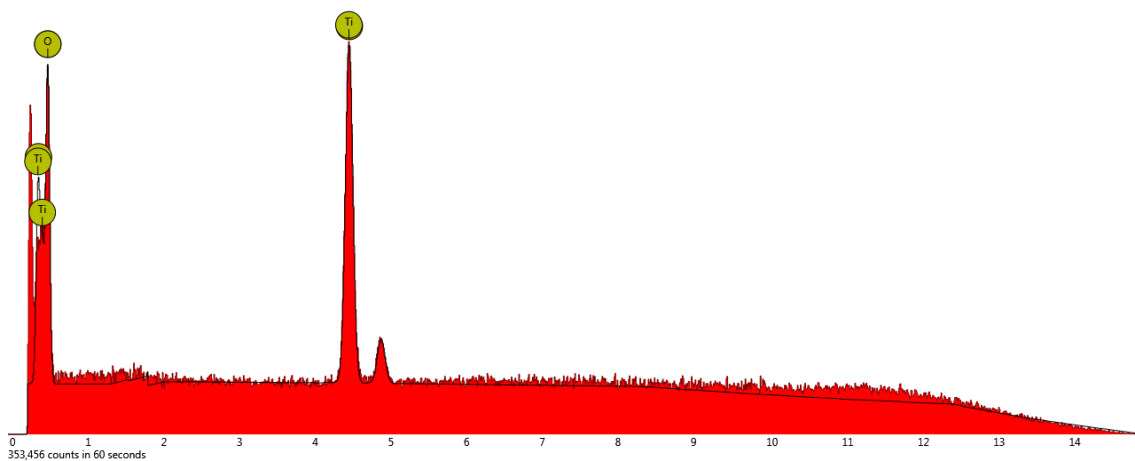


Figure A.6: EDS analysis of TiO₂ nanoparticles at point 3.

Table A.3: Chemical Elemental composition of TiO₂ nanoparticles by EDS analysis at point 3.

Element	Atomic (%)	Weight (%)
Ti	13.4	31.7
O	86.6	68.3

APPENDIX B: NANOPARTICLES SIZE MEASUREMENT

TEM image of Al_2O_3 -methanol, SiO_2 - methanol and TiO_2 -methanol nanofluids with measurements of the approximate diameter of some of the individual particle are shown in below.

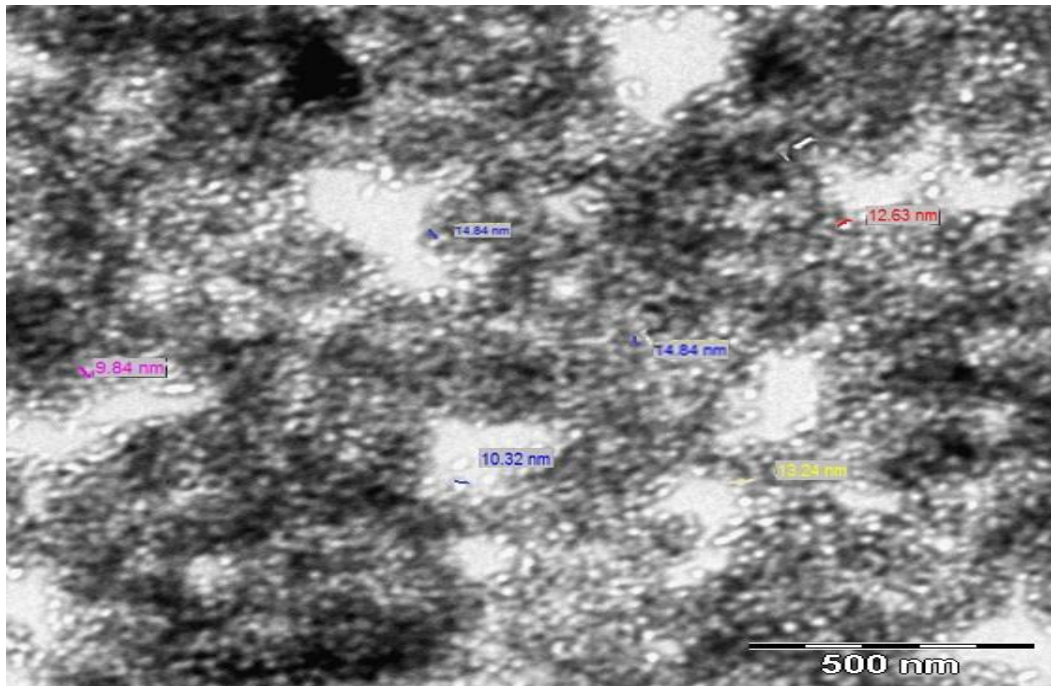


Figure B.1: TEM image of Al_2O_3 -methanol nanofluids with the approximate measurement of some particle's diameter.

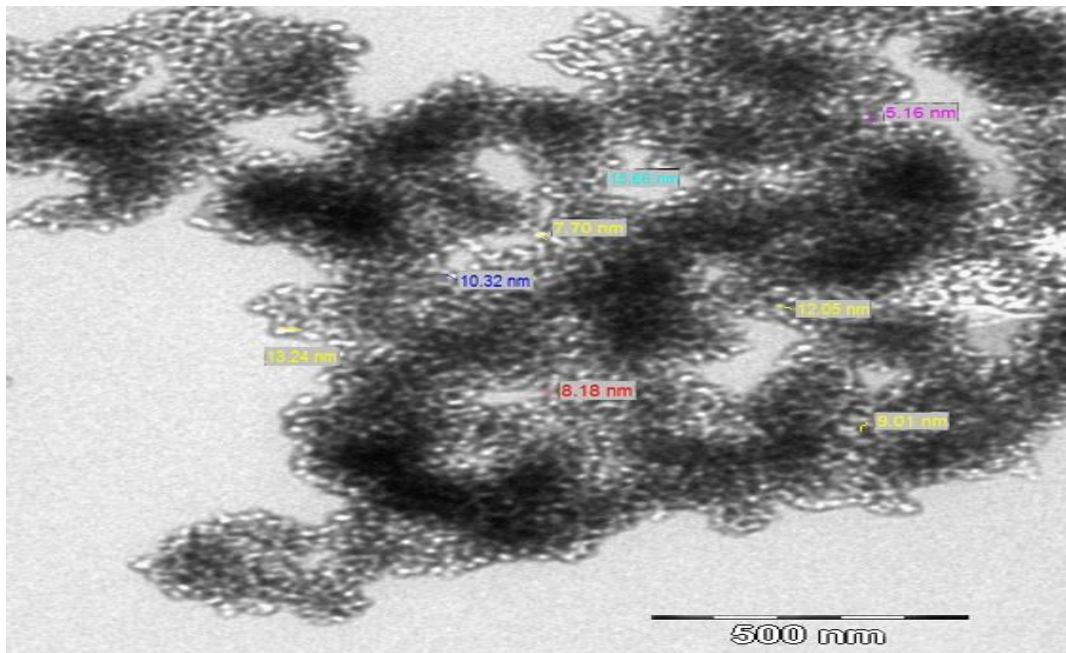


Figure B. 2: TEM image of SiO₂-methanol nanofluids with the approximate measurement of some particle's diameter.

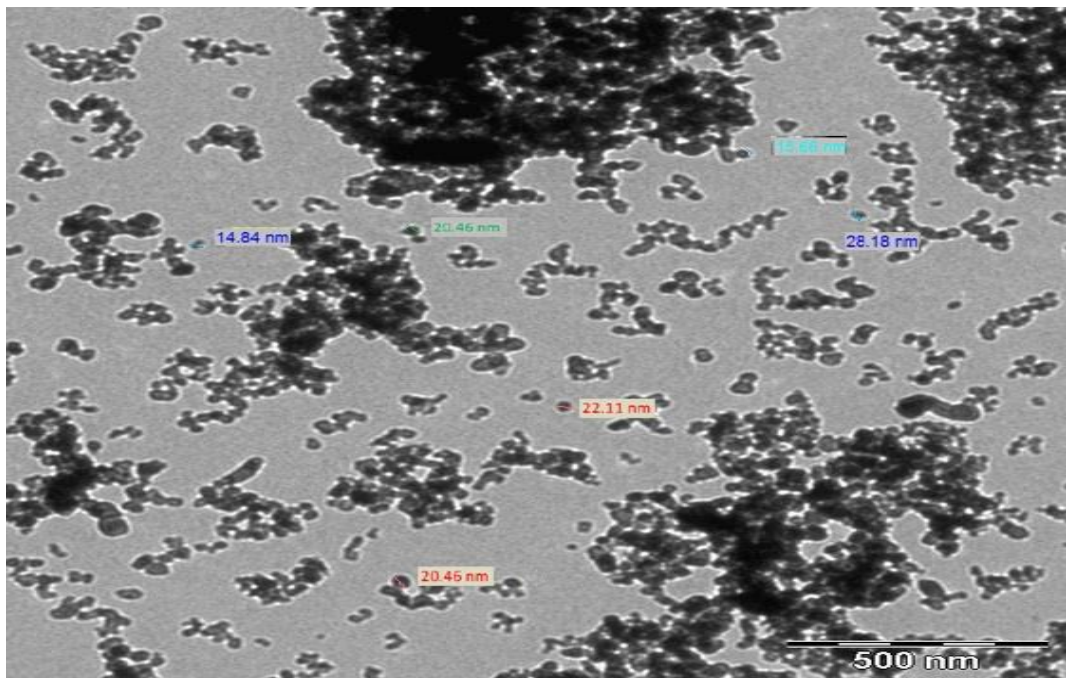


Figure B.3: TEM image of TiO₂-methanol nanofluids with the approximate measurement of some particle's diameter.

APPENDIX C: VOLUME DISTRIBUTION WITHIN THE NANOFLUIDS

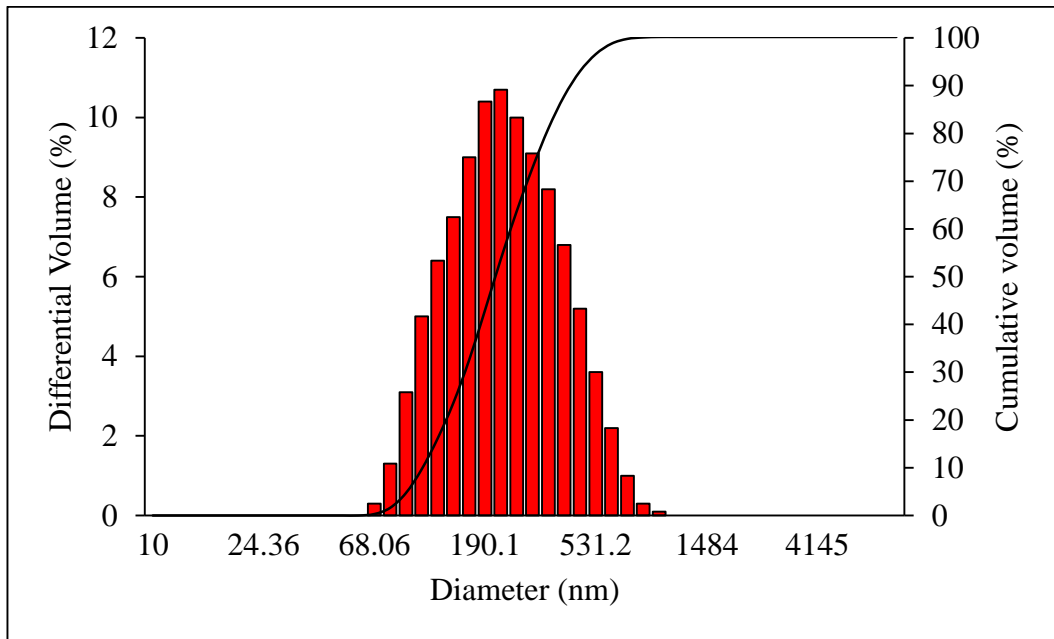


Figure C.1: Volume distribution of nanoparticle size within the 0.10 vol% of Al₂O₃-methanol nanofluids

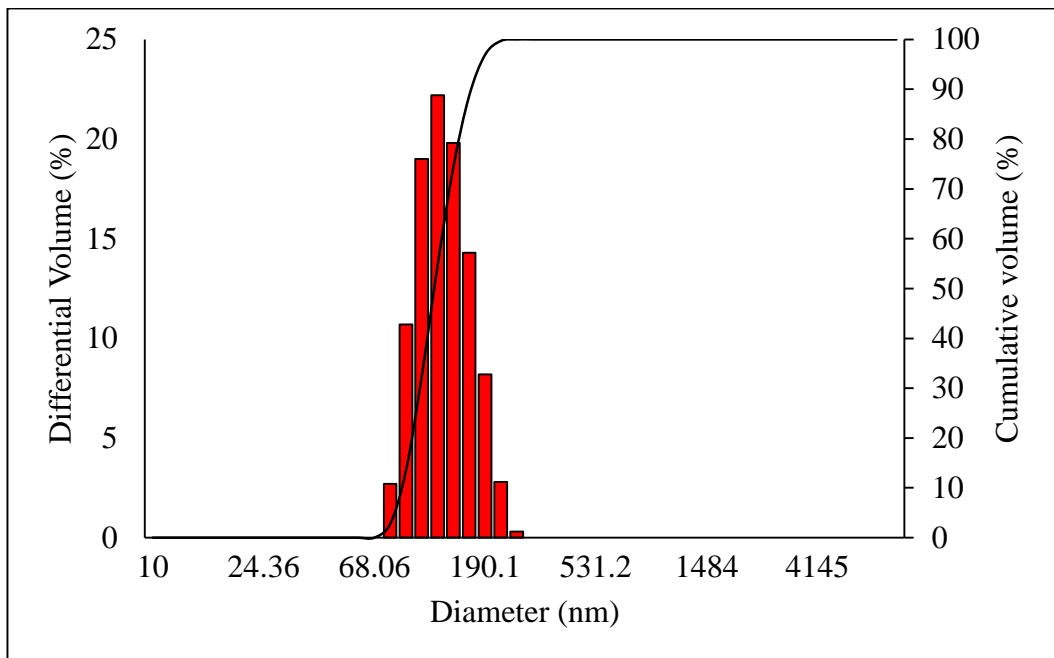


Figure C.2: Volume distribution of nanoparticle size within the 0.05 vol% of SiO₂-methanol nanofluids

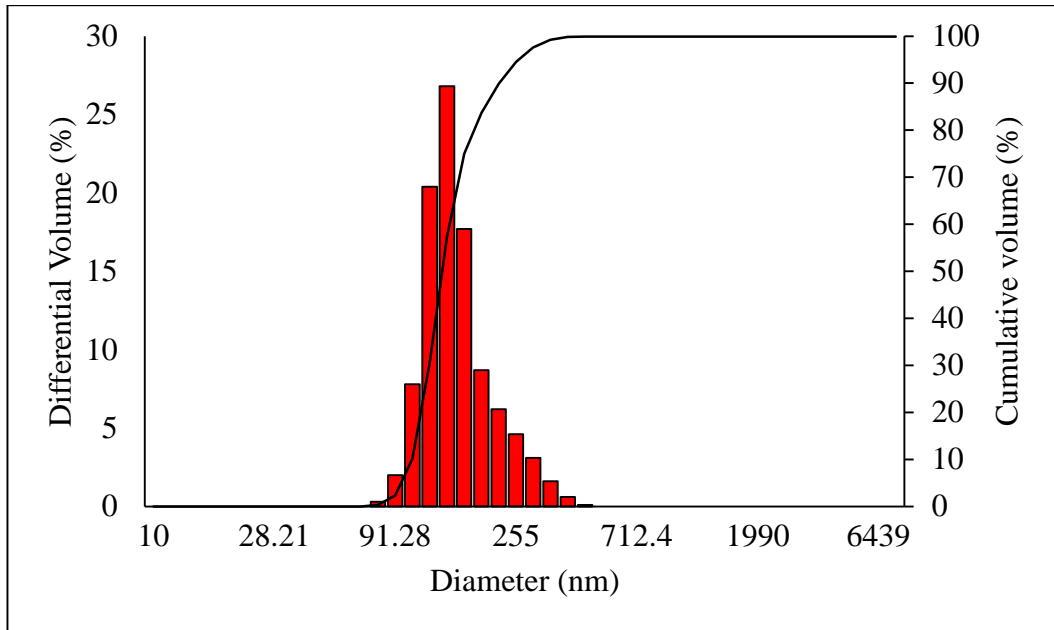


Figure C.3: Volume distribution of nanoparticle size within the 0.01 vol% of TiO₂-methanol nanofluids.